

6-1-1962

A Spectroscopic Study of Some Rare Earth Complexes

Richard M. Alire

Follow this and additional works at: https://digitalrepository.unm.edu/chem_etds



Part of the [Physical Chemistry Commons](#)

Recommended Citation

Alire, Richard M.. "A Spectroscopic Study of Some Rare Earth Complexes." (1962). https://digitalrepository.unm.edu/chem_etds/94

This Dissertation is brought to you for free and open access by the Electronic Theses and Dissertations at UNM Digital Repository. It has been accepted for inclusion in Chemistry ETDs by an authorized administrator of UNM Digital Repository. For more information, please contact disc@unm.edu.

UNIVERSITY OF NEW MEXICO-UNIVERSITY LIBRARIES



A14429 095596

A
SPECTRO-
SCOPIC
STUDY OF
SOME RARE
EARTH
COMPLEXES

ALIRE

378.789

Ua310a¹

1962

cop. 2

THE LIBRARY
UNIVERSITY OF NEW MEXICO

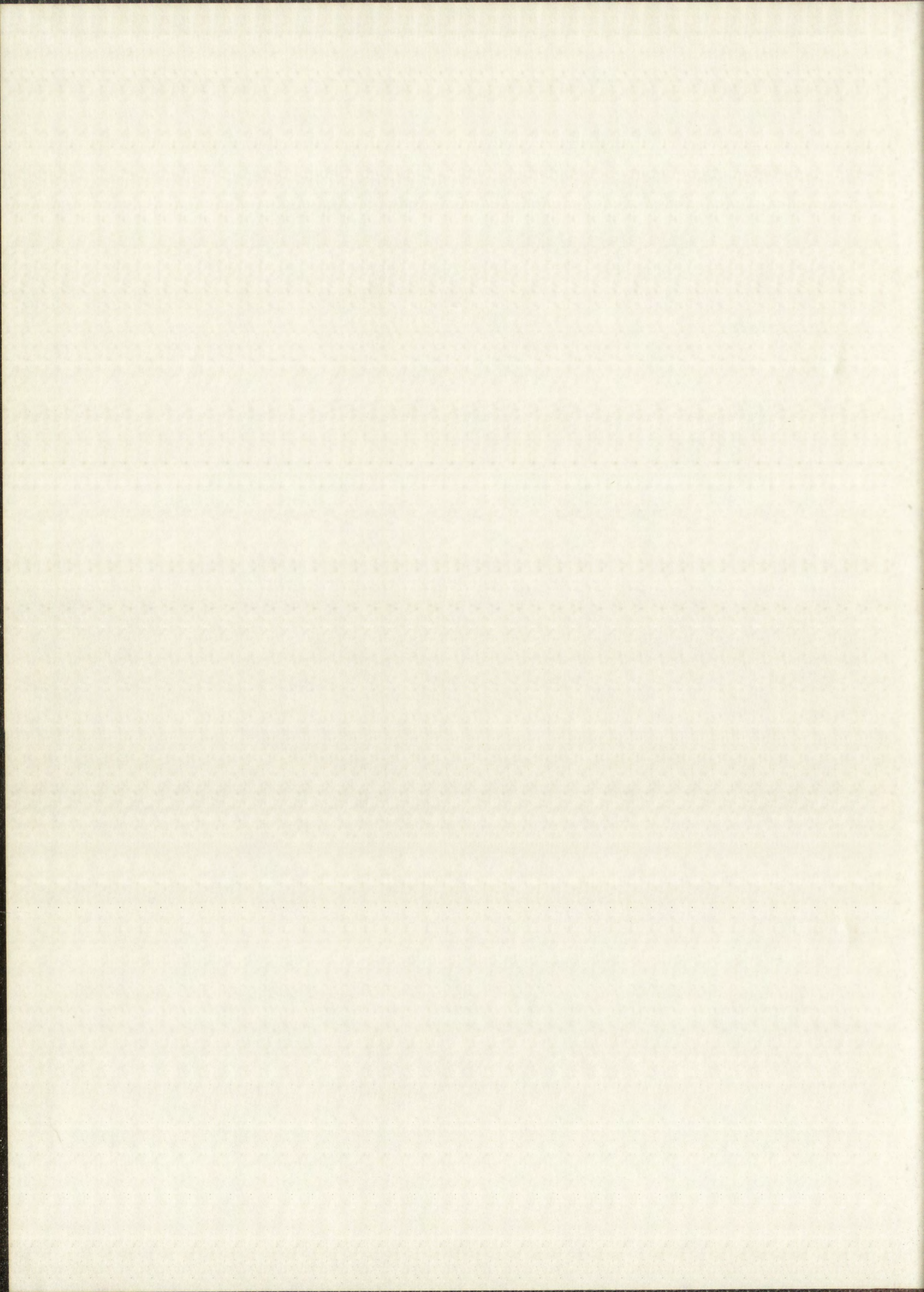


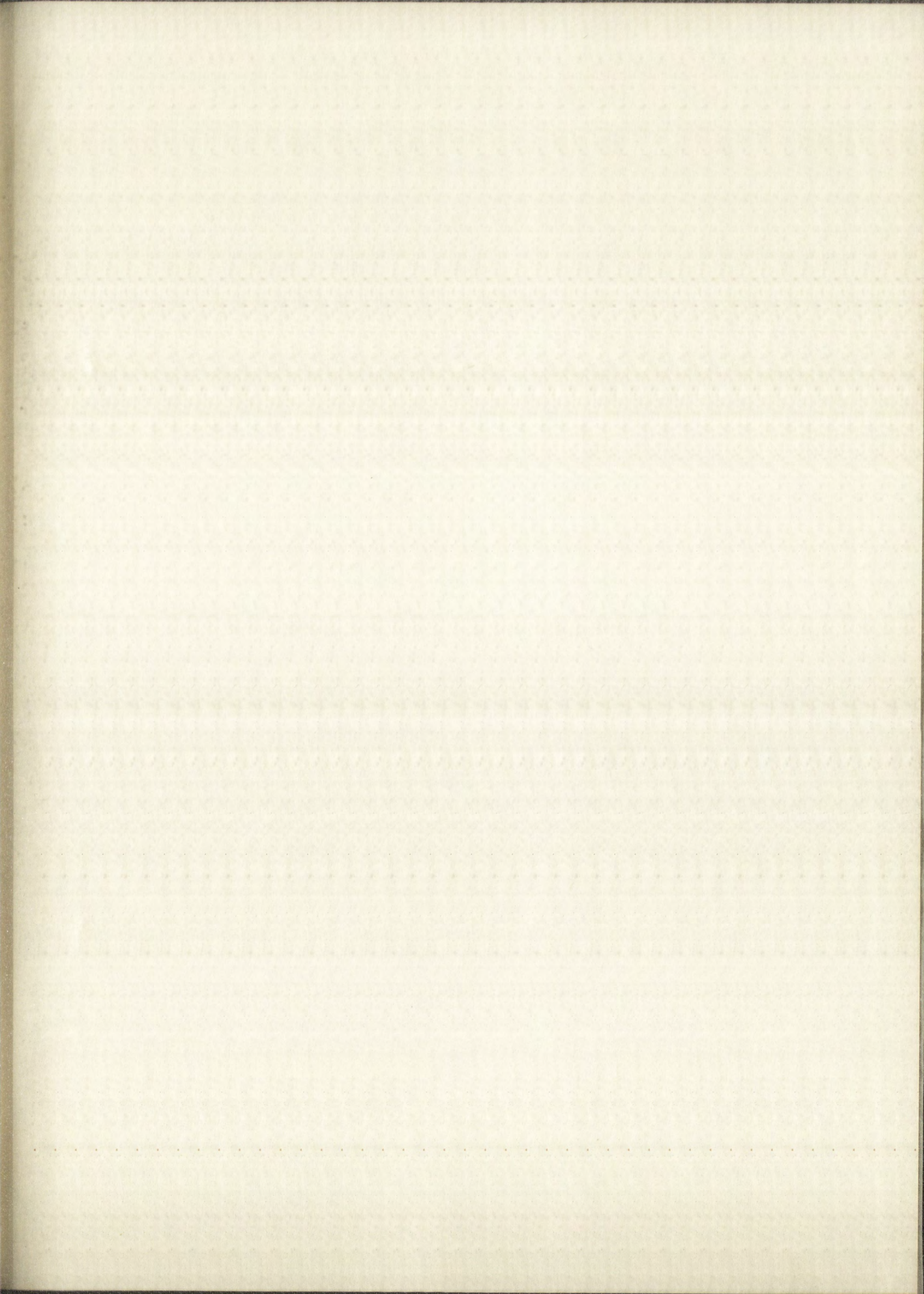
Call No.

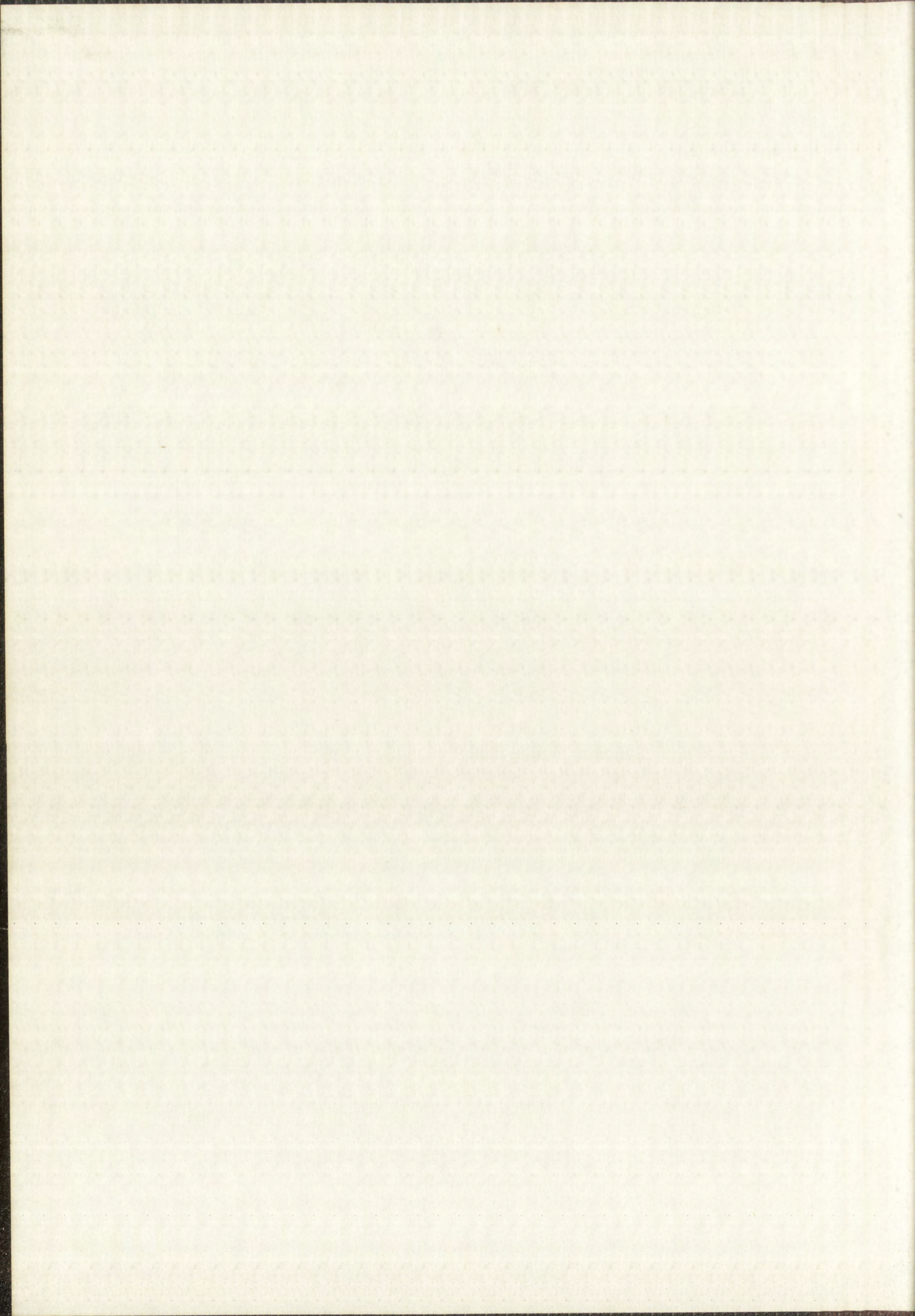
378.789
Un310a^l
1962
cop.2

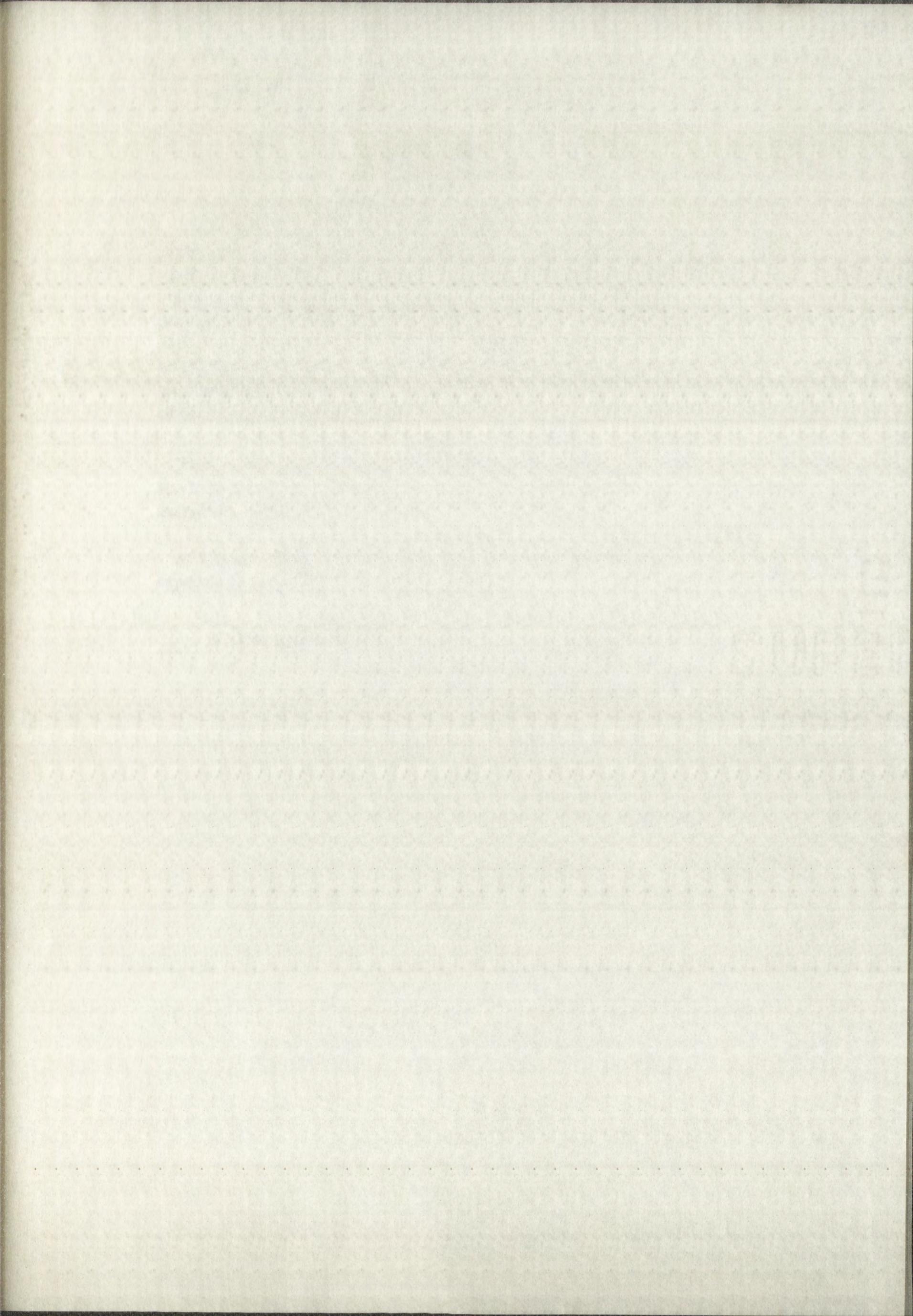
Accession
Number

291215









UNIVERSITY OF NEW MEXICO LIBRARY

MANUSCRIPT THESES

Unpublished theses submitted for the Master's and Doctor's degrees and deposited in the University of New Mexico Library are open for inspection, but are to be used only with due regard to the rights of the authors. Bibliographical references may be noted, but passages may be copied only with the permission of the authors, and proper credit must be given in subsequent written or published work. Extensive copying or publication of the thesis in whole or in part requires also the consent of the Dean of the Graduate School of the University of New Mexico.

This thesis by Richard M. Alire
has been used by the following persons, whose signatures attest their acceptance of the above restrictions.

A Library which borrows this thesis for use by its patrons is expected to secure the signature of each user.

NAME AND ADDRESS

DATE

MANUSCRIPT THESES

Unpublished theses submitted for the Master's and Doctor's degrees and deposited in the University of New Mexico Library are open for inspection, but are to be used only with due regard to the rights of the authors. Bibliographical references may be noted, but passages may be copied only with the permission of the author, and proper credit must be given in subsequent written or published work. Extensive copying or publication of the thesis in whole or in part requires also the consent of the Dean of the Graduate School of the University of New Mexico.

Richard M. Alfie

This thesis by

has been used by the following persons, whose signatures attest their acceptance of the above restrictions.

A library which borrows this thesis for use by its patrons is expected to secure the signature of each user.

DATE

NAME AND ADDRESS

A SPECTROSCOPIC STUDY OF SOME
RARE EARTH COMPLEXES

By

Richard M. Alire

A Dissertation

Submitted in Partial Fulfillment of the
Requirements for the Degree of
Doctor of Philosophy in Chemistry

The University of New Mexico

1962



A SPECIFIC STUDY OF
THE EASTERN CONCEPT

Richard W. Wright

A Dissertation
Submitted in Partial Fulfillment of the
Requirements for the Degree of
Doctor of Philosophy

The University of Toronto

1900

This dissertation, directed and approved by the candidate's committee, has been accepted by the Graduate Committee of the University of New Mexico in partial fulfillment of the requirements for the degree of

DOCTOR OF PHILOSOPHY

Stuart A. Northrop
DEAN

June 1, 1962
DATE

Committee

Glen A. Crosby
CHAIRMAN

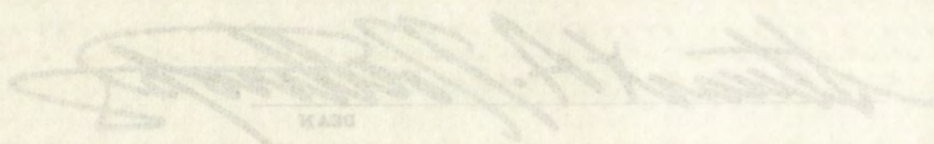
Guido H. Dault


Milton Kahn

J. H. Liebman

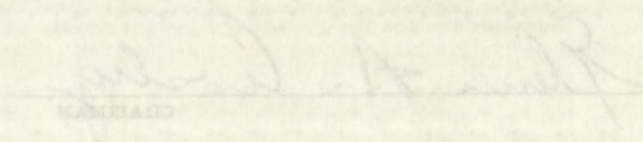
This dissertation, directed and approved by the candidate's committee, has been accepted by the Graduate Committee of the University of New Mexico in partial fulfillment of the requirements for the degree of

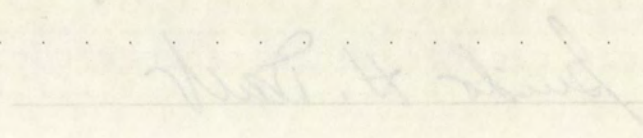
DOCTOR OF PHILOSOPHY

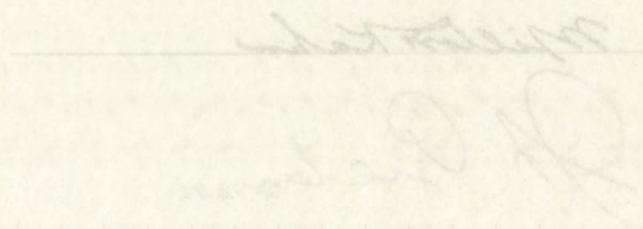

DEAN


DATE

Committee


CHAIRMAN


MEMBER


MEMBER

ABSTRACT

The phenomenon of intramolecular energy transfer was studied using anthranilate, 8-hydroxyquinolate, 2-methyl-8-hydroxyquinolate, and salicylaldehyde rare earth chelates. Line emission characteristic of the rare earth ion was observed whenever the lowest triplet (measured) of the complex was higher in energy than the emitting (resonance) level of the rare earth trivalent ion. The path of energy transfer from the organic portion of the chelate to the rare earth ion was verified as going via the lowest or a nearby triplet state of the complex.

Relative quantum yield measurements were made on the anthranilate rare earth series using a photographic method. Gadolinium anthranilate was used as an internal standard with a defined total quantum yield of 1.0. Fluorescence quantum yields varied from 0.04 for ytterbium anthranilate to 0.45 for lutecium and lanthanum anthranilates. Phosphorescence quantum yields varied from .037 for ytterbium anthranilate to 0.81 for gadolinium anthranilate with an estimated error of 25%. The relative quantum yields of the anthranilates have no simple relationship to the magnetic susceptibilities of the trivalent rare earth ions.

Dissociation and decomposition of the rare earth

291215

ABSTRACT

The phenomenon of intramolecular energy transfer was studied using anthracene, 8-hydroxyanthracene, hydroquinone, and naphthalene. The energy levels of the excited singlet state of the donor and acceptor were determined by laser spectroscopy. It was found that the energy transfer from the excited singlet state of the donor to the ground state of the acceptor was higher in energy than the energy of the excited singlet state of the acceptor. The rate of energy transfer from the excited singlet state of the donor to the ground state of the acceptor was verified as being the same as the rate of energy transfer from the excited singlet state of the donor to the excited singlet state of the acceptor.

Relative quantum yield measurements were made for anthracene, 8-hydroxyanthracene, hydroquinone, and naphthalene. The relative quantum yield of anthracene was found to be 0.45 for the excited singlet state and 0.51 for the excited triplet state. The relative quantum yield of 8-hydroxyanthracene was found to be 0.45 for the excited singlet state and 0.51 for the excited triplet state. The relative quantum yield of hydroquinone was found to be 0.45 for the excited singlet state and 0.51 for the excited triplet state. The relative quantum yield of naphthalene was found to be 0.45 for the excited singlet state and 0.51 for the excited triplet state. The relative quantum yield of anthracene was found to be 0.45 for the excited singlet state and 0.51 for the excited triplet state. The relative quantum yield of 8-hydroxyanthracene was found to be 0.45 for the excited singlet state and 0.51 for the excited triplet state. The relative quantum yield of hydroquinone was found to be 0.45 for the excited singlet state and 0.51 for the excited triplet state. The relative quantum yield of naphthalene was found to be 0.45 for the excited singlet state and 0.51 for the excited triplet state.

salicylaldehyde chelates were observed. The salicylaldehyde chelates demonstrate three different types of emission: (i) green phosphorescence (lifetime $\sim 10^{-3}$ sec.) attributed to the salicylaldehyde ion, (ii) a yellow phosphorescence with a lifetime of approximately 10^{-4} seconds in duration attributed to a triplet to ground state transition in a species containing the metal ion, (iii) a relatively long lived (10^{-1} sec.) afterglow attributed to an electronic transition occurring in either SA, solvated SA or both species.

Energy transfer to rare earth ions in salicylaldehyde chelates probably occurs from the excited state measured to be at approximately $17,700 \text{ cm}^{-1}$. This level is thought to be present in one or all three of the species $M(\text{SA})_3$, $M(\text{SA})_2^+$, $M(\text{SA})^{++}$.

salicylaldehyde anilates were observed. The salicylaldehyde
 chelates demonstrate three different types of emission: (i)
 green phosphorescence (lifetime $\sim 10^{-5}$ sec.) attributed to
 the salicylaldehyde ion, (ii) a yellow phosphorescence with
 a lifetime of approximately 10^{-4} seconds in duration attrib-
 uted to a triplet to ground state transition in a species
 containing the metal ion, (iii) a relatively long lived
 (10^{-1} sec.) afterglow attributed to an electronic transition
 occurring in either SA, solvated SA or both species.
 Energy transfer to rare earth ions in salicylaldehyde
 chelates probably occurs from the excited state measured to
 be at approximately $17,700 \text{ cm}^{-1}$. This level is thought to be
 present in one or all three of the species $\text{E}(\text{SA})$, $\text{E}(\text{SA})^+$,
 $\text{M}(\text{SA})^{++}$.

ACKNOWLEDGMENT

The author wishes to express his sincere appreciation to Dr. G. A. Crosby, who encouraged this investigation.

NOTICE

The author wishes to express his appreciation to Dr. J. J. [Name] for his assistance in the preparation of this manuscript.

Yours very truly,
[Signature]

TABLE OF CONTENTS

	Page
ABSTRACT	ii
ACKNOWLEDGMENT	iv
LIST OF TABLES	vii
LIST OF ILLUSTRATIONS	ix
INTRODUCTION	1
A. Purpose B. General Aspects of Absorption and Luminescence C. Spectroscopic Properties of the Hydrated Rare Earth Inorganic Salts D. Spectroscopic Properties of Rare Earth Chelates	
Chapter	
I. EXPERIMENTAL	20
A. Preparation of the Rare Earth Chelates B. Methods of Analysis C. Spectroscopic Measurements D. Relative Quantum Yields	
II. RESULTS	39
A. Spectroscopic Measurements of 8-Hydroxyquinolates, 2-Methyl-8-Hydroxyquinolates and Anthranilates B. Quantum Yield Measurements	
III. DISCUSSION	85
A. Absorption and Emission B. The Path of Energy Transfer C. Possible Reasons for Radiationless Intersystem Crossing	

TABLE OF CONTENTS

ABSTRACT

ACKNOWLEDGMENT

LIST OF TABLES

LIST OF ILLUSTRATIONS

INTRODUCTION

A. Purpose

B. General aspects of spectroscopy

C. Spectroscopic Principles

D. Spectroscopic Properties of

Chelates

Chapter

I. EXPERIMENTAL

A. Preparation of the compounds

B. Methods of Analysis

C. Spectroscopic Properties

D. Relative Quantum Yields

II. RESULTS

A. Spectroscopic Properties

B. Quantum Yield Measurements

III. DISCUSSION

A. Absorption and Emission

B. The Path of Energy Transfer

C. Possible Mechanisms of Energy Transfer

TABLE OF CONTENTS

Page

- D. Possible Reasons for Radiative
Triplet-Singlet Transitions
- E. Possible Reasons for Energy Transfer
to the Rare Earth Ion
- F. Electronic Transitions for Other
Rare Earth Chelate Series
- G. Other Mechanisms for Intramolecular
Energy Transfer

APPENDIX I	113
APPENDIX II.	125
BIBLIOGRAPHY	153

TABLE OF CONTENTS

D. Possible Reactions of Triplet-Singlet

E. Possible Reactions of Singlet-Singlet

F. Possible Reactions of Triplet-Triplet

G. Possible Reactions of Singlet-Triplet

APPENDIX I

APPENDIX II

BIBLIOGRAPHY

LIST OF TABLES

Table	Page
1. Analysis Reports of 2-Methyl-8-Hydroxyquinolate Rare Earth Chelates.	24
2. Analysis Reports of 8-Hydroxyquinolate Rare Earth Chelates.	25
3. Analysis Reports for the Rare Earth Anthranilates	26
4. Filtering Systems	28
5. Molar Absorption Coefficients of the Rare Earth Anthranilates	47
6. Molar Absorption Coefficients of the Rare Earth 8-Hydroxyquinolates	48-49
7. Molar Absorption Coefficients for the Rare Earth 2-Methyl-8-Hydroxyquinolates.	50
8. Classification of Luminescence Spectra of Rare Earth Chelates	51
9. Wavelength Measurements of the Fluorescence Band Maxima for the Rare Earth 8-Hydroxyquinolates, 2-Methyl-8-Hydroxyquinolates and Anthranilates	62-63
10. Wavelength Measurements of the Phosphorescence Band Maxima of the Rare Earth 8-Hydroxyquinolates, 2-Methyl-8-Hydroxyquinolates, and Anthranilates	64-65
11. Areas Obtained by Graphical Integration for the Emission Spectra of the Rare Earth Anthranilates	67-68
12. Integrated Intensities of the Rare Earth Anthranilates	78

LIST OF TABLES

Table	Page
13. Relative Quantum Yields and Crossing Constant Ratios for Rare Earth Anthranilates	84
14. Resonance Levels of Some Rare Earth Ions. . .	92
15. Ground State and Resonance Level Con- figurations of the Rare Earth Trivalent Ions.	107
16. Analysis Reports of Salicylaldehyde Rare Earth Chelates.	127
17. Measurements of the Phosphorescence Band Maxima for the Rare Earth Chelates of Salicylaldehyde	140-141
18. Summary of Spectral Data of Some Mixtures of Salicylaldehyde Chelates and the Rare Earth Chloride	144

LIST OF TABLES

Table		Page
13.	Relative Quantum Yields and Cross-Sectional Constant Factors for Rare Earth Antisymmetric	84
14.	Resonance Levels of Some Rare Earth Ions	93
15.	Ground State and Resonance Level Transitions of the Rare Earth Trivalent Ions	107
16.	Analytical Reports of Salicylaldehyde Rare Earth Complexes	127
17.	Measurements of the Phosphorescence Band Maxima for the Rare Earth Complexes of Salicylaldehyde	140-147
18.	Summary of Spectral Data of Some Mixtures of Salicylaldehyde Complexes and the Rare Earth Chlorides	148

LIST OF ILLUSTRATIONS

Figure	Page
1. Total Emission Filter Box	30
2. Phosphoroscope Schematic Diagram.	33
3. Dispersion Curve (short optics)	36
4-9. Typical Absorption Curves	42-46
10-17. Typical Fluorescence and Phosphorescence Spectra	55-61
18-20. Hurter-Driffield Plots.	71-75
21. Schematic Diagram of Triplet and Singlet Levels.	80
22. Energy Level Diagram, Triplet States of Chelates and Resonance Levels of Rare Earth Ions	94
23. Potential Well Diagram.	102
24. Typical Hurter-Driffield Plot	113
25. Decomposition of $\text{Sm}(\text{SA})_3$	129
26-33. Emission Spectra of Some Salicylaldehyde Rare Earth Chelates	133-139
34-35. Absorption Spectra of Salicylaldehyde	143

LIST OF FIGURES

Figure	
1.	Total Emission Spectrum
2.	Photographic Record of Total Emission Spectrum
3.	Dispersion Curve of Total Emission Spectrum
4-9.	Typical Absorption Curves
10-17.	Typical Fluorescence and Phosphorescence Spectra
18-20.	Harper-Driftfield Plots
21.	Schematic Diagram of Energy Levels
22.	Energy Level Diagram, Relative Intensities of Transitions and Relative Ionization Potentials
23.	Potential Well Diagram
24.	Typical Harper-Driftfield Plots
25.	Composition of Be ₁₂
26-33.	Emission Spectra of Be ₁₂ Vapor
34-35.	Absorption Spectra of Be ₁₂ Vapor

INTRODUCTION

A. Purpose

This investigation was initiated to attempt to establish the path of energy transfer from the organic portion of several rare earth chelates to the rare earth ion and to obtain information which would aid in elucidating the detailed mechanism of the transfer process.

B. General Aspects of Absorption and Luminescence

1. Absorption in the Visible and Ultraviolet Regions.-- Studies on the absorption properties in the visible and ultraviolet regions of unsaturated compounds indicate that the π - electrons are responsible for most low-lying electronic states which correspond to the absorption bands in these regions of the spectrum.¹ These transitions are ascribed to ones in which π -electrons go from a π -bonding state to a π^* antibonding state.²

Non-bonding electrons, which are generally referred to as "lone pair", may be excited to unfilled π^* -electron antibonding orbitals thereby giving rise to other absorption bands in the visible and ultraviolet regions.³ These latter types of electronic transitions are found in molecules containing

Purpose

This investigation was carried out to determine the effect of the presence of several ions on the rate of absorption of light by a solution of a certain substance. The results of the investigation are presented in the following tables.

B. General Remarks

1. Absorption in the visible and ultraviolet regions of the spectrum of a substance is determined by the presence of certain ions in the solution. The results of the investigation are presented in the following tables.

Non-bonding electrons, which are free to move, may be excited to a higher energy state by the absorption of light. This process is called photochemical reaction. The results of the investigation are presented in the following tables.

nitro, nitroso, and carbonyl compounds. Transitions which involve non-bonding electrons have been experimentally observed to be significantly weaker than those which involve π electrons only.

2. Multiplicities of Electronic States.--All molecules that have an even number of electrons, with electron pairing, exhibit a diamagnetic singlet ground state.⁴ Electron pairing is usually maintained in electronic transitions which are the origin of the commonly observed absorption bands. States of higher multiplicity are observed in cases where electron pair uncoupling takes place⁵ and the common state of higher multiplicity is the triplet state. Numerous singlet and triplet states are available in a molecule for such electronic transitions. In chelate molecules the singlet and triplet states have been used to explain their spectroscopic properties. Yuster,⁶ however, has pointed out for rare earth chelates that the electronic states are not pure singlets and triplets but admixtures of both multiplicities. In order to avoid complication of the nomenclature, however, these states will be referred to as singlets and triplets.

3. Vibronic States.--Each of the electronic states of either singlet or triplet multiplicity have superimposed vibrational levels which are responsible for vibrational fine structure in absorption and emission spectra. Excitation of a given electronic level also results in excitation of the

nitro, nitroso, and carbonyl compounds. Transitions which involve non-bonding electrons have been experimentally observed to be significantly weaker than those which involve π electrons only.

3. Multiplicities of Electronic States.--All molecules that have an even number of electrons, with electron pairing, exhibit a diamagnetic singlet ground state. Electron pairing is usually maintained in electronic transitions which are the origin of the commonly observed absorption bands. States of higher multiplicity are observed in cases where electron pairing uncoupling takes place, and the common state of higher multiplicity is the triplet state. Numerous singlet and triplet states are available in a molecule for such electronic transitions. In chelate molecules the singlet and triplet states have been used to explain their spectroscopic properties. Yuster,⁶ however, has pointed out for rare earth chelates that the electronic states are not pure singlet and triplet but admixtures of both multiplicities. In order to avoid complication of the nomenclature, however, these states will be referred to as singlets and triplets.

5. Vibrronic States.--Each of the electronic states of either singlet or triplet multiplicity have superimposed vibrational levels which are responsible for vibrational fine structure in absorption and emission spectra. Excitation of a given electronic level also results in excitation of the

vibrational levels associated with it, although vibrational fine structure is not always well-defined in absorption and emission studies in solution because the vibrational levels are perturbed by collisions.

4. Internal Conversion.--Studies on molecular luminescence have demonstrated that only the lowest (in energy) excited state of a given multiplicity is able to emit its excitation energy in the form of light.⁷ For a series of electronic levels of the same multiplicity, the higher electronic levels lose some energy by collisions and the molecule undergoes a radiationless transition to the lowest excited state of that multiplicity. This internal conversion process is far more rapid than any emission process. It is to be emphasized that the concept of internal conversion is based entirely on experimental observations.

5. Fluorescence.--The short lived emission observed for molecules with an even number of electrons is considered to be a singlet-singlet transition and is called fluorescence. This type of emission normally occurs at lower frequencies than the corresponding singlet-singlet absorption. The reason for this shift to lower frequencies is that the fluorescence usually originates from transitions of the lower vibrational levels of the first excited singlet to higher vibrational levels of the ground state. On the other hand, the source of the absorption bands are transitions from the lower vibrational

vibrational levels separated by small energy intervals. The line structure is not observed in the emission studies in solution and is perturbed by collisions. 4. Interval between the two lowest vibrational levels is small.

Measurements have demonstrated that the excited state of a molecule is not a simple electronic level but is a complex of electronic levels. The energy of the excited state of a molecule is not a simple function of the electronic level but is a function of the electronic level and the vibrational level. The energy of the excited state of a molecule is not a simple function of the electronic level but is a function of the electronic level and the vibrational level. It is to be expected that the energy of the excited state of a molecule is not a simple function of the electronic level but is a function of the electronic level and the vibrational level.

5. Fluorescence. The energy of the excited state of a molecule is not a simple function of the electronic level but is a function of the electronic level and the vibrational level. The energy of the excited state of a molecule is not a simple function of the electronic level but is a function of the electronic level and the vibrational level. This type of emission is called fluorescence. The energy of the excited state of a molecule is not a simple function of the electronic level but is a function of the electronic level and the vibrational level. The energy of the excited state of a molecule is not a simple function of the electronic level but is a function of the electronic level and the vibrational level. The energy of the excited state of a molecule is not a simple function of the electronic level but is a function of the electronic level and the vibrational level.

levels of the ground state to higher vibrational levels of the first excited singlet state. The consequence is that the energy gap for the emission process is smaller than that for the corresponding absorption process. The emission and absorption spectra are usually mirror images of each other for most compounds. The area of overlap for the emission and absorption spectra is designated as the transition which occurs from the lowest vibrational level of the first excited state to the lowest vibrational level of the ground state (0-0 transition). The (0-0) band only occurs for allowed transitions.

6. Intersystem Crossing and Phosphorescence.--The long lived luminescence which is usually observed only at low temperatures is attributed to a transition from the lowest triplet state to the singlet ground state of the molecule and is called phosphorescence.⁴ This emission is preceded by a radiationless transition from the vibrational levels of the first excited singlet state to the vibrational levels of the low-lying triplet states. In accordance with the idea of internal conversion, the lowest triplet state is the only electronic state of that multiplicity that emits energy in the form of light. The radiationless transition, which is called a singlet-triplet transition, is spin forbidden.⁸ The fact that it occurs at all in certain cases is explained by spin-orbit interaction. In qualitative terms, this process occurs

levels of the ground state to higher vibrational levels of the first excited singlet state. The consequence is that the energy gap for the emission process is smaller than that for the corresponding absorption process. The emission and absorption spectra are usually well separated for each other for most compounds. The area of overlap for the emission and absorption spectra is designated as the transition with energy from the lowest vibrational level of the first excited state to the lowest vibrational level of the ground state (0-0 transition). The (0-0) band only occurs for allowed transitions.

6. Intersystem Crossing and Phosphorescence. -- The long-lived luminescence which is usually observed only at low temperatures is attributed to a transition from the lowest triplet state to the singlet ground state of the molecule and is called phosphorescence. This emission is preceded by a radiationless transition from the vibrational levels of the first excited singlet state to the vibrational levels of the low-lying triplet states. It is associated with the loss of vibrational energy, the lowest triplet state is the only electronic state of that multiplicity that emits energy in the form of light. The radiationless transition, which is called a singlet-triplet transition, is spin-forbidden. The fact that it occurs at all in certain cases is explained by spin-orbit interaction. In qualitative terms, this process occurs

because of the magnetic interactions present in the molecule.

Spin-orbit coupling in atoms is greatly increased with increasing atomic number. McClure⁹ has applied this principle by heavy atom substitution of organic molecules which includes the monohalobenzenes and naphthalenes. The conclusion reached in his study is that the probability for the radiationless singlet-triplet transition increases rapidly along with the radiative triplet-singlet transition probability as the atomic number of the substituent is increased.

Paramagnetism of the atoms in molecules also enhances the singlet-triplet radiationless transition. The correlation between the increase in singlet-triplet mixing and the degree of paramagnetism is not simple. Porter and Wright¹⁰ have reported that the probability of triplet emission of naphthalene is definitely increased in the presence of paramagnetic inorganic ions, but no definite correlation to the magnetic moments of these ions has been established.

7. Oscillator Strengths.--A measure of the interaction between optical electrons and light, resulting in a given absorption band is called the oscillator strength. It can be shown¹¹ that the oscillator strength is: $f_1 = 4.319 \times 10^9 \int \epsilon_i d\tilde{\nu}$. ϵ_i = molar absorption coefficient and $\tilde{\nu}$ = frequency expressed in cm^{-1} .

An experimental evaluation of the oscillator strength for a given absorption band can be made by plotting absorption

curves in terms of absorption coefficient versus frequency in wavenumbers and determining the area under the resulting curve by graphical integration.

The oscillator strength is also an experimental measurement of the transition probabilities between the electronic levels which are the source of absorption bands. The actual life of the emission process is related to the oscillator strength whenever no quenching processes are involved.

The oscillator strength for a typical singlet-triplet absorption is approximately 10^6 smaller than that for a singlet-singlet absorption. It is evident that an experimental measurement of singlet-triplet absorption requires highly concentrated solutions and long optical paths, which tend to increase errors from impurities.

D. F. Evans¹² has measured singlet-triplet absorptions for many organic compounds by using paramagnetic oxygen to increase the intensity of these transitions. The exact nature of this paramagnetic oxygen effect is not fully understood but experiments indicate that the singlet-triplet absorption intensity increases in the presence of oxygen and that it does not increase in the presence of diamagnetic gases.

8. Quenching.--The amount of energy that is not emitted as light following absorption is referred to as quenched energy.¹³ There are three general ways by which excitation energy may be quenched: (i) intermolecular energy transfer

curve in case of absorption coefficient versus frequency
in wave-lengths and the curve of the absorption
curve of the absorption coefficient.
The oscillation theory is also of great interest
and of the oscillation coefficient between the absorption
levels which are the basis of the oscillation theory. The actual
life of the emission process is related to the oscillator
strength whether in the oscillation process or in the
oscillation process. The oscillation coefficient is a
absorption is approximately 10⁶ smaller than that for a
single-oscillator absorption. It is evident that an absorp-
tion coefficient of single-oscillator absorption is
highly concentrated in the oscillation and the oscillation
and to the oscillation theory from the oscillation.
D. E. Evans, has recently suggested a hypothesis
for many organic compounds of which the oscillation is
increased the intensity of the oscillation. The oscillation
nature of the oscillation is not fully under-
stood but experimental evidence is that the oscillation is
oscillation intensity in the presence of oxygen and
that it does not increase in the presence of diatomic gases.
8. Oscillation. The oscillation is not related
as light in the oscillation is related to the oscillation
energy. 1) There are two types of oscillation energy
energy may be oscillation. (1) Oscillation energy

from the excited states of one molecule to electronic states of other surrounding molecules of a different kind, (ii) intramolecular energy transfer to other electronic or vibrational states near in energy to the excited states, (iii) intermolecular or intramolecular collisional interaction.

Terrenin and Ermolaev¹⁴ have reported quenching due to intermolecular energy transfer. The amount of interaction was found to increase with increasing concentration of the quenching agent.

The second general way for radiationless deactivation of excitation energy is considered to be important for explaining the spectral behavior of rare earth chelates. Previous investigations¹⁶ on emission spectra of the rare earth chelates have presupposed that there is no quenching or that quenching is small. Investigations in this laboratory have shown that the amount of quenching varies as the rare earth ion is varied and the ligand is kept constant. Quenching and its relation to the mechanism of energy transfer will be discussed in a later section.

All the luminescence spectra studied in this investigation were taken at liquid nitrogen temperature and any quenching due to collisional interaction is considered to be negligible. At room temperature the energy lost by collisions becomes a significant factor.

9. Quantum Yields.--Molecules emit by radiative

from the other side of the barrier.

at other points of the barrier.

transmission of energy.

at other points of the barrier.

molecular of energy.

transmission of energy.

intermolecular energy.

was found to be the same.

quenching agent.

The second part of the experiment.

of excitation energy.

plasma in the gas.

transmission of energy.

chances have been made.

quenching is small.

shown that the energy of the plasma.

ion is varied in the plasma.

and the relation to the energy of the plasma.

discussed in a later section.

All the experiments were made in this manner.

gation were carried out in the same manner.

quenching due to the plasma.

negligible. At the same time the energy of the plasma.

becomes a small fraction of the total energy.

2. Quenching of the plasma.

transitions only a certain fraction of the quanta absorbed and the quantum yield is defined as $\frac{\text{No. of quanta emitted}}{\text{No. of quanta absorbed}}$. Absolute measurements of this fraction on various organic compounds were made by D. McClure and co-workers.¹⁷ Experimental difficulties associated with absolute measurements have limited the number of measurements made. Total luminescence yields include phosphorescence and fluorescence. The fluorescence quantum yield is defined as:

$\frac{\text{No. of quanta emitted from the first excited singlet}}{\text{Total No. of quanta absorbed}}$; the phosphorescence quantum yield is defined as:

$\frac{\text{No. of quanta emitted from the lowest triplet state}}{\text{Total No. of quanta absorbed}}$. These

two quantum yields are dependent on the degree of singlet-triplet crossing. In the absence of quenching an increase in phosphorescence quantum yield is coupled with a decrease in fluorescence quantum yield.

A distinction is made between intrinsic quantum yields which have been corrected for external quenching and observed quantum yields which include quenching. At low temperatures external quenching is negligible for cases involving dilute solutions of only one compound, consequently the observed and intrinsic quantum yields are nearly equal. In solutions containing mixtures of compounds, intermolecular quenching is present so that the quantum yields measured even at low temperatures include quenching. The investigations here show the existence of large intramolecular quenching in dilute

transitions only a certain fraction of the quanta absorbed and
the quantum yield is defined as $\frac{\text{No. of quanta emitted}}{\text{No. of quanta absorbed}}$
These measurements of the fraction of the quanta absorbed
were made by E. McGlynn and co-workers. The fluorescence
intensities associated with absolute measurements have limited the
number of measurements made. Total fluorescence yield is the
ratio of fluorescence and phosphorescence. The fluorescence
quantum yield is defined as:
$$\frac{\text{No. of quanta emitted from the triplet excited state}}{\text{Total No. of quanta absorbed}}$$

phosphorescence quantum yield is defined as:
$$\frac{\text{No. of quanta emitted from the lowest triplet state}}{\text{Total No. of quanta absorbed}}$$

The quantum yields are dependent on the degree of singlet-
triplet conversion. In the absence of quenching an increase in
phosphorescence quantum yield is coupled with a decrease in
fluorescence quantum yield.
A distinction is made between intrinsic quantum yields
which have been corrected for external quenching and observed
quantum yields which include quenching. At low temperatures
external quenching is negligible for cases involving dilute
solutions of only one compound, consequently the observed and
intrinsic quantum yields are nearly equal. In solutions con-
taining mixtures of compounds, intermolecular quenching is pre-
sent so that the quantum yields measured even at low tempera-
tures include quenching. The investigations here show the
existence of large intramolecular quenching in dilute

solutions of rare earth chelates at low temperatures.

The sum of intrinsic quantum yields for fluorescence and phosphorescence added to the total quenching yield equals unity. This is expressed as follows: $\phi_p^0 + \phi_f^0 + \phi_q^0 = 1$. In other words, all of the absorbed energy must be emitted as fluorescence and phosphorescence or be internally quenched.

10. Lifetimes.--The duration of luminescence is a spectroscopic measurement which is very valuable in characterizing emission spectra. The reciprocal of the intrinsic mean life which is the observed mean life corrected for quenching of any form is the probability of radiative transition. The intrinsic lifetime is proportional to the reciprocal of the oscillator strength. In view of the definition of the oscillator strength, the intrinsic lifetime can be calculated from the integrated absorption curve. Direct measurement of the decay time constant does not always result in a value for the intrinsic mean life because internal quenching might still be present even when external quenching is zero.

Intrinsic lifetimes are an important factor in the utilization of excitation energy in photochemical processes. The short-lived fluorescence may be so rapid that energy transfer cannot effectively compete with the spontaneous fluorescence emission.

11. Energy Transfer.--Mechanisms of energy transfer in atoms and molecules have been the subject of many investigations.

Energy transfer in atoms was first reported¹⁸ for the mercury-thallium mixture in the gas phase. Energy was transferred from the mercury to the thallium atom upon selective excitation of the mercury atom alone. Subsequent studies by Förster and co-workers¹⁵ revealed that this type of energy transfer occurs only when the emission spectra of the acceptor overlaps the absorption spectra of the donor. The requirement for energy transfer is very specific; however, it seems to be of general occurrence. A slight shift to lower frequency of the emission spectra usually occurs. This shift is sometimes a prerequisite for the requirement of spectral overlap.

Terrenin and Ermolaev¹⁴ have recently reported energy transfer between organic molecules. The main conclusion reached in their study is that energy transfer occurs only when the triplet state energy of the donor is higher than that of the acceptor. Possible complexes formed by the organic mixtures were considered to be unimportant because absorption spectra of the components were additive. It is significant to point out that the energy transfer occurs via the triplet state of the donor to the triplet state of the acceptor. Intramolecular energy transfer from the triplet state of the complex to the ions in rare earth chelates has also been reported and this will be discussed in a later section.

12. Characterization of $n \rightarrow \pi^*$ Transitions.--The dependence of electronic spectra of solute molecules on the

properties of solvents has been successfully used for an empirical classification of the electronic spectra. Kasha⁷ first suggested that solvent effects could be used to distinguish $n-\pi^*$ transitions from $\pi-\pi^*$ transitions. H. McConnell¹⁹ found that $n-\pi^*$ transitions undergo a shift to higher frequencies as the solvent is changed from a hydrocarbon to a hydroxylic one. Most $n-\pi^*$ transitions which have been characterized are at longer wavelengths and have lower intensities than $\pi-\pi^*$ transitions. Allowed $n-\pi^*$ transitions have intensities which result in molar absorption coefficients which range from 100-1000, while forbidden $n-\pi^*$ transitions have a range of absorption coefficient from 10 to 100. $\pi-\pi^*$ transitions, on the other hand, have molar absorption coefficients which are about 10,000 or higher and they undergo a shift to lower frequencies as the solvent is changed from a hydrocarbon to a hydroxylic one. The band shifts which $n-\pi^*$ transitions undergo in hydroxylic solvents are commonly referred to as blue shifts.

The qualitative explanation which has been proposed for the fact that $n-\pi^*$ transitions undergo shifts to higher frequencies by solvent variation is as follows: The ground state of the solute molecule has a charge distribution such that the polar solvent binds strongly with it, while the excited state of the solute molecule has a charge distribution such that the polar solvent molecules do not bind as strongly

relative to the ground state. The consequence is a larger energy gap between the ground state and the excited state which means a shift to a higher frequency as the solvent is changed from a hydrocarbon to a hydroxylic one.

Brealey and Kasha²⁰ have shown that hydrogen bonding plays an important role in blue shifts of $n \rightarrow \pi^*$ absorption bands which are present in pyridazine and benzophenone. The blue shifts which $n \rightarrow \pi^*$ transitions undergo in hydroxylic solvents have been attributed to hydrogen bonding of the n -electrons by the hydroxylic solvent. The blue shift is caused by greater stabilization of the ground state compared to the excited state of the solute molecule. Association constants for pyridazine with ethanol and benzophenone with ethanol have been calculated on the basis of the UV spectra. A continuous range of mixtures of hexane and ethanol was used for the determination of the association constant which agrees well with the constant determined from infrared data.

C. Spectroscopic Properties of the Hydrated Rare Earth Inorganic Salts

1. Line Emission.--Appreciable intensity of line emission has been observed for certain rare earth hydrated inorganic salts upon direct excitation of the ion by near ultraviolet light.²¹ Only the rare earth ions which are near to gadolinium in the periodic table show significant fluorescence.²² The observed lines are usually "atomic like" and relatively

relative to the ground state. The corresponding is a larger energy gap between the ground state and the excited state which means a shift to a higher frequency as the solvent is changed from a hydrocarbon to a hydroxylic one. Inceley and Kohn²⁰ have shown that hydrogen bonding plays an important role in the shift of a $\pi \rightarrow \pi^*$ absorption band which are present in pyridine and benzophenone. The blue shift with $\pi \rightarrow \pi^*$ transitions undergo in hydroxylic solvents have been attributed to hydrogen bonding of the π electrons by the hydroxylic solvent. The blue shift is caused by greater stabilization of the ground state compared to the excited state of the solute molecule. Association constants for pyridine with ethanol and benzophenone with ethanol have been calculated on the basis of the UV spectra. A constant ratio of extinction of benzene and ethanol was used for the determination of the association constant which agrees well with the constant determined from infrared data.

C. Spectroscopic Properties of the Hydroxylic Solvent

1. The absorption spectra of the solute in the hydroxylic solvent has been observed for certain rare earth hydrated ions. The absorption spectra of the rare earth ions in the hydroxylic solvent are very similar to those in the hydrocarbon solvents. The observed lines are usually "atomic like" and relatively

sharp. Absorption spectra of the hydrated rare earth salts have determined the spectral region that is necessary to properly excite the crystals. A considerable amount of work has been done with rare earth spectra in an attempt to characterize the line emission and the investigations have been aided recently by the fact that rare earth oxides have become available in very high purity.

2. Origin of Absorption and Emission Spectra.--It is now generally recognized that absorption and fluorescence lines of rare earth ions in the visible region are produced by transitions between various possible levels of the $(4f)^n$ configurations in rare earth ions.²³ (n indicates the number of $4f$ electrons present in the rare earth trivalent ion and varies from one to thirteen.) Any ions or molecules, surrounding the rare earth ion establish an electric field which splits the atomic levels through Stark effects into various components. The observed sharp lines in absorption and emission are due to transitions between these components and the number of components depends on the symmetry of the field. The number of components decreases as the symmetry of the field increases and the degree of splitting is dependent on the strength of the field.²⁴

A determination of the field symmetry requires a correct assignment of the observed spectra. The transition assignments are extremely difficult because many possible levels

sharp. Absorption of the light is due to the presence of the dye in the solution. The absorption spectrum of the dye in the solution is shown in Figure 1. The absorption maximum is at 450 mμ. The absorption minimum is at 600 mμ. The absorption is proportional to the concentration of the dye in the solution. The absorption is also proportional to the path length of the light through the solution. The absorption is independent of the wavelength of the light. The absorption is independent of the temperature of the solution. The absorption is independent of the pH of the solution. The absorption is independent of the ionic strength of the solution. The absorption is independent of the nature of the solvent. The absorption is independent of the nature of the dye. The absorption is independent of the nature of the solution. The absorption is independent of the nature of the light. The absorption is independent of the nature of the observation. The absorption is independent of the nature of the measurement. The absorption is independent of the nature of the instrument. The absorption is independent of the nature of the operator. The absorption is independent of the nature of the environment. The absorption is independent of the nature of the time. The absorption is independent of the nature of the space. The absorption is independent of the nature of the universe. The absorption is independent of the nature of everything.

result as the number of electrons increase, and some of these may interact with each other leading to a very complicated set of energy levels. Direct assignments are possible for the hydrated salts of ytterbium and cerium trivalent ions, because the ions have thirteen electrons and one electron respectively. In both cases only an F doublet arises and the transition between the two doublet components is the only possible spectral line. In a field the doublet will be split into the various Stark components. Gobrect²⁵ found sharp absorption lines at 9700 Å in crystalline ytterbium sulfate octahydrate and assigned the transition as being between the $^2F_{7/2}$ and $^2F_{5/2}$ levels of the ytterbium trivalent ion. Assignments for the observed spectra of most of the rare earth ions are reviewed by D. McClure.²⁶

3. The Mechanism of Line Emission.--Upon irradiation with light of the required wavelength, the absorbed photons cause the ion in the crystal to attain the various excited states. The lifetimes of most of these states are generally too short for radiative transitions to be competitive. It is possible for some of these excited states to interact with the crystal lattice thereby converting some of the excitation energy to thermal vibrations of the crystal.²⁷ The remainder of the energy is transferred to the resonance level, which is usually a level far removed from the next lowest excited state, by a radiationless process. The observed lines in the

result of the...
any...
set of energy levels...
hydrogen...
the ions have...
In both cases...
between the two...
line. In a...
state...
9700 A...
aligned the...
levels of the...
observed...
by D. McG...
The...
with...
cause...
states. The...
too short...
possible...
the...
energy...
of the...
usually a...
state, by a...

spectrum are due to transitions from the resonance level to the lower states which are components of the ground multiplet. At low temperatures the transitions may originate from more than one resonance level.

4. Lifetime and Quenching of Line Emission.--In most cases the measured mean life of the excited state which is the origin of line emission is considerably shorter than the intrinsic mean life obtained from the absorption spectra. Dieke and Hall²² attribute this difference in lifetimes to depletion of the excited levels through radiationless interactions with the crystal lattice. The lifetime measurements on samarium, europium, gadolinium, terbium, and dysprosium trivalent ions, however, do not change appreciably with temperature indicating only small temperature dependence of the interaction of the excited state with the crystal lattice. The measurements show that there is considerable variation in lifetime from ion to ion in this series, but no significant change in lifetime as the salt of a given ion is varied. All the ions studied have a unique mean life with the exception of trivalent europium which demonstrated two lifetimes, although the two were not resolved. These results on europium corroborate the work by Sayer and Freed³⁰ where they assign two distinct resonance levels to this ion. A direct correlation between the degree of brightness and the lifetimes was found. The brightest emitter of all (Gd^{+++}) demonstrated the

spectrum are the two transitions from the resonance level to the lower states which are components of the ground multiplet. At low temperatures the transitions may originate from more than one resonance level.

4. Lifetime and branching of the $^2D_{3/2}$ state. - In most cases the measured mean life of the excited state which is the origin of the emission is considerably shorter than the intrinsic mean life obtained from the absorption spectra. These and other results indicate that transitions in lifetime to depletion of the excited levels through radiative transitions with the crystal lattice. The lifetime measurements on samarium, europium, gadolinium, cerium, and dysprosium trivalent ions, however, do not change appreciably with temperature indicating only small temperature dependence of the interaction of the excited state with the crystal lattice. The measurements show that there is considerable variation in lifetime from ion to ion in this series, but no significant change in lifetime as the salt of a given ion is varied. All the ions studied have a unique mean life within the exception of trivalent europium which demonstrated two lifetimes, 25- though the two were not resolved. These results on europium corroborate the work by Sayer and Ruedel¹⁰ where they assign two distinct resonance levels to this ion. A direct correlation between the degree of polarization and the lifetime was found. The highest lifetime of all (4.1×10^{-8} sec) demonstrated the

longest mean life (7500 micro-seconds) and the other ions whose lifetimes were measured have mean lives decreasing in the following order: $\text{Tb}^{+++} > \text{Eu}^{+++} > \text{Dy}^{+++} \approx \text{Sm}^{+++}$.

D. Spectroscopic Properties of Rare Earth Chelates

1. Line Emission.--Characteristic line emission from rare earth chelates was first observed by Weissman³¹. Sevchenko et al³² later studied this phenomenon. Chelates of trivalent europium, samarium, and terbium were studied using various chelating agents. The illumination was accomplished with light containing frequencies which were absorbed essentially by the organic constituent of the chelate. Energy was transferred from the organic constituent to the rare earth ion with subsequent characteristic line emission. The line emission was found to be much brighter than that observed for hydrated inorganic salts. These investigations were made at liquid nitrogen temperature in rigid glasses.

Crosby and Kasha³³ have reported line emission occurring for the dibenzoylmethide chelate of ytterbium. A single luminescence line was reported at 9710 ± 40 Å and the transition was assigned as the ${}^2\text{F}_{5/2} \rightarrow {}^2\text{F}_{7/2}$ intramultiplet transition. Other rare earth ions (Dy^{+++} , Tm^{+++} , Tb^{+++} , Ho^{+++}) have been reported to emit characteristic lines when chelated to dibenzoylmethane.³⁴⁻³⁵

2. Fluorescence and Phosphorescence.--Yuster and Weissman¹⁶ reported fluorescence and phosphorescence for

for the purpose of the investigation.

who were interviewed in the course of the investigation.

in the course of the investigation.

of the investigation.

of the investigation.

of the investigation.

of the investigation.

of the investigation.

of the investigation.

of the investigation.

of the investigation.

of the investigation.

of the investigation.

of the investigation.

of the investigation.

of the investigation.

of the investigation.

of the investigation.

of the investigation.

of the investigation.

of the investigation.

of the investigation.

of the investigation.

of the investigation.

of the investigation.

of the investigation.

dibenzoylmethide chelates of trivalent lanthanum, gadolinium and lutecium. No line emission has been observed for lanthanum and lutecium trivalent ions even in the hydrated inorganic crystals, because there are no 4f transitions which would appear in the visible or near ultraviolet region. Line emission has been observed for hydrated inorganic salts of gadolinium but not for the corresponding chelates. The absence of gadolinium line emission in chelates is due to the fact that it is energetically impossible for energy transfer to the ion to take place since the resonance level is higher in energy than either the singlet states or the triplet states of the chelates studied.

3. Fluorescence and Phosphorescence Lifetimes.-- Lifetime studies on the fluorescence and phosphorescence spectra of rare earth chelates of dibenzoylmethane demonstrate that each rare earth chelate for a given ligand has a unique mean life and that the trisdibenzoylmethide Gd(III) has a shorter mean life than any of the other rare earth chelates studied.¹⁶ No lifetime measurements of lines observed from chelates have been reported. However, on the basis of Dieke and Hall's²² investigations, the lifetimes of the lines in chelates can be expected to be nearly equal to those which were reported for the corresponding hydrated rare earth salts.

4. Fluorescence and Phosphorescence Quantum Yields.-- Relative intensity measurements of fluorescence and

phosphorescence have been reported¹⁶ for some rare earth chelates of dibenzoylmethane. No absolute quantum yield measurements on rare earth chelates have been reported. Investigations in this laboratory have shown the presence of phosphorescence, fluorescence and line emission in varying intensities for the chelates studied.

5. Energy Transfer.--The mechanism of energy transfer in rare earth chelates has not been completely established. Crosby and Whan³⁴ have suggested that the path of energy transfer from the organic portion of a chelate is via the lowest triplet state of the chelate. Dibenzoylmethide chelates of trivalent dysprosium, terbium and europium were the compounds reported. It has been suggested that vibrational interaction plays an important role in the mechanism of energy transfer.³³ This interaction involves excited states of the chelate coupling with vibrational levels of the rare earth ion. Further discussion on this problem by H. Sponer³⁶ points out that energy transfer in the case of ytterbium trisdibenzoylmethide has to bridge an energy gap of $\sim 10,500 \text{ cm}^{-1}$ between the lowest triplet state of the chelate and the resonance level of the ion. The energy gap is $13,500 \text{ cm}^{-1}$ if the energy is being transferred from the singlet state. This large energy gap indicates a weak vibrational coupling and consequently leads to a weak luminescence. A large amount of electronic energy has to be converted to

vibrational energy to be dissipated thermally. The important details of energy transfer have not been completely resolved and further work needs to be done.

6. Quenching of Line Emission.--The relative intensities of line emission from ion to ion vary considerably. No satisfactory explanation for the difference in luminescence efficiency of the lines in rare earth chelates has been reported. An ionic effect on the line emission efficiency has been observed.³¹ The ligand was varied for a given ion, and line intensities were observed to decrease as the degree of ionic bonding between the ligand and the ion increased. This suggests that energy transfer is not as efficient for compounds with a large amount of ionic bonding.

7. Quenching of Fluorescence and Phosphorescence.--Quantum yields of some trivalent rare earth chelates of dibenzoylmethane have been reported.¹⁶ A quantum yield close to unity was estimated by a comparison to the luminescence of fluorescein. No line emission was observed for any of the compounds so the total luminescence yield which was reported represented fluorescence and phosphorescence only. Studies on quantum yields in this laboratory indicate that there is considerable variation of the efficiency of emission with change of ion. Intramolecular quenching seems to play the most important role here.

CHAPTER I

EXPERIMENTAL

A. Preparation of the Rare Earth Chelates

1. 8-Hydroxyquinolates and Anthranilates.--The entire series of the rare earth 8-hydroxyquinolates and anthranilates (except for promethium and cerium) was synthesized in the following manner: Three tenths gram of the rare earth oxide was first converted to the chloride by boiling in concentrated hydrochloric acid until hydrated crystals appeared upon cooling. The hydrated chloride was then dissolved in about fifty milliliters of water. The rare earth chloride solution was added to five tenths gram of 8-hydroxyquinoline or anthranilic acid which was dissolved in fifty milliliters of 2N acetic acid. To this mixture 6N ammonium hydroxide was added dropwise and accompanied by vigorous stirring until a pH of 8 was reached. The resulting precipitate was digested at 70-80°C for thirty minutes and filtered while hot through a fritted glass funnel. The compound was air dried for two hours and finally dried in vacuum at 100°C.

The 8-hydroxyquinoline used was Eastman, white label and was sublimed in vacuo. The rare earth oxides were obtained from Research Chemicals, Burbank, California, and The Institute

for Atomic Research, Ames, Iowa. The anthranilic acid used was reagent grade from K & K Laboratories, Jamaica, New York, and was recrystallized twice from absolute ethanol.

2. 2-Methyl-8-hydroxyquinolates.--The synthesis of this series was accomplished by making a solution of three tenths gram of the rare earth chloride in fifty milliliters of ethanol, mixing with a solution containing five tenths gram of 2-methyl-8-hydroxyquinoline in 50ml. of ethanol and adding piperidine dropwise until a pH of 8 was reached. The precipitate was digested for fifteen minutes at 70-80°C and filtered while hot through a fritted glass funnel. The compound was dried in vacuo at 150°C.

The piperidine and 2-methyl-8-hydroxyquinoline were obtained from K & K Laboratories, Jamaica, New York. The piperidine was fractionally distilled and the fraction boiling at 90-91°C was used, and the 2-methyl-8-hydroxyquinoline was recrystallized from ethanol until a reproducible melting point of 74°C was obtained.

B. Methods of Analysis

1. Analysis of the 8-hydroxyquinolates.--A quantitative bromination of 8-hydroxyquinoline in acid medium, as described by Kolthoff and Sandell³⁷ was used to determine the composition of these chelates. A 20-50 milligram sample, accurately weighed, was dissolved in 25 milliliters of 2N hydrochloric acid. The volume was adjusted to 75 milliliters with the same

for Atomic Research, Ames, Iowa. The antihistamine was used
was reagent grade from R. K. Laboratories, Jamaica, New York,
and was recrystallized twice from absolute ethanol.

2. 2-Methyl-3-hydroxyphenylamine--The synthesis of

this series was accomplished by making a solution of three
tenths gram of the pure earth chloride in fifty milliliters
of ethanol, mixing with a solution containing five tenths gram
of 2-methyl-3-hydroxyphenylamine in 50 ml. of ethanol and adding
piperidine dropwise until a pH of 8 was reached. The resulting
mixture was digested for fifteen minutes at 70-80°C and filtered
while hot through a fitted glass funnel. The compound was
dried in vacuo at 150°C.

The piperidine and 2-methyl-3-hydroxyphenylamine were
obtained from R. K. Laboratories, Jamaica, New York. The
piperidine was fractionally distilled and the reaction boiling
at 90-91°C was used, and the 2-methyl-3-hydroxyphenylamine was
recrystallized from ethanol until a mother liquor melting
point of 74°C was obtained.

B. Methods of Analysis

1. Analysis of the 3-hydroxyphenylamine--A quantitative
bromination of 3-hydroxyphenylamine in acid medium, as described
by Kolthoff and Sandell¹⁷ was used to determine the concen-
tration of these esters. A 20-50 milligram sample, accurately
weighed, was dissolved in 25 milliliters of 0.1N hydrochloric
acid. The volume was adjusted to 75 milliliters with the same

acid. One gram of potassium bromide, and 5-10 drops of a 0.1% solution of the sodium salt of methyl red was added to the solution. This solution was titrated with standard potassium bromate to the color change from red to yellow. The excess potassium bromate was determined by adding one gram of potassium iodide, allowing the solution to stand for two minutes, and titrating the liberated iodine with sodium thiosulfate to a starch end-point.

2. Analysis of the Anthranilates.--A modified procedure used for the analysis of the 8-hydroxyquinolates was utilized for the analysis of the anthranilates. A 30-50 milligram sample, accurately weighed, was dissolved in 6N hydrochloric acid. The volume was adjusted to 75 milliliters with the same acid. The titration was done with standard mixture of potassium bromate and potassium bromide. Methyl red was used as an indicator for the first end-point. The excess potassium bromate was determined in the presence of excess potassium iodide followed by titration with sodium thiosulfate to a starch end-point.

3. Analysis of the 2-methyl-8-hydroxyquinolates.--The analysis of this series was done by the analytical section of the Los Alamos Scientific Laboratories. The percentage of rare earth in the compounds was determined by ignition of the sample to the metal oxide.

Samples of the other series of chelates were selected

acid. One gram of potassium permanganate and 0.1 g. of
0.1% solution of the sodium salt of potassium permanganate
the solution. This solution was filtered with a fine filter
excess potassium permanganate was determined by adding the same
potassium iodide, allowing the solution to stand for 10 minutes
in water, and titrating the liberated iodine with a 0.1%
solution of a starch end-point.

2. Analysis of the 2-hydroxy-3-methyl-2-butenoic acid
used for the synthesis of the 2-hydroxy-3-methyl-2-butenoic acid
for the synthesis of the 2-hydroxy-3-methyl-2-butenoic acid.
A 0.5 g. sample, accurately weighed, was dissolved in 10 ml. of water
acid. The volume was adjusted to 10 ml. with water.
same acid. The titration was done with a 0.1% solution of
potassium permanganate and potassium iodide. The end-point was
as an indicator for the first end-point. The second end-point
bromate was determined in the presence of a 0.1% solution of
iodine followed by titration with sodium thiosulfate to a
starch end-point.

3. Analysis of the 2-hydroxy-3-methyl-2-butenoic acid
analysis of this series was done by the analytical method of
the Los Alamos Scientific Laboratory. The potassium
rare earth in the compounds was determined by titration with
sample to the metal oxide.

Examples of the other members of the series are as follows:

at random for analysis by the Los Alamos Scientific Laboratories. These independent analyses served as a check on the analytical scheme used for a particular series. The analytical results are shown in Tables 1, 2, and 3. No melting points are reported because all the chelates in this study decompose before melting.

C. Spectroscopic Measurements

1. Absorption Spectra.--The absorption spectra were all taken at 20°C in absolute ethanol using the Cary Model 14 automatic recording spectrophotometer. The insolubility of the 8-hydroxyquinolates and the 2-methyl-8-hydroxyquinolates, accompanied by their dissociation and decomposition in ethanolic solutions, made it extremely difficult to obtain accurate molar extinction coefficients. The anthranilates appeared to obey Beer's law, but all of the other series of chelates reported here did not obey Beer's law. The molar extinction coefficients were also found to be time dependent. The variations of molar extinction coefficients with concentration and time are attributed to decomposition and dissociation of the complexes in ethanolic solutions. Precautions were taken to minimize these effects by using freshly prepared solutions at all times. The 8-hydroxyquinolates and the 2-methyl-8-hydroxyquinolates, however, had to be heated to accomplish solution.

TABLE 1

ANALYSIS REPORTS OF 2-METHYL-8-HYDROXYQUINOLATE
RARE EARTH CHELATES

Compound	% Metal Found	% Metal Theoretical
La(2 Me ₈ HQ) ₃	22.1	22.7
Eu(2 Me ₈ HQ) ₃	24.6	24.2
Gd(2 Me ₈ HQ) ₃	24.2	24.6
Tb(2 Me ₈ HQ) ₃	25.4	25.0
Dy(2 Me ₈ HQ) ₃	25.1	25.5
Tm(2 Me ₈ HQ) ₃	25.9	25.9
Yb(2 Me ₈ HQ) ₃	27.2	26.8
Lu(2 Me ₈ HQ) ₃	26.6	27.0

2 Me₈HQ = 2 methyl-8-hydroxyquinolate ion

CONFIDENTIAL

SECRET

UNITED STATES DEPARTMENT OF THE ARMY
OFFICE OF THE CHIEF OF STAFF

COMMEMORATIVE OF THE ARMY
OFFICE OF THE CHIEF OF STAFF

IN (S. 1000)
IN (S. 1000)
IN (S. 1000)
IN (S. 1000)
IN (S. 1000)
IN (S. 1000)
IN (S. 1000)
IN (S. 1000)

IN (S. 1000) IN (S. 1000) IN (S. 1000)

CONFIDENTIAL

TABLE 2

ANALYSIS REPORTS OF 8-HYDROXYQUINOLATE RARE EARTH CHELATES

Compound	% 8HQ		% Metal	
	Found	Theoretical	Found	Theoretical
$\text{La}(\text{8HQ})_3 \cdot \text{H}_2\text{O}$	72.7	73.4		
$\text{Pr}(\text{8HQ})_3 \cdot \text{H}_2\text{O}$	72.5	73.1		
$\text{Nd}(\text{8HQ})_3 \cdot \text{H}_2\text{O}$	72.3	72.7		
$\text{Sm}(\text{8HQ})_3 \cdot \text{H}_2\text{O}$	71.2	71.9		
$\text{Eu}(\text{8HQ})_3 \cdot \text{H}_2\text{O}$	70.8	71.8		
$\text{Gd}(\text{8HQ})_3$	73.2	73.4		
$\text{Tb}(\text{8HQ})_3$	72.7	73.1	25.8	26.8
$\text{Dy}(\text{8HQ})_3$	73.3	72.7	26.4	27.4
$\text{Ho}(\text{8HQ})_3$	74.3	72.4	26.9	27.6
$\text{Er}(\text{8HQ})_3$	72.8	72.3	26.7	27.9
$\text{Tm}(\text{8HQ})_3$	72.6	71.9	27.0	28.0
$\text{Yb}(\text{8HQ})_3$	73.2	71.4	27.8	28.6
$\text{Lu}(\text{8HQ})_3$	--	--	29.2	28.8

8HQ = 8-hydroxyquinolate ion

TABLE 3
ANALYSIS REPORTS FOR THE RARE EARTH ANTHRANILATES

Compound	% AnAc		% Metal	
	Found	Theoretical	Found	Theoretical
La (AnAc) ₃	76.3	74.7		
Pr (AnAc) ₃	69.5	72.0	26.1	25.8
Nd (AnAc) ₃	71.6	72.3	26.9	26.1
Sm (AnAc) ₃	70.2	70.7	26.8	27.1
Eu (AnAc) ₃	71.5	72.9		
Gd (AnAc) ₃	75.0	72.6	26.3	27.8
Tb (AnAc) ₃	71.6	71.9	28.7	28.2
Dy (AnAc) ₃	70.2	70.5	28.1	28.4
Ho (AnAc) ₃	70.5	71.5	30.7	28.7
Er (AnAc) ₃	69.0	70.8		
Tm (AnAc) ₃	70.2	70.7		
Yb (AnAc) ₃	69.7	70.0		
Lu (AnAc) ₃			30.4	30.0

AnAc = Anthranilate ion

UNITED STATES DEPARTMENT OF THE INTERIOR
BUREAU OF LAND MANAGEMENT
WASHINGTON, D. C. 20250

CONTRACT NO.		DATE
1	100-100000	10/1/50
2	100-100000	10/1/50
3	100-100000	10/1/50
4	100-100000	10/1/50
5	100-100000	10/1/50
6	100-100000	10/1/50
7	100-100000	10/1/50
8	100-100000	10/1/50
9	100-100000	10/1/50
10	100-100000	10/1/50
11	100-100000	10/1/50
12	100-100000	10/1/50
13	100-100000	10/1/50
14	100-100000	10/1/50
15	100-100000	10/1/50
16	100-100000	10/1/50
17	100-100000	10/1/50
18	100-100000	10/1/50
19	100-100000	10/1/50
20	100-100000	10/1/50
21	100-100000	10/1/50
22	100-100000	10/1/50
23	100-100000	10/1/50
24	100-100000	10/1/50
25	100-100000	10/1/50
26	100-100000	10/1/50
27	100-100000	10/1/50
28	100-100000	10/1/50
29	100-100000	10/1/50
30	100-100000	10/1/50
31	100-100000	10/1/50
32	100-100000	10/1/50
33	100-100000	10/1/50
34	100-100000	10/1/50
35	100-100000	10/1/50
36	100-100000	10/1/50
37	100-100000	10/1/50
38	100-100000	10/1/50
39	100-100000	10/1/50
40	100-100000	10/1/50
41	100-100000	10/1/50
42	100-100000	10/1/50
43	100-100000	10/1/50
44	100-100000	10/1/50
45	100-100000	10/1/50
46	100-100000	10/1/50
47	100-100000	10/1/50
48	100-100000	10/1/50
49	100-100000	10/1/50
50	100-100000	10/1/50
51	100-100000	10/1/50
52	100-100000	10/1/50
53	100-100000	10/1/50
54	100-100000	10/1/50
55	100-100000	10/1/50
56	100-100000	10/1/50
57	100-100000	10/1/50
58	100-100000	10/1/50
59	100-100000	10/1/50
60	100-100000	10/1/50
61	100-100000	10/1/50
62	100-100000	10/1/50
63	100-100000	10/1/50
64	100-100000	10/1/50
65	100-100000	10/1/50
66	100-100000	10/1/50
67	100-100000	10/1/50
68	100-100000	10/1/50
69	100-100000	10/1/50
70	100-100000	10/1/50
71	100-100000	10/1/50
72	100-100000	10/1/50
73	100-100000	10/1/50
74	100-100000	10/1/50
75	100-100000	10/1/50
76	100-100000	10/1/50
77	100-100000	10/1/50
78	100-100000	10/1/50
79	100-100000	10/1/50
80	100-100000	10/1/50
81	100-100000	10/1/50
82	100-100000	10/1/50
83	100-100000	10/1/50
84	100-100000	10/1/50
85	100-100000	10/1/50
86	100-100000	10/1/50
87	100-100000	10/1/50
88	100-100000	10/1/50
89	100-100000	10/1/50
90	100-100000	10/1/50
91	100-100000	10/1/50
92	100-100000	10/1/50
93	100-100000	10/1/50
94	100-100000	10/1/50
95	100-100000	10/1/50
96	100-100000	10/1/50
97	100-100000	10/1/50
98	100-100000	10/1/50
99	100-100000	10/1/50
100	100-100000	10/1/50

APPROVED AND FORWARDED:
Special Agent in Charge

UNITED STATES DEPARTMENT OF THE INTERIOR
BUREAU OF LAND MANAGEMENT
WASHINGTON, D. C. 20250

2. Emission Spectra.--The luminescence studies were done in 5:5:2 (parts by volume) mixtures of ethyl ether, 3-methyl pentane, and absolute ethanol, which were frozen in a liquid nitrogen bath to form transparent rigid glass solutions, approximately $10^{-5}M$ in concentration of complex. The absolute ethanol, USI, reagent quality, was purified by distilling over magnesium ethoxide using a six foot column. The ethyl ether used was Mallinckrodt anhydrous ethyl ether, analytical reagent. The ether was used without further purification because it exhibited no emission when excited in the near ultraviolet region. The 3-methylpentane, Phillips pure grade was purified by pouring it through a baked silica gel column.

The molecular band emissions were recorded on Eastman 103a-F spectroscopic plates using a 3 prism Steinheil Universal GH spectrograph equipped with glass optics, and a 195/255 millimeter combination of collimator and objective lenses. The settings used for proper focus in the region of 4500-6000 Å were determined by Mrs. R. E. Whan.³⁸ The settings which were recommended by the manufacturer for proper focus in the 3800-5000 Å region were used.

The excitation of the chelate samples in rigid media by near ultraviolet light was done by means of a General Electric AH6, water cooled mercury lamp. Corning glass filters combined with solutions having appropriate transmission in the

desired region were used. The filters were placed in a light tight box as described in Figure 1. The total emission was photographed using this apparatus.

The filtering systems were selected on the basis of two main requirements, (i) maximum band pass being in the region of the near ultraviolet absorption band of the chelate, (ii) minimum of exciting light overlapping the luminescence of the chelate samples. The filters used are tabulated in Table 4.

TABLE 4

Chelate	Filters	Band Pass (Approx.)
$M(8HQ)_3$ (a)	$\begin{cases} 5840^{(b)} \\ 5840, CuSO_4 \cdot 5H_2O \end{cases}$	3000 - 4100 A
$M(2 Me8HQ)_3$	$\begin{cases} 5840 \\ 5840, CuSO_4 \cdot 5H_2O^{(c)} \end{cases}$	3000 - 4100 A
$M(AnAc)_3$	$\begin{cases} 9863 \\ 5840, KCr(SO_4)_2 \cdot 12H_2O^{(d)} \end{cases}$	3000 - 3900 A
$M(SA)_3$	$\begin{cases} 5840 \\ 5840, KCr(SO_4)_2 \cdot 12H_2O \\ 3389, CuSO_4 \cdot 5H_2O \end{cases}$	3000 - 3900 A 4000 - 6000 A

(a) See Tables 1-4 for formula abbreviations

(b) Corning filter code number--standard thickness

(c) 100g/l water, in a 5 cm. optical path

(d) 30g/l water, in a 5 cm. optical path

FIGURE 1

TOTAL EMISSION FILTER BOX

- A and C. 4 inch focal length quartz lens
- B. 5 centimeter cell with quartz windows
- D. Corning glass filter
- E. Front surface mirror
- F. Optical quartz Dewar flask, partially silvered
- G. AH6 lamp housing

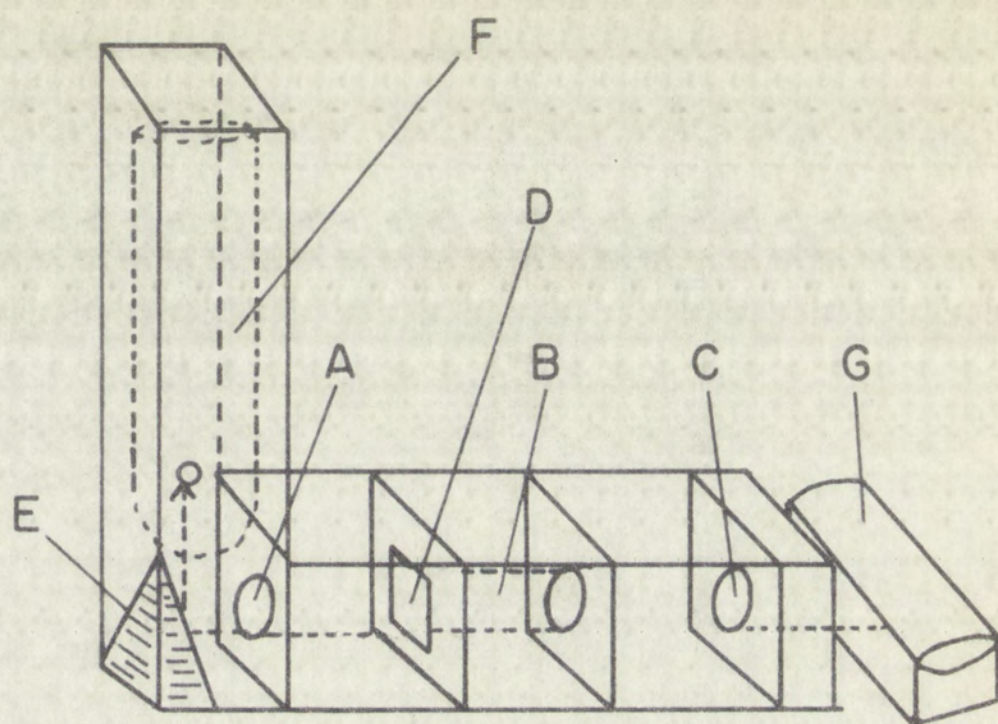
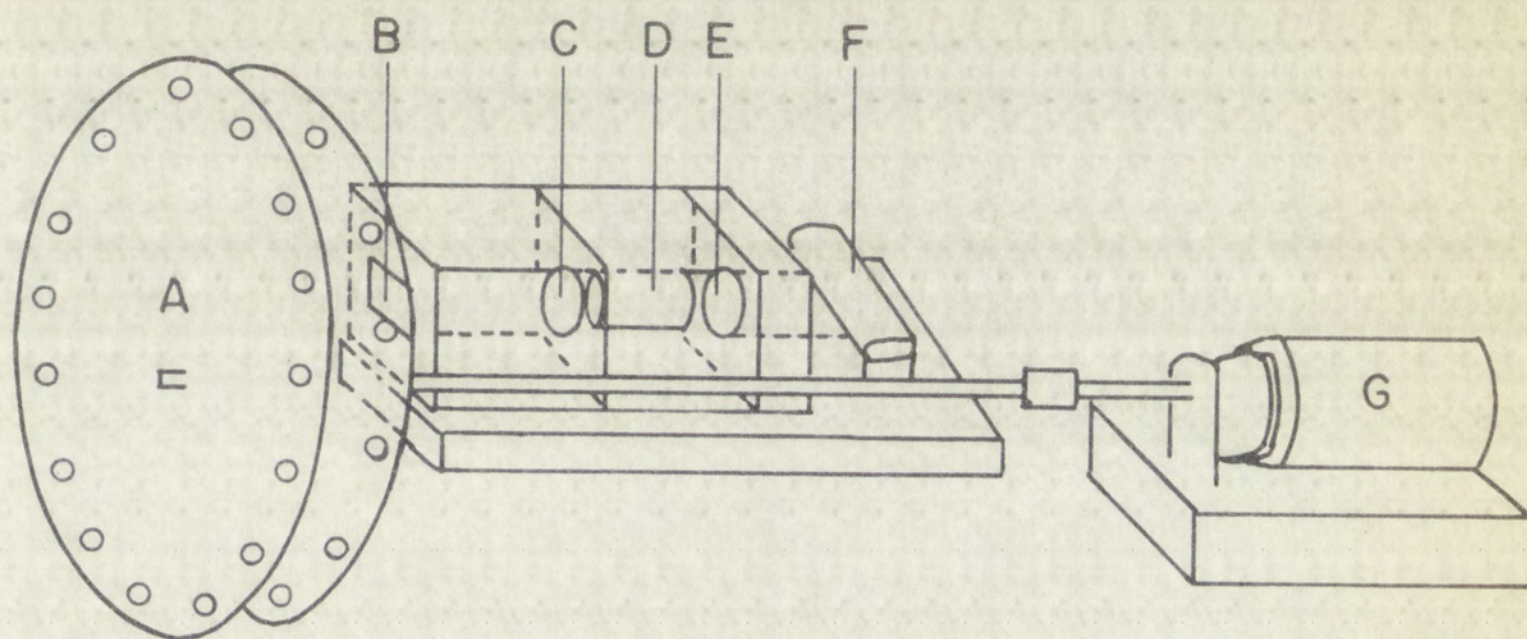
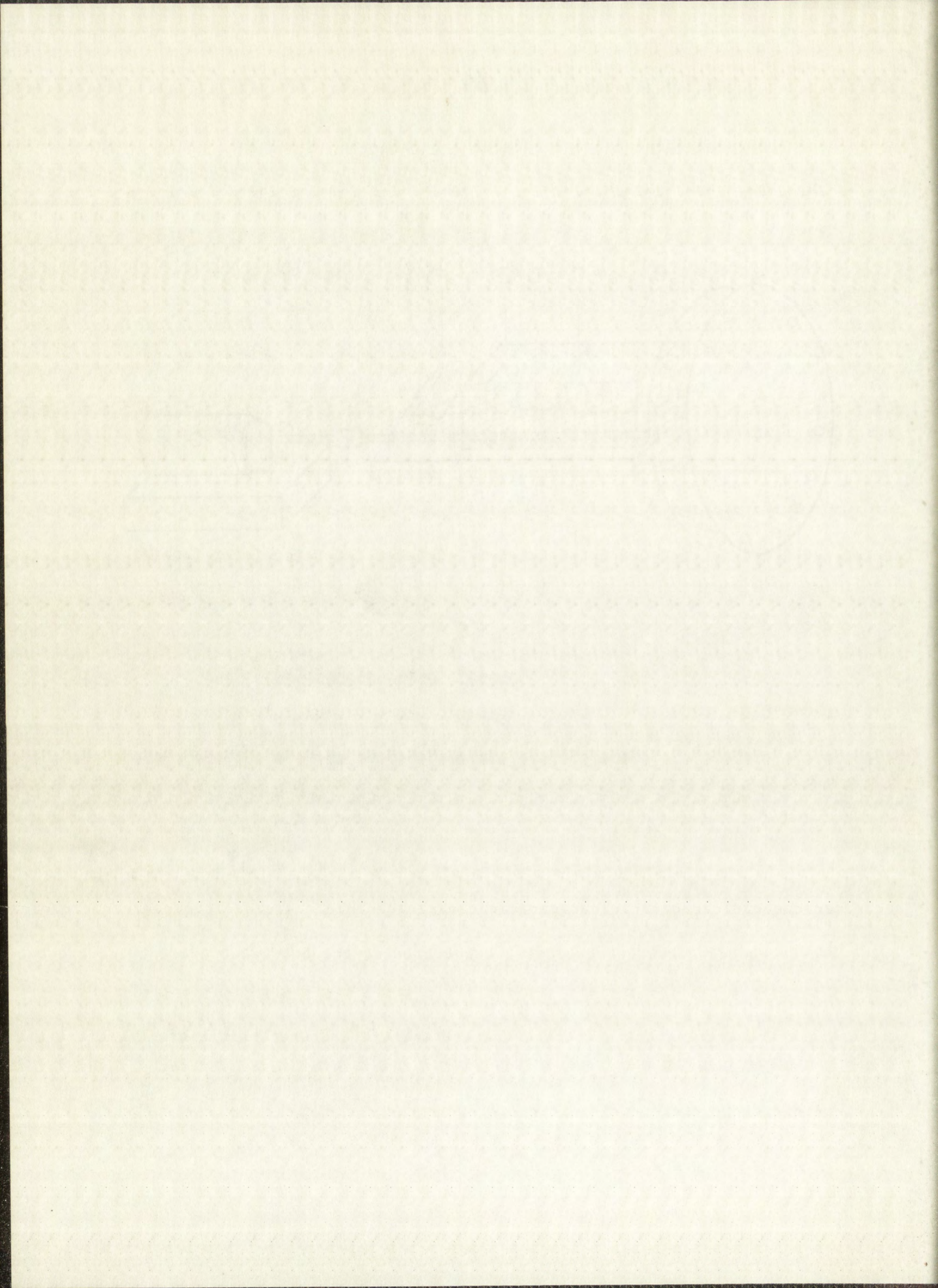


FIGURE 2

PHOSPHOROSCOPE SCHEMATIC DIAGRAM

- A. Phosphoroscope discs
- B. Corning glass filter
- C and E. 4 inch focal length quartz lens
- D. 5 cm. cell for solution filters with quartz windows
- F. Light source
- G. Motor





Better dispersion than was available with the camera lens combination 195/255 millimeter (45A/mm at 5000A) of the spectrograph was required for photographing characteristic line emission of the rare earth ions. A 650 millimeter lens, the collimator, and a 640 millimeter lens, the objective, with proper extensions for the camera gave a dispersion of 17A/mm at 5000A. The line emitters were all photographed using these optics for the spectrograph. Slit widths of 10-100 microns and exposure times, varying from a few seconds to four hours, were used to obtain well exposed lines on the spectroscopic plates. Argon and neon discharge tubes were used for calibration in both the line and molecular band emissions.

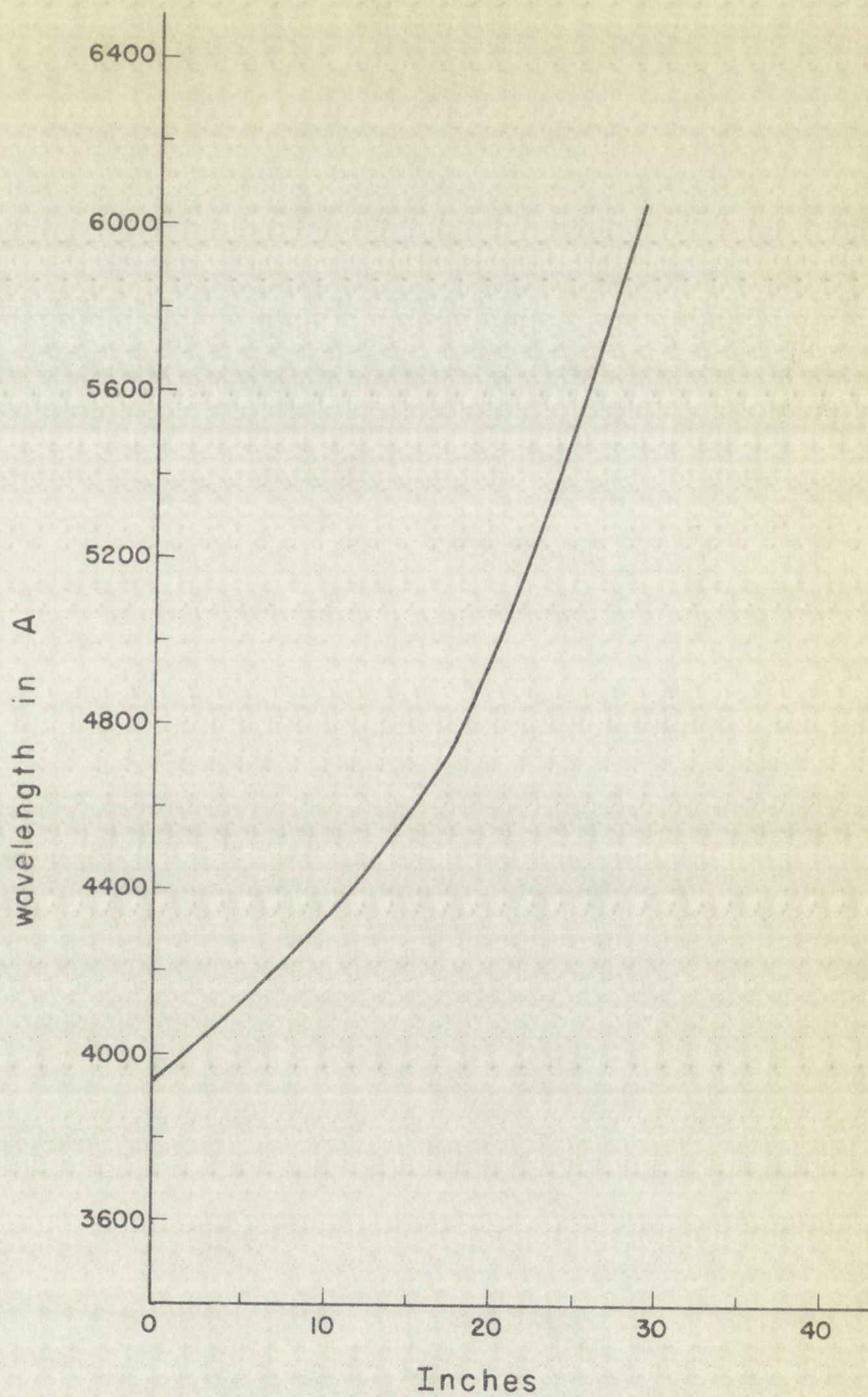
In order to photograph the lines characteristic of the ytterbium ion, Eastman IM, ammonia hypersensitized spectroscopic plates were used. The sensitivity of the IM plates was increased in the near infrared region by treatment with dilute ammonia and ethanol at 4°C as recommended by the manufacturer.

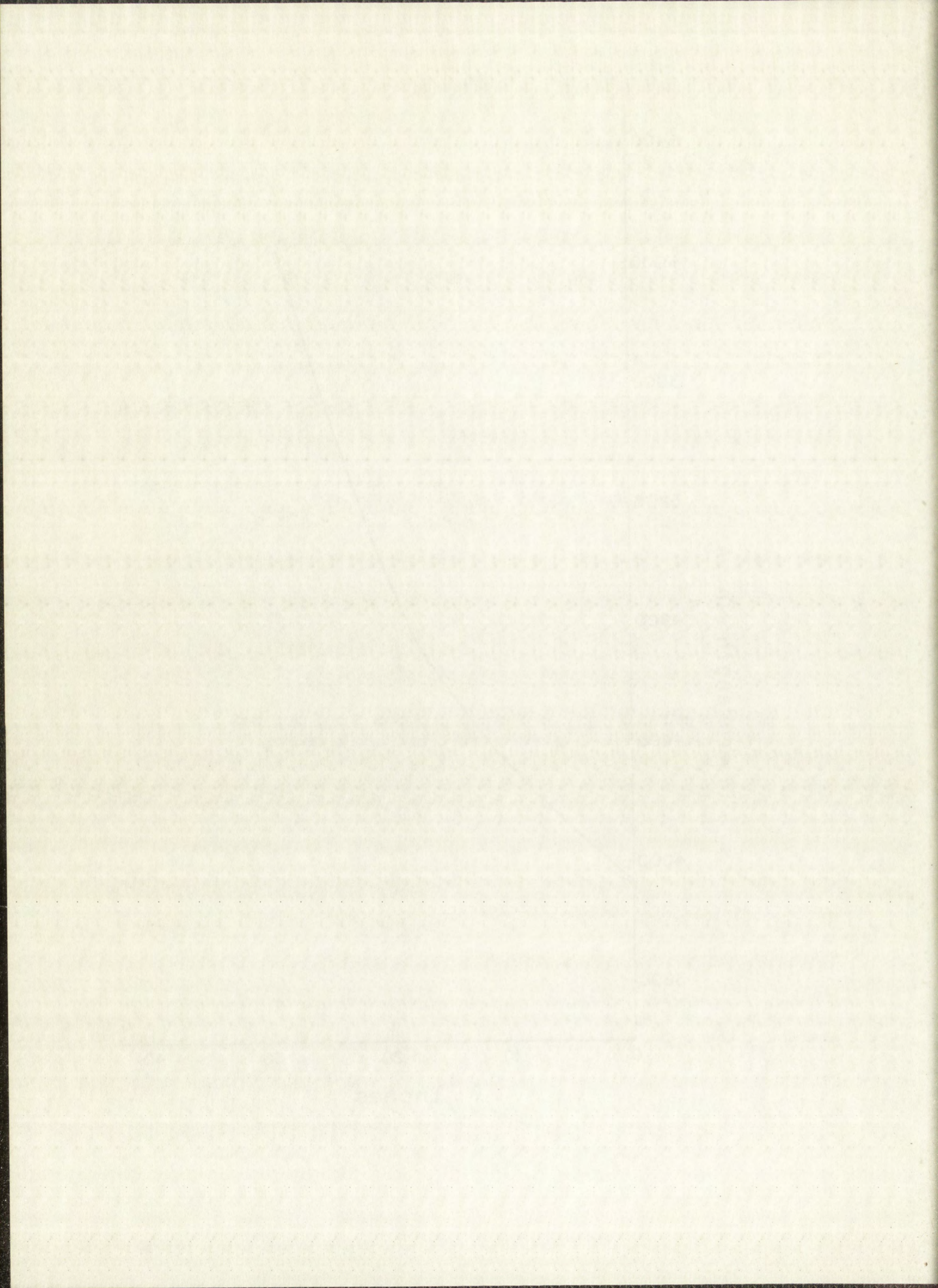
Densitometer traces were obtained using a Jarrall Ash automatic recording microdensitometer. Wavelength measurements of the molecular band emissions were carried out with the aid of a dispersion curve obtained from argon and neon calibrations. (See Figure 3.) Assignment of wavelengths to the calibration lines was done by comparison of their observed relative intensities to those recorded in the literature.³⁹

FIGURE 3

DISPERSION CURVE (Short Optics)

Camera lens combination 195/255 millimeters on
3 prism Steinheil Universal G-H Spectrograph





D. Relative Quantum Yields

1. Photographic Technique.--The total emission (fluorescence and phosphorescence) for the entire anthranilate rare earth series was photographed using well controlled experimental conditions. Two Corning 9863 and one Corning 5840 filters with a chrome alum solution filter were used in the total emission apparatus shown in Figure 1 for photographing the luminescence of the anthranilate rare earth series. External fogging of the optical Dewar flask was prevented by passing nitrogen gas over the outside of the flask. The exposure times were different because of the variation in brightness of the individual chelates studied. The concentrations were nearly the same for all samples used. (The data are contained in Table 12 in the Results Section.)

2. Mathematical Analysis.--Appendix I describes the mathematical technique which was used for the evaluation of the integrated fluorescence and phosphorescence intensities from the photographic plates. Values for the integrated optical densities on the plate were required for the evaluation of the integrated intensities. The contour of the phosphorescence emission along with the peak maxima and spectral range was determined from densitometer traces of the phosphorescence alone. The overlap of the fluorescence and phosphorescence emission made it necessary to graphically resolve the two emissions. The phosphorescence emission resulted in a

1. The following conditions were maintained (approximate):

Relative humidity (approximate) 70-80%
Temperature (approximate) 25-30°C
Light intensity (approximate) 100-200 lux
Air flow (approximate) 0.5-1.0 m/s
The humidity was maintained by the use of a saturated salt solution in a closed container. The temperature was maintained by the use of a water bath. The light intensity was maintained by the use of a tungsten lamp. The air flow was maintained by the use of a fan. The relative humidity was measured by the use of a hygrometer. The temperature was measured by the use of a thermometer. The light intensity was measured by the use of a light meter. The air flow was measured by the use of an anemometer.

2. The following conditions were maintained (approximate):

Relative humidity (approximate) 70-80%
Temperature (approximate) 25-30°C
Light intensity (approximate) 100-200 lux
Air flow (approximate) 0.5-1.0 m/s
The humidity was maintained by the use of a saturated salt solution in a closed container. The temperature was maintained by the use of a water bath. The light intensity was maintained by the use of a tungsten lamp. The air flow was maintained by the use of a fan. The relative humidity was measured by the use of a hygrometer. The temperature was measured by the use of a thermometer. The light intensity was measured by the use of a light meter. The air flow was measured by the use of an anemometer.

curve that was close to a Gaussian distribution. A knowledge of the spectral range and peak maximum was the basis used for sketching in the phosphorescence emission on a densitometer trace of the total emission. The fluorescence spectrum was then determined by subtraction of the phosphorescence spectrum from the total emission spectrum. The densitometer traces of the entire series with the exception of gadolinium anthranilate show no resolution of the phosphorescence and fluorescence. The intensities of the phosphorescence and fluorescence for gadolinium anthranilate are different enough in magnitude so that resolution of the fluorescence and phosphorescence is possible in this case.

drive the car into the garage
of the property. The car was
sketching in the driveway and
there is no indication of a
then returned to the garage and
from this the car was driven
of the car was in the garage
while the car was in the garage
cense. The car was in the garage
cense for the car was in the garage
magnitude as the car was in the garage
possession as the car was in the garage

CHAPTER II

RESULTS

A. Spectroscopic Measurements of 8-Hydroxyquinolates, 2-Methyl- 8-Hydroxyquinolates and Anthranilates

1. Absorption.--The absorption coefficients for the anthranilates are considered to be the most accurate of all the compounds studied. Dissolution of the chelate samples in absolute ethanol was accomplished easily without heat. Dilution experiments indicate that Beer's law is obeyed by the entire anthranilate series. Errors in dilution and weighing are estimated to be $\pm 4\%$.

Typical absorption spectra are shown in Figures 4 and 5. Only typical spectra are shown because all the anthranilates have absorption spectra that are very nearly the same. The absorption coefficients at the band maxima are reported in Table 5.

Difficulties were encountered in measuring the absorption spectra of the 8-hydroxyquinolates and the 2-methyl-8-hydroxyquinolates because of their insolubility and the fact that they undergo dissociation, decomposition and photolysis under irradiation by ultraviolet light in solution. Absorption spectra were always taken on freshly prepared

solutions but the error in the absorption coefficients for these two series is estimated to be $\pm 6\%$.

Typical absorption spectra are shown in Figures 6 through 9 and the absorption coefficients at the peak maxima are reported in Tables 6 and 7. Absorption spectra for gadolinium chelates only are shown because the other members of the series have similar spectral features but the absorption coefficients vary somewhat in magnitude.

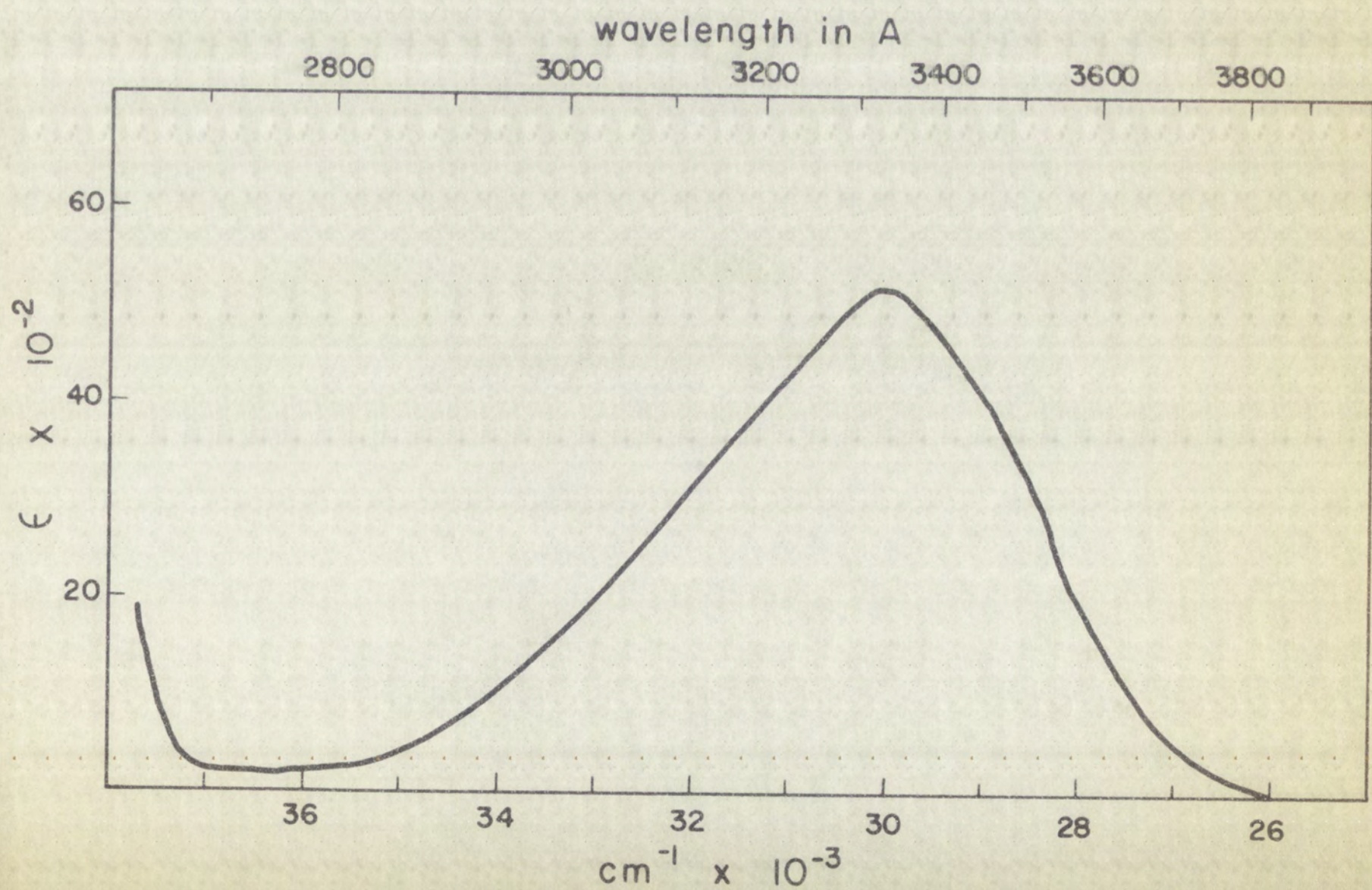
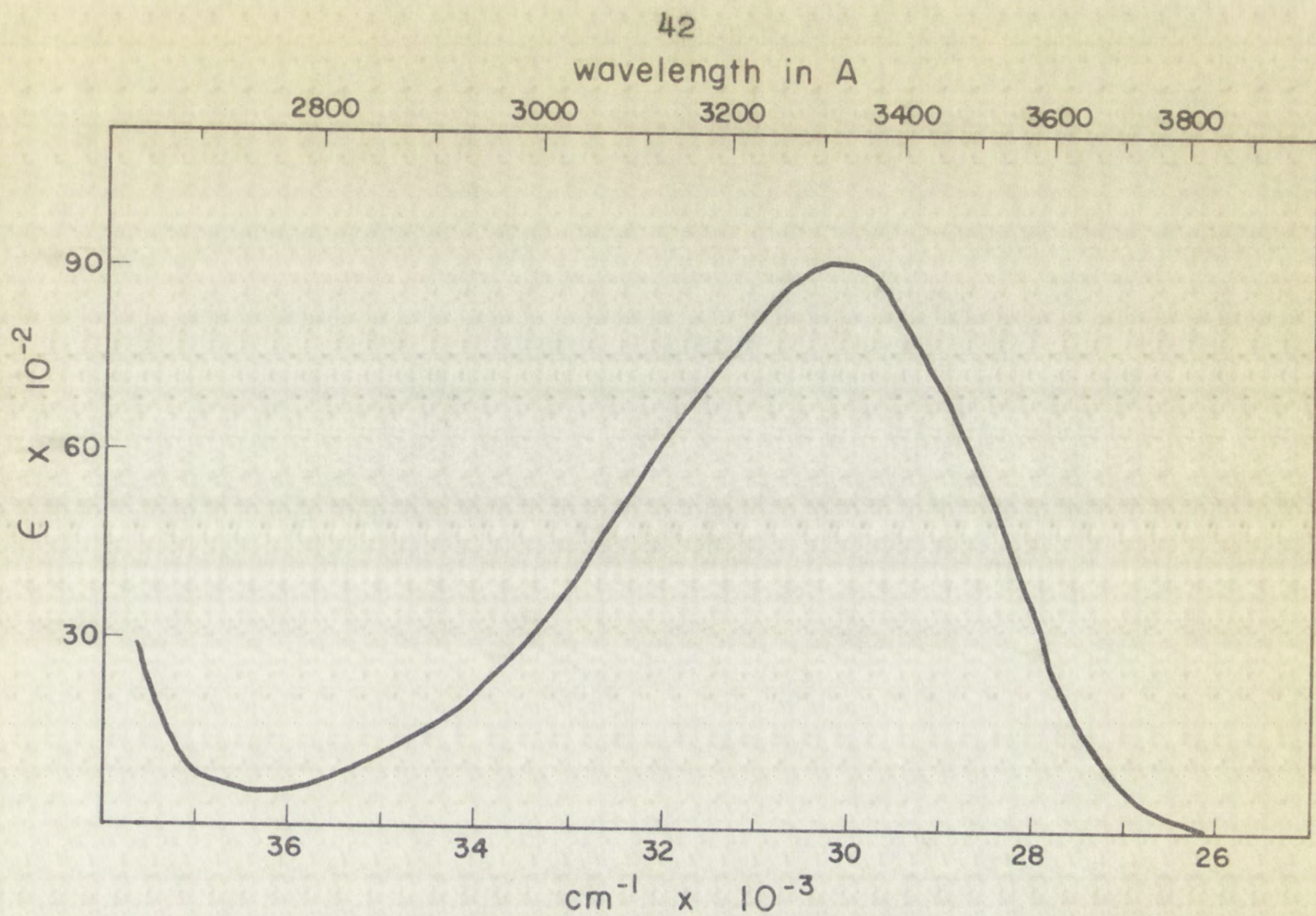
2. Emission.--The emission spectra are classified into categories in Table 8. The basis of the classification is the existence or nonexistence of line emission from the metal ion. The classification includes both phosphorescence and fluorescence emission. The data indicate that the majority of chelates studied exhibited band emission only.

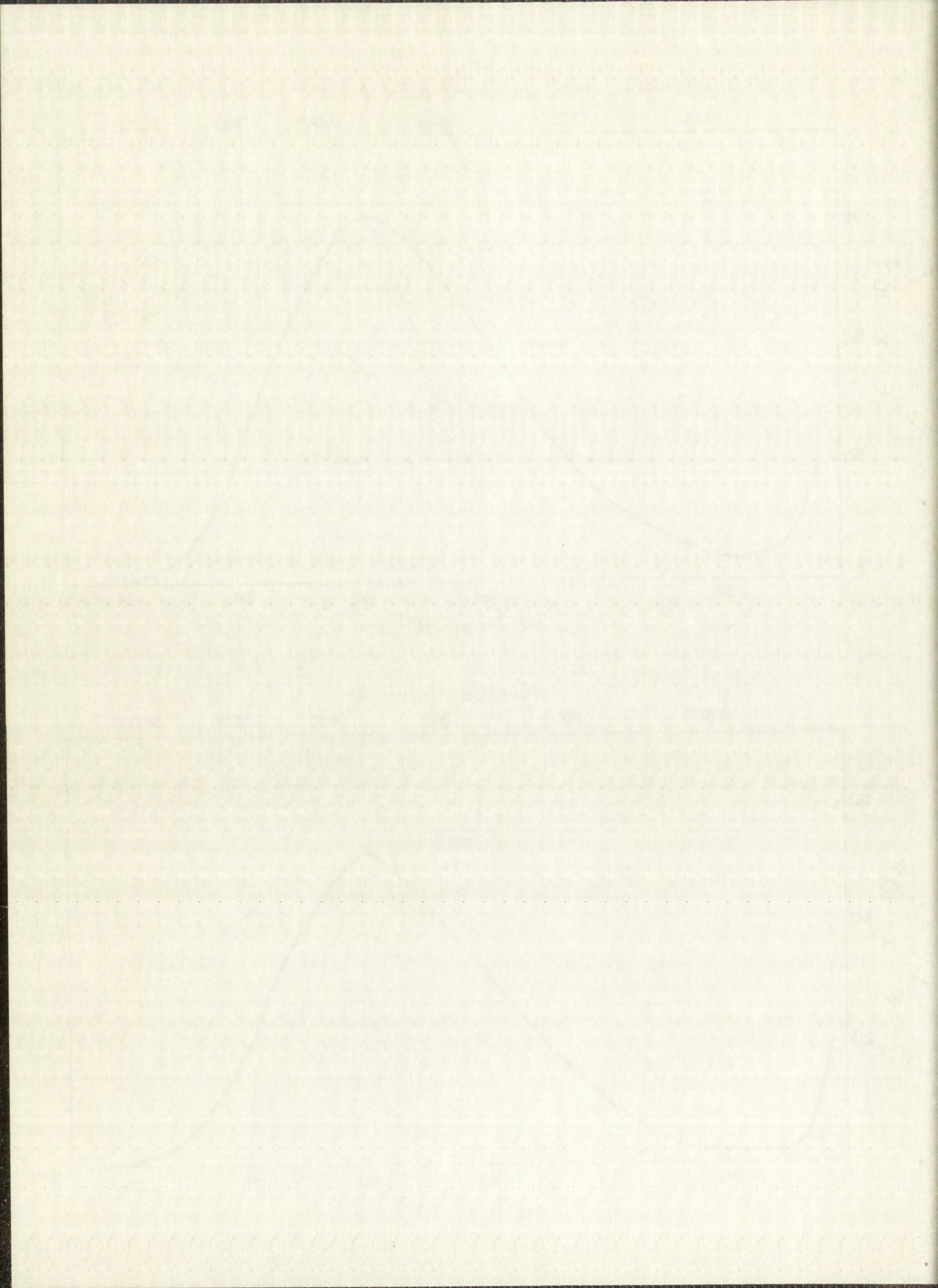
FIGURE 4

$\text{Gd}(\text{AnAc})_3$ $1.59 \times 10^{-5} \text{M}$ Abs. Eth.

FIGURE 5

AnAc $5.45 \times 10^{-5} \text{M}$ Abs. Eth.





FORM 10

CLERK JAMES

1870

1870

1870

1870

1870

FIGURE 6

$Tm(8HQ)_3$ $1.41 \times 10^{-4} M$ in Abs. Eth.

FIGURE 7

8HQ $4.15 \times 10^{-5} M$ in Abs. Eth.

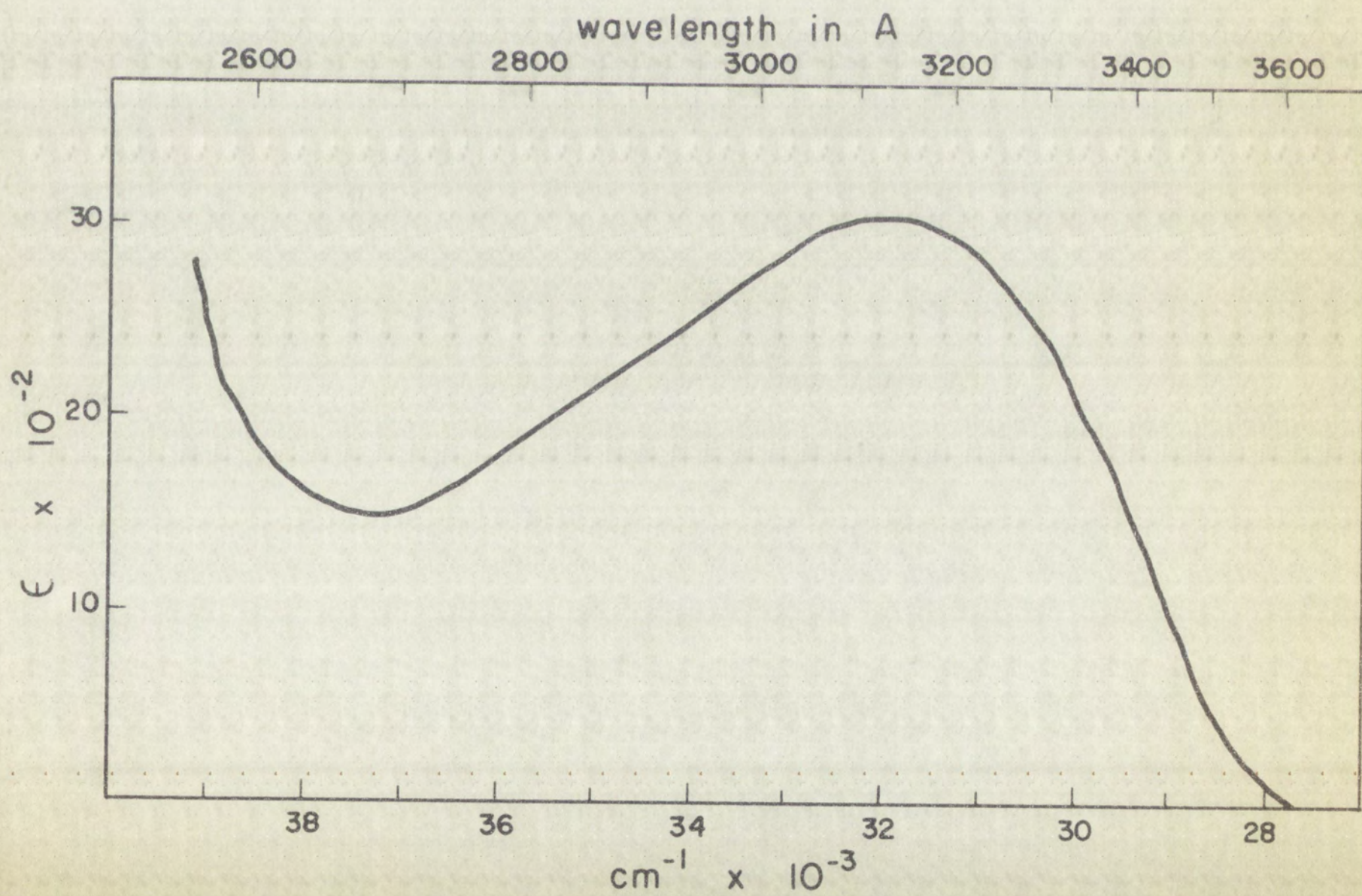
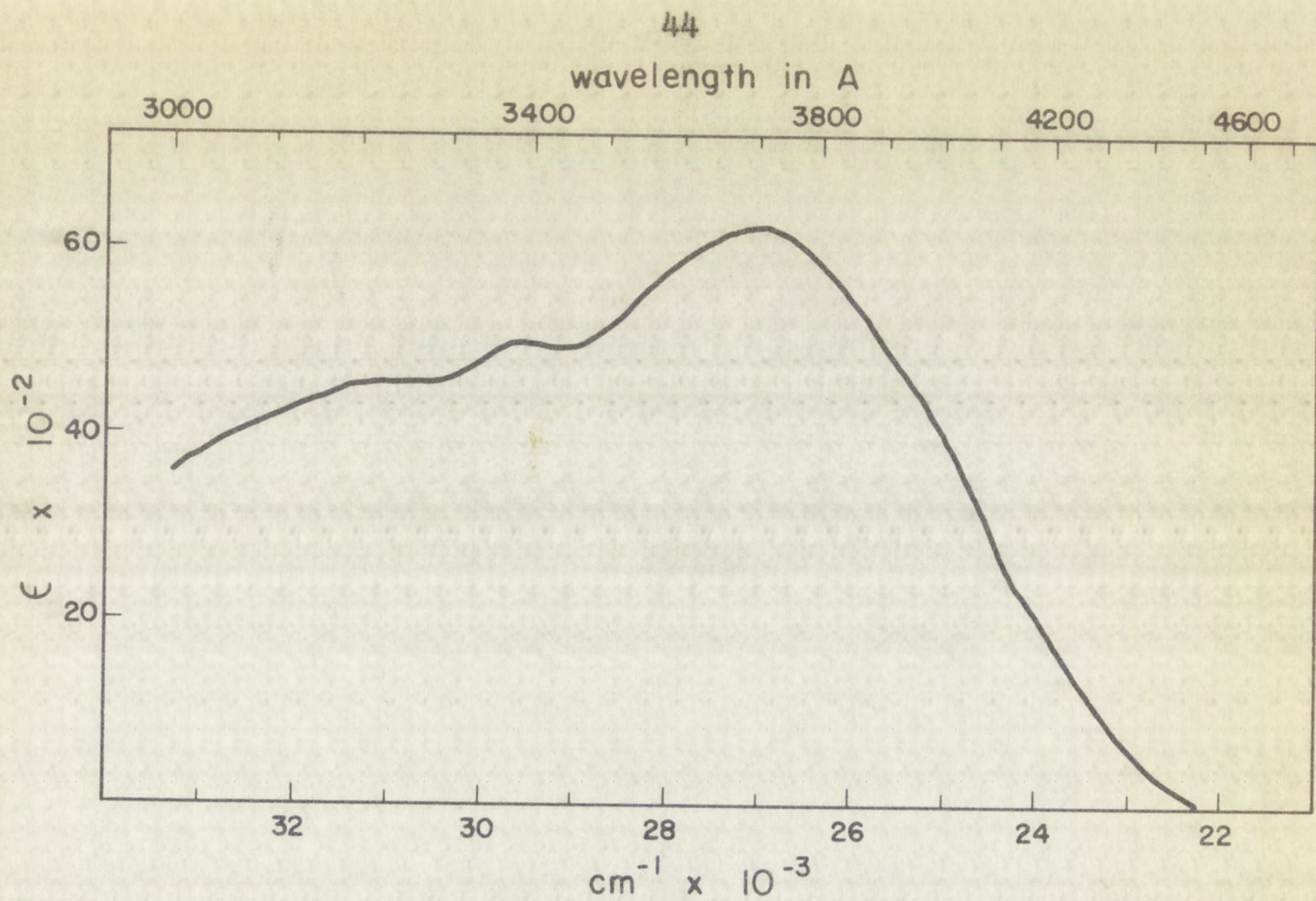


FIGURE 8

$\text{Gd}(\text{2 Me8HQ})_3$ $9.64 \times 10^{-4} \text{M}$ in Abs. Eth.

FIGURE 9

2-Me8HQ $4.82 \times 10^{-5} \text{M}$ in Abs. Eth.

46

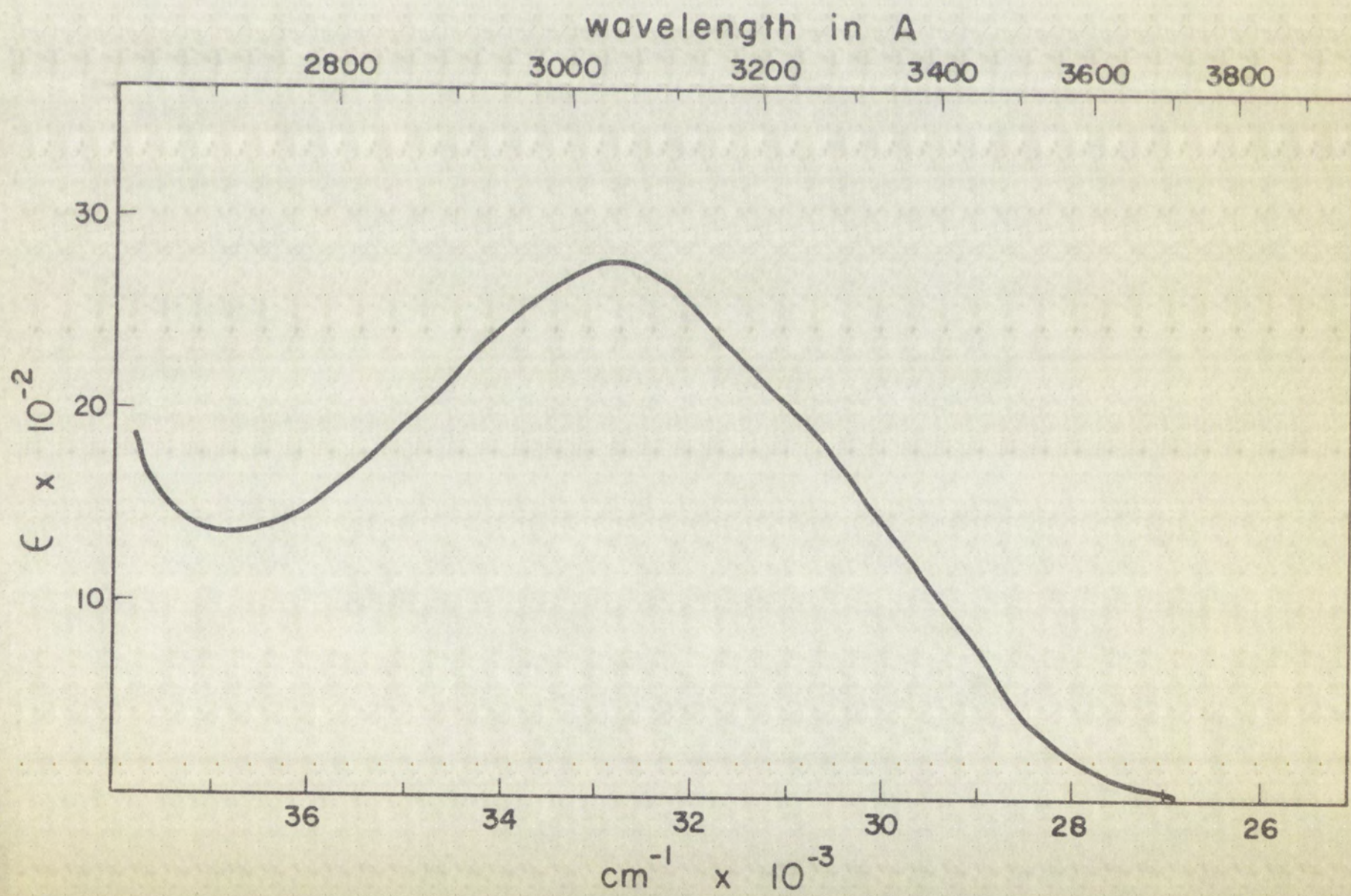
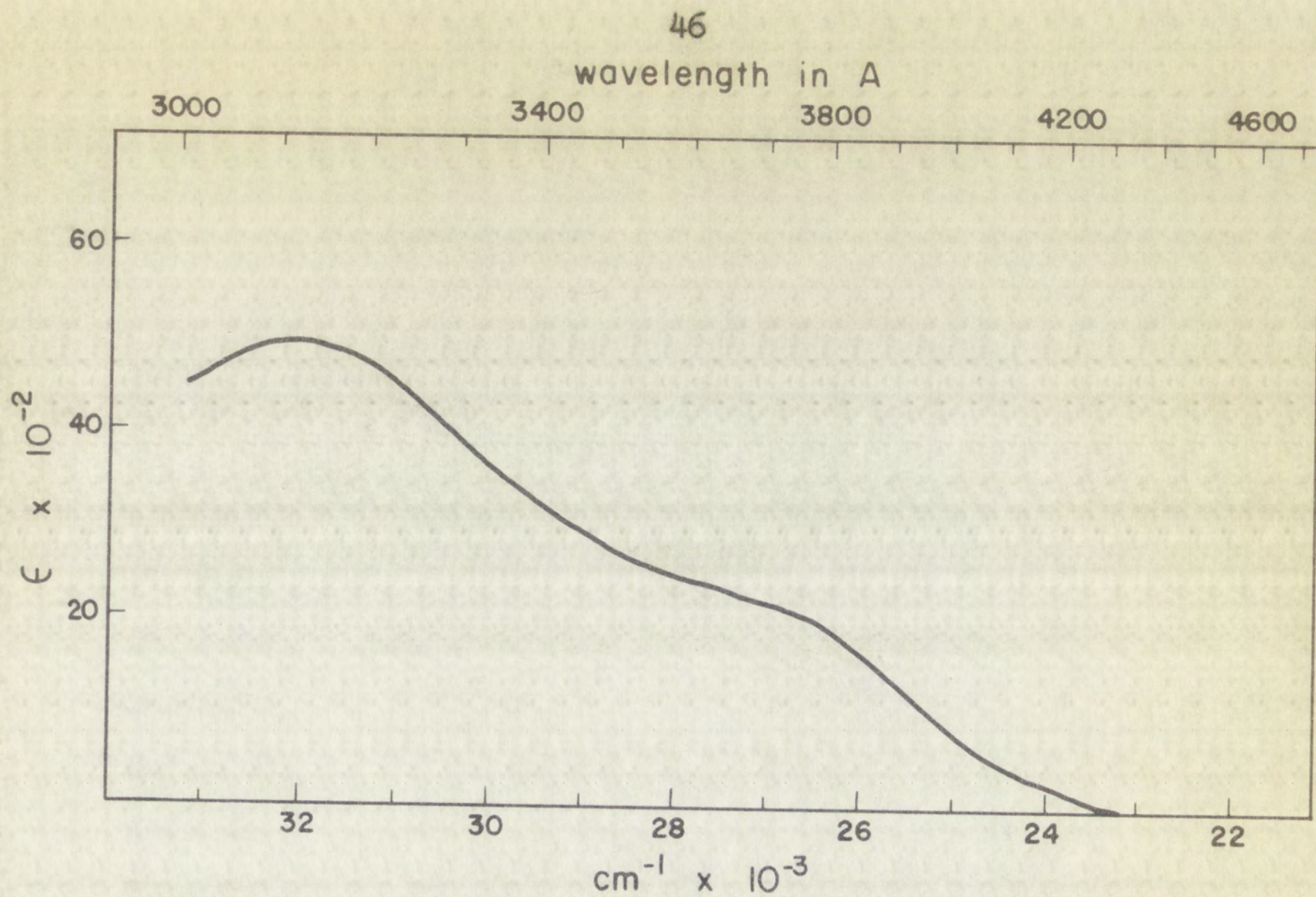


TABLE 5
MOLAR ABSORPTION COEFFICIENTS OF THE
RARE EARTH ANTHRANILATES

Compound	λ (a) ($\pm 20\text{\AA}$)	ϵ ($\pm 4\%$)	Concentration
La(AnAc) ₃	3,300	8,358	$1.35 \times 10^{-5} \text{M}$
Pr(AnAc) ₃	3,300	8,768	$1.38 \times 10^{-5} \text{M}$
Nd(AnAc) ₃	3,310	8,912	$1.12 \times 10^{-5} \text{M}$
Sm(AnAc) ₃	3,300	9,090	$1.32 \times 10^{-5} \text{M}$
Eu(AnAc) ₃	3,320	8,923	$1.36 \times 10^{-5} \text{M}$
Gd(AnAc) ₃	3,320	9,359	$1.59 \times 10^{-5} \text{M}$
Tb(AnAc) ₃	3,320	8,481	$1.53 \times 10^{-5} \text{M}$
Dy(AnAc) ₃	3,320	9,626	$1.44 \times 10^{-5} \text{M}$
Ho(AnAc) ₃	3,330	9,106	$1.78 \times 10^{-5} \text{M}$
Er(AnAc) ₃	3,330	13,309	$1.39 \times 10^{-5} \text{M}$
Tm(AnAc) ₃	3,320	9,044	$1.76 \times 10^{-5} \text{M}$
Yb(AnAc) ₃	3,320	9,388	$1.34 \times 10^{-5} \text{M}$
Lu(AnAc) ₃	3,320	12,014	$1.75 \times 10^{-5} \text{M}$
AnAc	3,350	5,321	$5.45 \times 10^{-5} \text{M}$

(a) 3350 \AA $\sim 29,850 \text{ cm}^{-1}$

3320 \AA $\sim 30,120 \text{ cm}^{-1}$

3300 \AA $\sim 30,300 \text{ cm}^{-1}$

Compound	2,4,6-trinitrophenol
1a (ArAc)	1.0000
1b (ArAc)	1.0000
1c (ArAc)	1.0000
1d (ArAc)	1.0000
1e (ArAc)	1.0000
1f (ArAc)	1.0000
1g (ArAc)	1.0000
1h (ArAc)	1.0000
1i (ArAc)	1.0000
1j (ArAc)	1.0000
1k (ArAc)	1.0000
1l (ArAc)	1.0000
1m (ArAc)	1.0000
1n (ArAc)	1.0000
1o (ArAc)	1.0000
1p (ArAc)	1.0000
1q (ArAc)	1.0000
1r (ArAc)	1.0000
1s (ArAc)	1.0000
1t (ArAc)	1.0000
1u (ArAc)	1.0000
1v (ArAc)	1.0000
1w (ArAc)	1.0000
1x (ArAc)	1.0000
1y (ArAc)	1.0000
1z (ArAc)	1.0000
ArAc	1.0000

(a) 2,4,6-trinitrophenol
 1.0000
 1.0000
 1.0000

TABLE 6

MOLAR ABSORPTION COEFFICIENTS OF THE
RARE EARTH 8-HYDROXYQUINOLATES

Compound	λ (a) \pm 20A	$\epsilon \pm 6\%$	λ (b) \pm 20A
La(8HQ) ₃	3,710	5,185	3,365
Pr(8HQ) ₃	3,710	5,215	3,360
Nd(8HQ) ₃	3,710	6,421	3,360
Sm(8HQ) ₃	3,705	6,121	3,370
Eu(8HQ) ₃	3,710	5,862	3,370
Gd(8HQ) ₃	3,710	5,373	3,365
Tb(8HQ) ₃	3,700	6,300	3,350
Dy(8HQ) ₃	3,710	6,251	3,360
Ho(8HQ) ₃	3,710	8,188	3,370
Er(8HQ) ₃	3,710	8,138	3,360
Tm(8HQ) ₃	3,700	6,250	3,365
Yb(8HQ) ₃	3,700	5,940	3,370
Lu(8HQ) ₃ (d)	3,695	5,200	3,360

(a) 3700 Å \sim 27,030 cm⁻¹

(b) 3370 Å \sim 29,675 cm⁻¹

(c) 3200 Å \sim 31,250 cm⁻¹

(d) The analyses of the 8-hydroxyquinolates indicate that some of the chelates are hydrates (see Table 2 in Experimental Section). This was accounted for in the evaluation of the absorption coefficients.

TABLE 6--Continued

$\pm 6\%$	(c) $\pm 20A$	$\pm 6\%$	Moles/l Conc.
4,510	3,200	4,105	$1.61 \times 10^{-4} M$
4,981	3,210	4,210	$1.58 \times 10^{-4} M$
4,821	3,205	4,350	$1.71 \times 10^{-4} M$
4,321	3,200	4,405	$1.46 \times 10^{-4} M$
4,721	3,210	4,860	$1.42 \times 10^{-4} M$
4,652	3,210	4,700	$1.38 \times 10^{-4} M$
5,850	3,195	6,011	$1.39 \times 10^{-4} M$
5,012	3,200	4,850	$1.73 \times 10^{-4} M$
6,484	3,210	5,975	$1.62 \times 10^{-5} M$
6,315	3,220	5,892	$1.92 \times 10^{-4} M$
4,998	3,210	4,260	$1.41 \times 10^{-4} M$
4,800	3,210	4,420	$7.25 \times 10^{-5} M$
4,550	3,210	4,320	$1.81 \times 10^{-4} M$

100

+ 2			
1. 100.00	100.00	100.00	100.00
2. 100.00	100.00	100.00	100.00
3. 100.00	100.00	100.00	100.00
4. 100.00	100.00	100.00	100.00
5. 100.00	100.00	100.00	100.00
6. 100.00	100.00	100.00	100.00
7. 100.00	100.00	100.00	100.00
8. 100.00	100.00	100.00	100.00
9. 100.00	100.00	100.00	100.00
10. 100.00	100.00	100.00	100.00
11. 100.00	100.00	100.00	100.00
12. 100.00	100.00	100.00	100.00
13. 100.00	100.00	100.00	100.00
14. 100.00	100.00	100.00	100.00
15. 100.00	100.00	100.00	100.00
16. 100.00	100.00	100.00	100.00
17. 100.00	100.00	100.00	100.00
18. 100.00	100.00	100.00	100.00
19. 100.00	100.00	100.00	100.00
20. 100.00	100.00	100.00	100.00

100.00

100.00

100.00

100.00

TABLE 7

MOLAR ABSORPTION COEFFICIENTS FOR THE RARE
EARTH 2-METHYL-8-HYDROXYQUINOLATES

Compound	$\lambda^{(a)}_A$	ϵ	$\lambda^{(b)}_A$	ϵ	Concentration
	$\pm 20A$	$\pm 6\%$	$\pm 20A$	$\pm 6\%$	
La(2 Me ₈ HQ) ₃	3,500	1,466	2,980	6,000	$7.51 \times 10^{-5}M$
Eu(2 Me ₈ HQ) ₃	3,500	2,414	3,100	5,859	$1.28 \times 10^{-4}M$
Gd(2 Me ₈ HQ) ₃	3,500	1,548	3,100	6,224	$9.64 \times 10^{-4}M$
Tb(2 Me ₈ HQ) ₃	3,530	2,535	3,100	5,320	$1.50 \times 10^{-4}M$
Dy(2 Me ₈ HQ) ₃	3,510	3,160	3,120	4,816	$1.36 \times 10^{-4}M$
Tm(2 Me ₈ HQ) ₃	3,520	2,554	3,100	4,635	$1.37 \times 10^{-5}M$
Yb(2 Me ₈ HQ) ₃	3,500	2,468	3,100	4,285	$1.32 \times 10^{-4}M$
Lu(2 Me ₈ HQ) ₃	3,500	3,250	3,100	4,093	$1.47 \times 10^{-4}M$
2-Me ₈ HQ	-	-	3,060	2,800	$4.82 \times 10^{-5}M$

(a) $3500 \text{ A} \sim 28,570 \text{ cm}^{-1}$

(b) $3100 \text{ A} \sim 32,260 \text{ cm}^{-1}$

TABLE 8

CLASSIFICATION OF LUMINESCENCE
SPECTRA OF RARE EARTH CHELATES

Chelate (a)	La	Pr	Nd	Sm	Eu	Gd	Tb	Dy	Ho	Er	Tm	Yb	Lu
M(8HQ) ₃	B	B	B	B	CL	B	B	B	B	B	B	CB	B
M(AnAc) ₃	B	B	B	CB	C	B	CL	CB	B	B	B	CB	B
M(2 Me8HQ) ₃	B	-	-	B	CL	B	B	B	-	-	B	CB	B
M(SA) ₃ (b) & (c)	B	B	B	B	CL	B	CB	B	B	B	B	CB	B
- - - - -	-	-	-	-	-	-	-	-	-	-	-	-	-

B. Molecular fluorescence and phosphorescence band emission only

L. Line emission characteristic of the lanthanide ion with only negligible molecular band emission

C. Combination of both band and line emission of comparable intensity

CL. Combination of band and line emission with lines predominating

CB. Combination of band and line emission with bands predominating

(a) In some cases the preparative methods yielded solvates of the chelates (see Table 3 in the Experimental Section) especially for the first half of the series (La⁺⁺⁺ through Gd⁺⁺⁺). The fact that solvates were used in some cases is considered unimportant for this study.

(b) Very weak Tb⁺⁺⁺ lines observed, and they are considered to be from a decomposition product.

(c) See Appendix II.

UNITED STATES DEPARTMENT OF AGRICULTURE
BUREAU OF PLANT INDUSTRY

Washington, D. C., January 1, 1914.

My dear Sir:

I have the honor to acknowledge the receipt of your letter of the 29th inst. and in reply to inform you that the same has been forwarded to the proper authorities for their consideration.

I am, Sir, very respectfully,
Yours very truly,
J. H. ...

(2) In the event of a ...
...
...

(3) ...

Typical densitometer traces of the fluorescences and phosphorescences are shown in Figures 10 through 17. Only typical emission spectra are shown because the traces are nearly the same for the members of a chelate series with any one ligand.

The energy of the lowest triplet level, in all cases, was assumed to be equal to the highest energy phosphorescence band. The energy of the lowest singlet was estimated from the band maximum of the fluorescence band. The broad band maxima of the anthranilates along with the fact that there was no discernible structure in both the phosphorescence and fluorescence made accurate measurements impossible for this series. The measurements on the peaks of the anthranilates are estimated within $\pm 100 \text{ cm}^{-1}$. The position of the lowest triplet is certainly higher in energy than the values reported because the high energy tail of the phosphorescence band is removed by 2000 cm^{-1} from the peak maxima to shorter wavelengths. (See Figure 15.) Since the fluorescence high energy tail extends to about $25,700 \text{ cm}^{-1}$ for the anthranilates (see Figure 15), the position of the lowest singlet is certainly higher in energy than the values reported here.

The phosphorescence spectra for chelates of gadolinium, lanthanum and lutecium of the 8-hydroxyquinolate and 2-methyl-8-hydroxyquinolate series were the only ones sufficiently intense for reliable measurements of band maxima. The triplet measurements reported were made on these three samples

typical form of the ...
reactions ...
existence ...
range ...
the ...
was ...
band ...
the ...
maximum ...
was ...
and ...
this ...
laser ...
lowest ...
reported ...
beam ...
wavelength ...
energy ...
factor ...
generative ...
The ...
laser ...
neutral ...
by ...
triple ...

only. The relatively well defined structure made more accurate measurements possible (see Figures 11 and 17), however, the error is still considered to be approximately $\pm 50 \text{ cm}^{-1}$. The fluorescence emission for both series exhibited a broad band maximum and no discernible structure. As in the case of the anthranilates, the lowest singlet energy is undoubtedly higher than values reported here. All the spectra were reproducible and the compounds were reasonably pure as indicated by analysis so that the measurements reported are considered to be reliable within the specified limits of error.

B. Quantum Yield Measurements

1. The Anthranilate Rare Earth Series.--The anthranilates were selected for a quantum yield study because: (i) Gadolinium anthranilate is the brightest emitter of the series and can be used as an internal standard for comparison of the luminescence efficiencies of other chelates. Since it is a bright emitter, the phosphorescence quenching was assumed to be zero and all the quenching yields for the remainder of the series were determined on the basis of this assumption. The quenching yields are, therefore, relative to gadolinium anthranilate. (ii) The entire series luminesces relatively bright so that good exposures can be obtained in a short time. (iii) The emission spectra have no discernible structure, thereby making it less difficult to integrate the curves graphically.

THE UNIVERSITY OF CHICAGO

1911

CHICAGO, ILL.

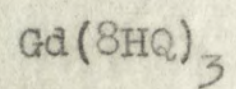
(1911)

VOLUME 1

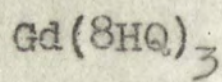
1911

CHICAGO, ILL.

(1911)

FIGURE 10

Fluorescence

FIGURE 11

Phosphorescence

55

wavelength in Å

4000

4200

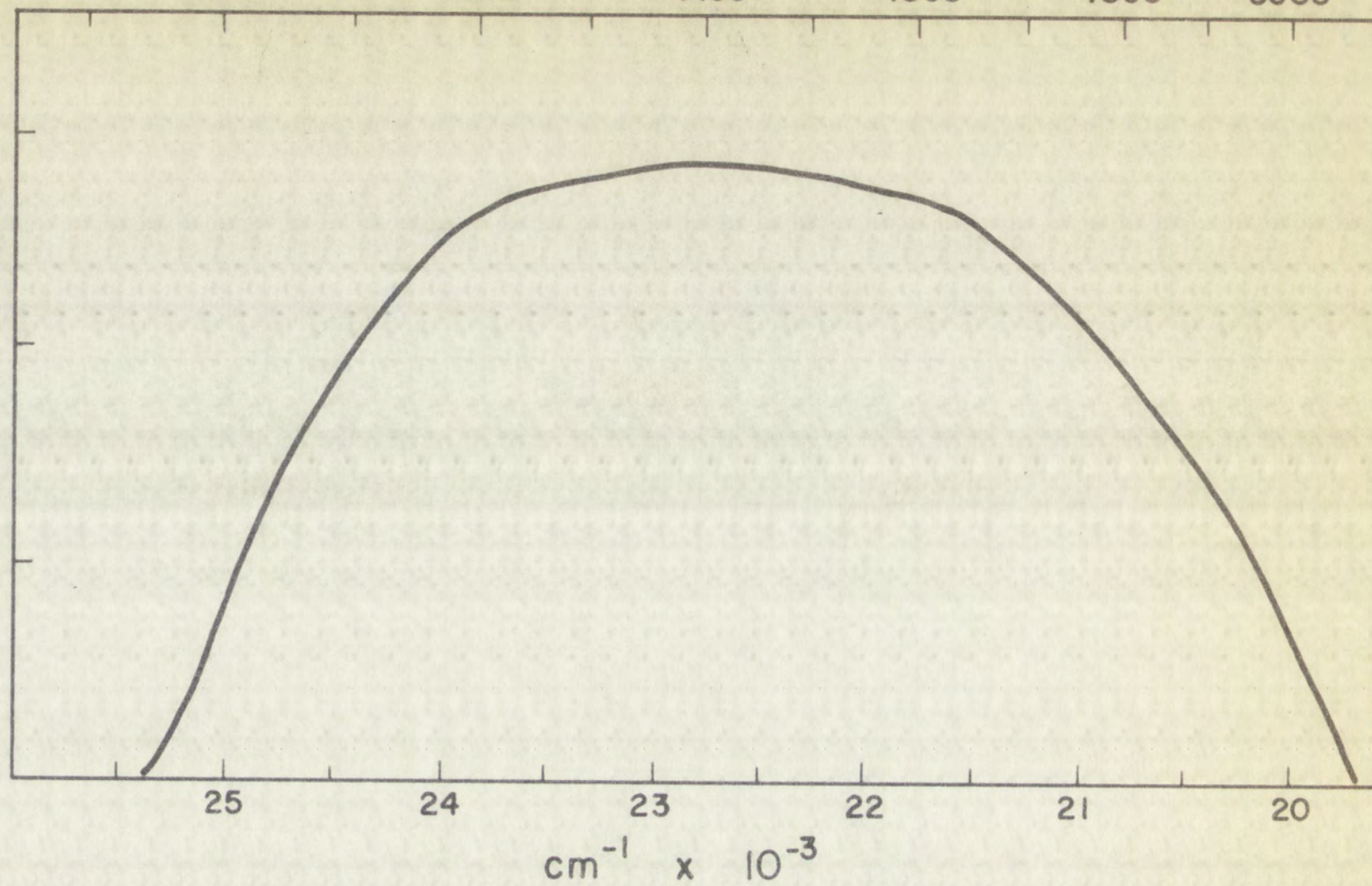
4400

4600

4800

5000

plate blackening



wavelength in Å

5400

5600

5800

6000

6200

plate blackening

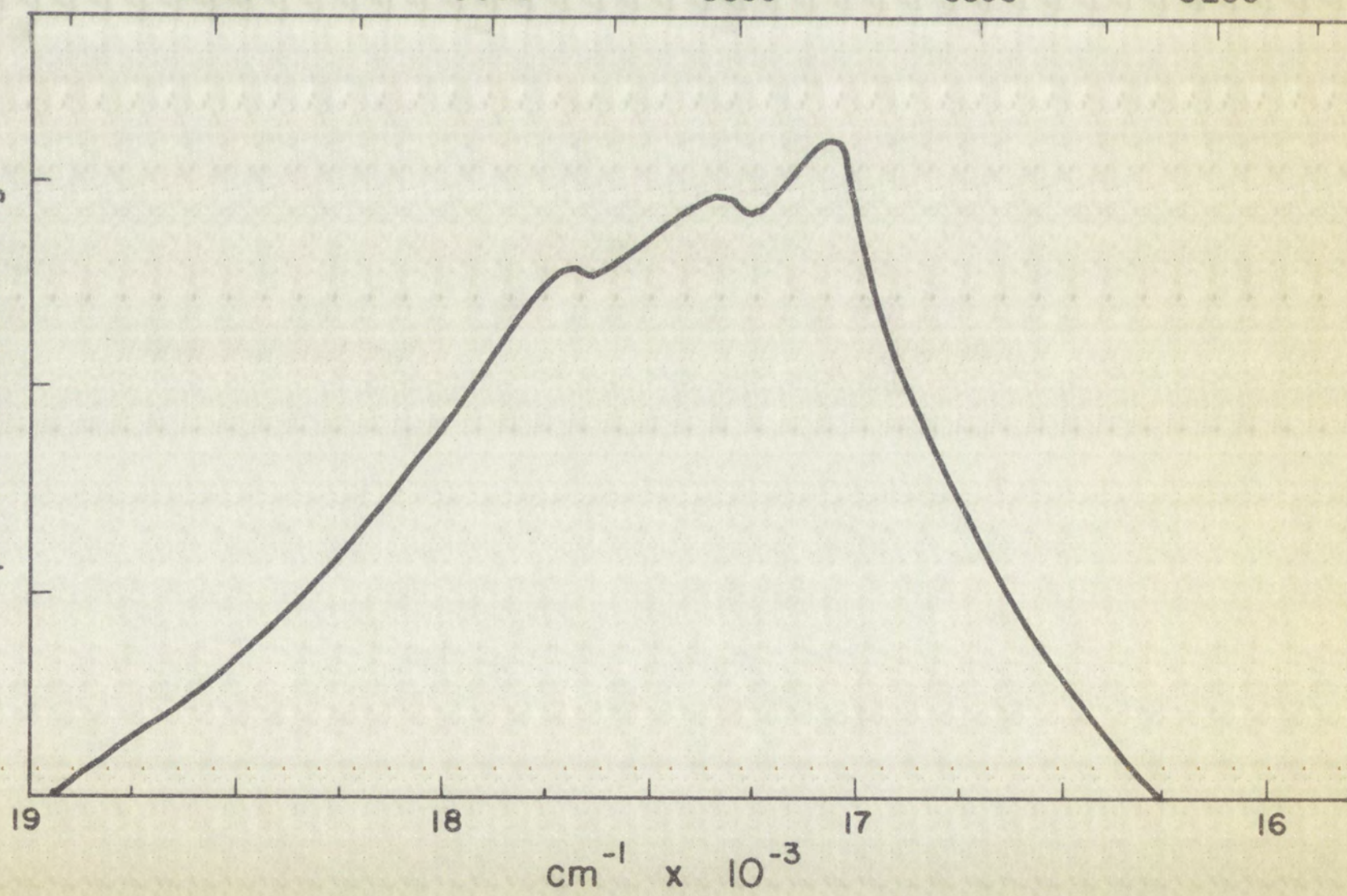


FIGURE 12 $\text{Gd}(\text{AnAc})_3$

Total Emission

FIGURE 13 $\text{Gd}(\text{AnAc})_3$

Phosphorescence

57

wavelength in Å

4000

4200

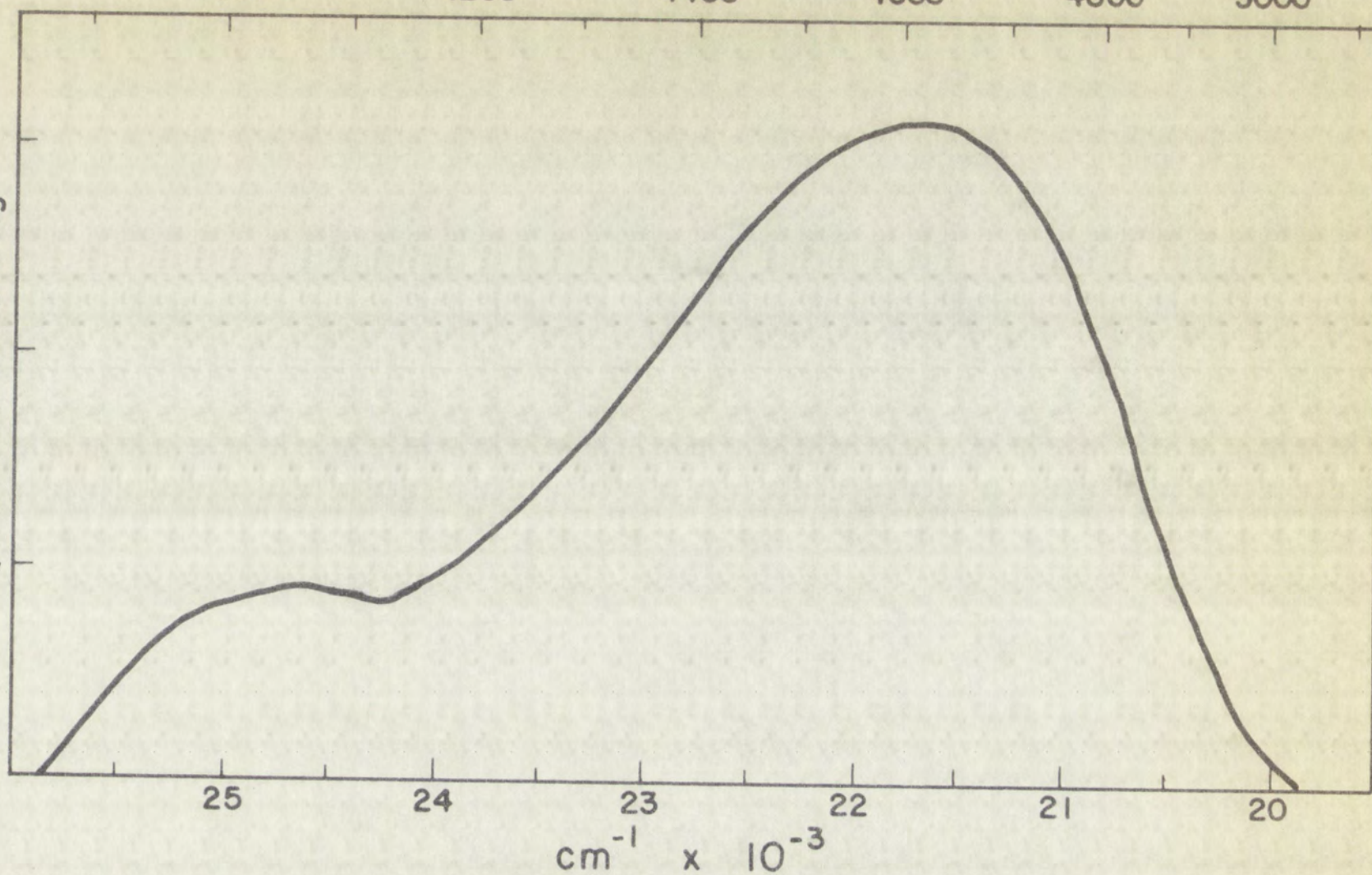
4400

4600

4800

5000

plate blackening



wavelength in Å

4000

4200

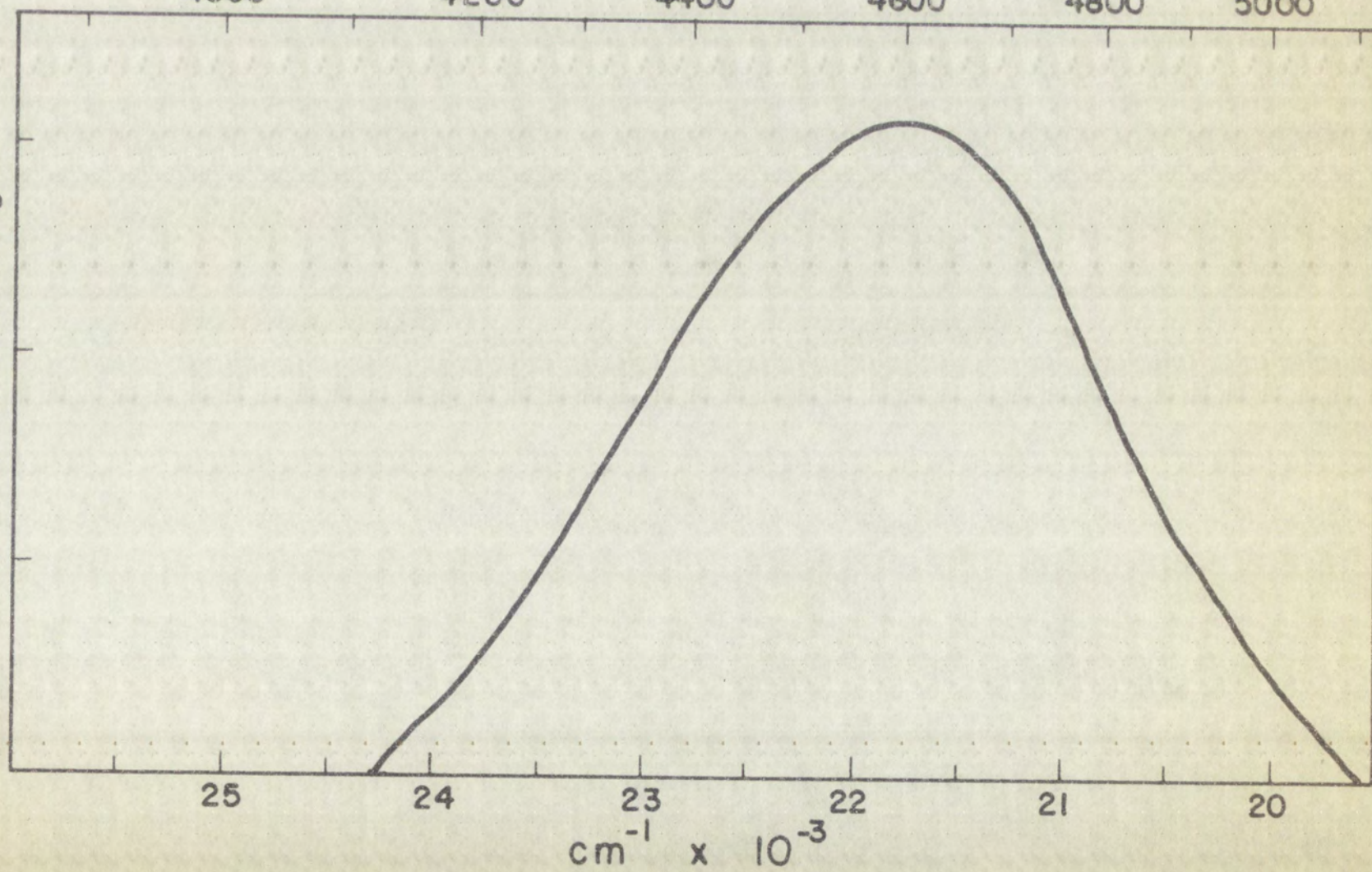
4400

4600

4800

5000

plate blackening



1911

1911

1911

1911

1911

1911

1911

1911

1911

1911

FIGURE 14 $\text{Dy}(\text{AnAc})_3$

Phosphorescence

FIGURE 15 $\text{Dy}(\text{AnAc})_3$

Total Emission

59

wavelength in Å

4200

4400

4600

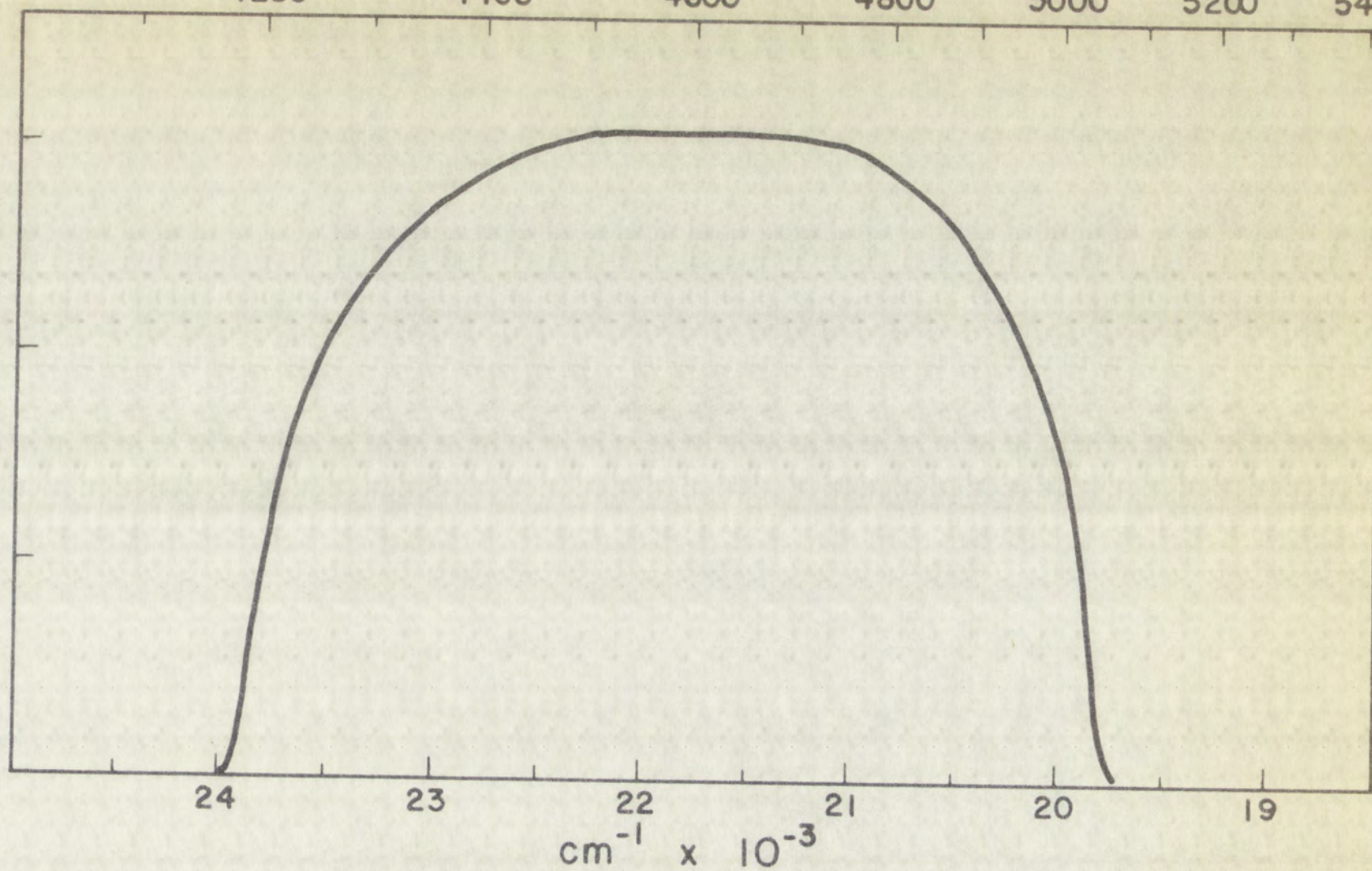
4800

5000

5200

5400

plate blackening



wavelength in Å

4000

4200

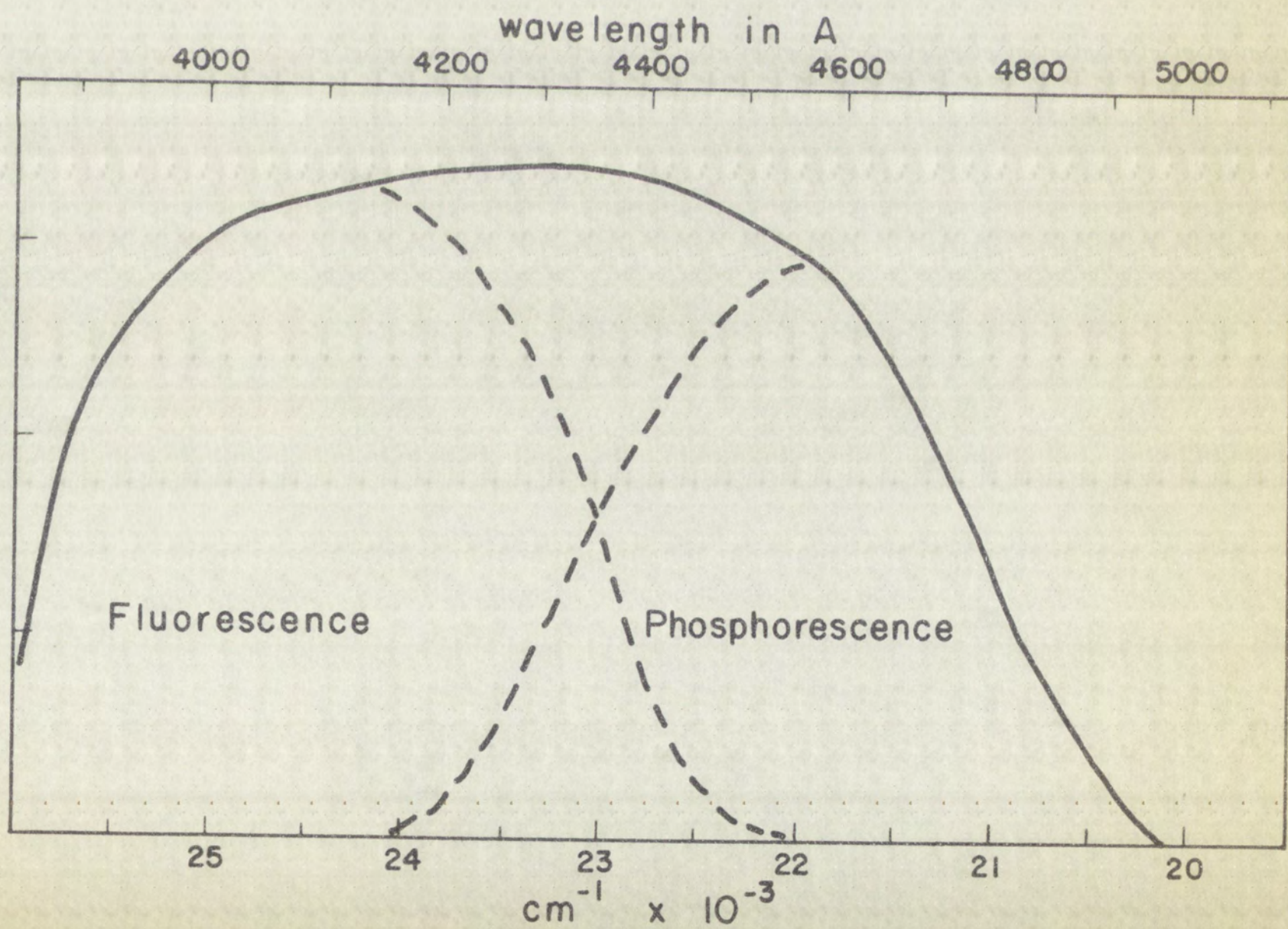
4400

4600

4800

5000

plate blackening



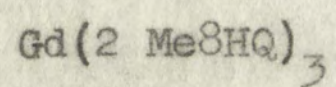
1911

1911

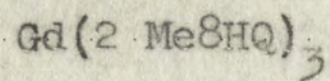
1911

1911

1911

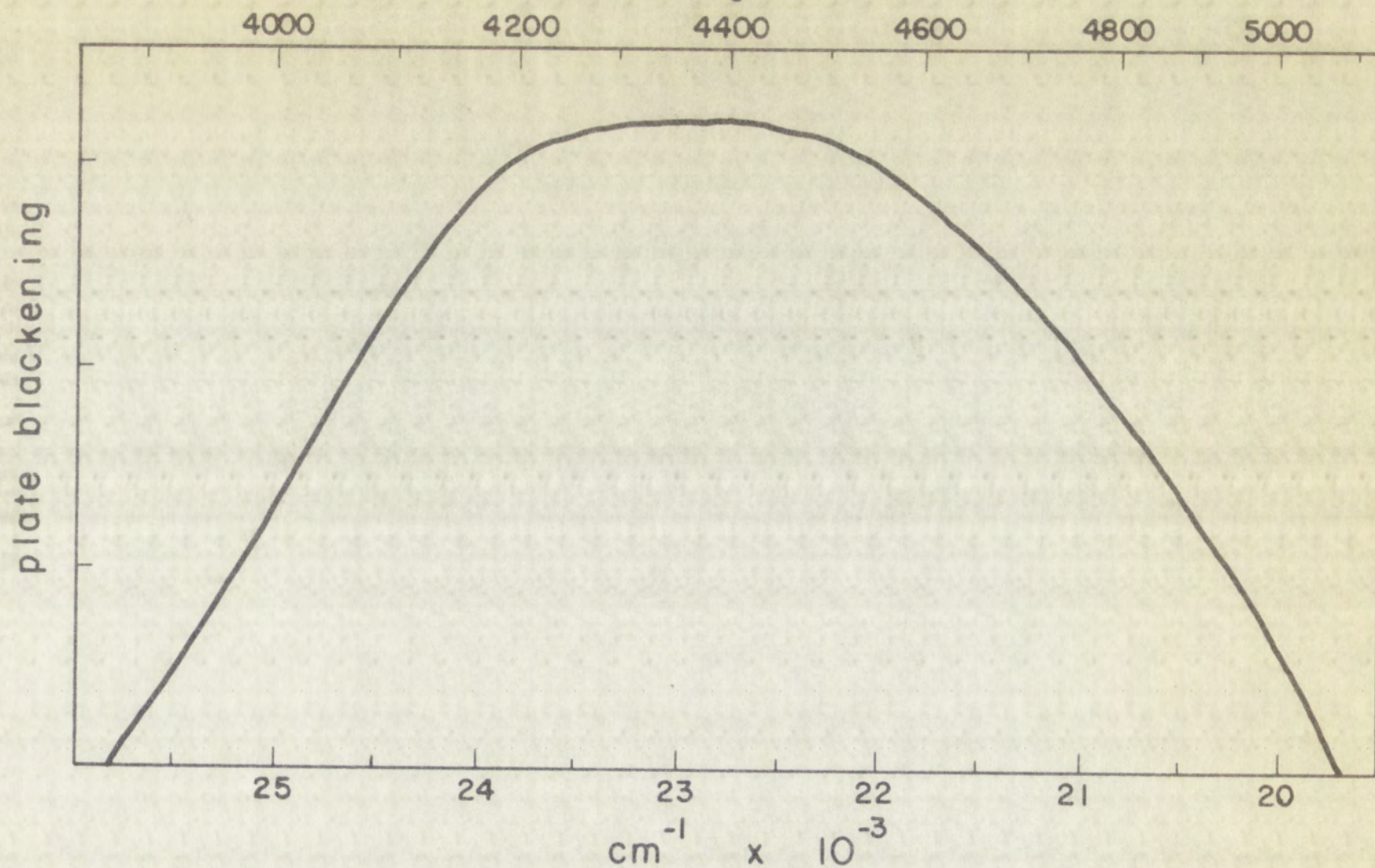
FIGURE 16

Fluorescence

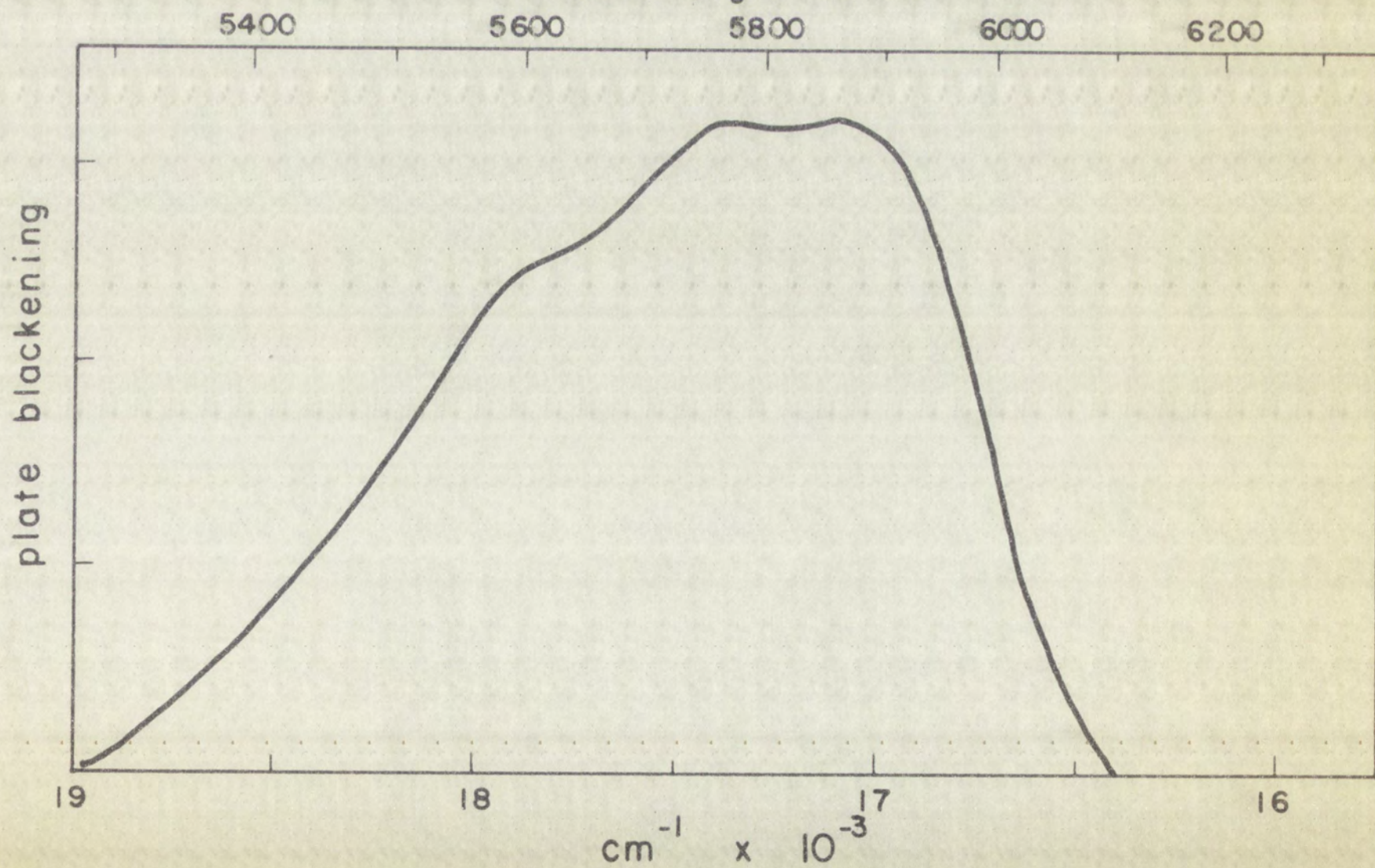
FIGURE 17

Phosphorescence

61
wavelength in A



wavelength in A



THE UNITED STATES OF AMERICA DEPARTMENT OF THE INTERIOR BUREAU OF LAND MANAGEMENT

<p>1-10</p>	<p>1-10</p>	<p>1-10</p>
<p>1-10</p>	<p>1-10</p>	<p>1-10</p>
<p>1-10</p>	<p>1-10</p>	<p>1-10</p>

(1) The land is located in the State of California, County of San Diego, and is situated in the Township of San Diego, Range 14 North, and Section 14, 15, 16, 17, 18, 19, 20, 21, 22, 23, 24, 25, 26, 27, 28, 29, 30, 31, 32, 33, 34, 35, 36, 37, 38, 39, 40, 41, 42, 43, 44, 45, 46, 47, 48, 49, 50, 51, 52, 53, 54, 55, 56, 57, 58, 59, 60, 61, 62, 63, 64, 65, 66, 67, 68, 69, 70, 71, 72, 73, 74, 75, 76, 77, 78, 79, 80, 81, 82, 83, 84, 85, 86, 87, 88, 89, 90, 91, 92, 93, 94, 95, 96, 97, 98, 99, 100.

(2) The land is located in the State of California, County of San Diego, and is situated in the Township of San Diego, Range 14 North, and Section 14, 15, 16, 17, 18, 19, 20, 21, 22, 23, 24, 25, 26, 27, 28, 29, 30, 31, 32, 33, 34, 35, 36, 37, 38, 39, 40, 41, 42, 43, 44, 45, 46, 47, 48, 49, 50, 51, 52, 53, 54, 55, 56, 57, 58, 59, 60, 61, 62, 63, 64, 65, 66, 67, 68, 69, 70, 71, 72, 73, 74, 75, 76, 77, 78, 79, 80, 81, 82, 83, 84, 85, 86, 87, 88, 89, 90, 91, 92, 93, 94, 95, 96, 97, 98, 99, 100.

(3) The land is located in the State of California, County of San Diego, and is situated in the Township of San Diego, Range 14 North, and Section 14, 15, 16, 17, 18, 19, 20, 21, 22, 23, 24, 25, 26, 27, 28, 29, 30, 31, 32, 33, 34, 35, 36, 37, 38, 39, 40, 41, 42, 43, 44, 45, 46, 47, 48, 49, 50, 51, 52, 53, 54, 55, 56, 57, 58, 59, 60, 61, 62, 63, 64, 65, 66, 67, 68, 69, 70, 71, 72, 73, 74, 75, 76, 77, 78, 79, 80, 81, 82, 83, 84, 85, 86, 87, 88, 89, 90, 91, 92, 93, 94, 95, 96, 97, 98, 99, 100.

TABLE 9

(a) WAVELENGTH MEASUREMENTS OF THE FLUORESCENCE BAND MAXIMA FOR THE RARE EARTH 8-HYDROXYQUINOLATES, 2-METHYL-8-HYDROXYQUINOLATES AND ANTHRANILATES

Chelate	La		Pr		Nd	
	A	cm ⁻¹	A	cm ⁻¹	A	cm ⁻¹
M(8HQ) ₃ ^(b)	4648	21,514				
M(2 Me8HQ) ₃	4656	21,477				
M(AnAc) ₃ ^(c)	4061	24,624	4056	24,655	4066	24,594

	Dy		Ho		Er	
	A	cm ⁻¹	A	cm ⁻¹	A	cm ⁻¹
M(8HQ) ₃	4190	23,866	4251	23,524	4261	23,469
M(2 Me8HQ) ₃	4170	23,981				
M(AnAc) ₃	4062	24,618	4078	24,522	4081	24,504

(a) The wavelengths in Table 9 are the band maxima of the fluorescence, and they are assumed to represent the approximate position of the first excited singlet.

(b) The energy of the lowest singlet for the 2-methyl-8-hydroxyquinolates and the 8-hydroxyquinolates could be as much as 2000 cm⁻¹ higher than the tabulated values.

(c) The energy of the lowest singlet for the anthranilates could be as much as 2000 cm⁻¹ higher, but not lower than the tabulated values.

TABLE 9--Continued

Sm	Eu	Gd	Tb
A cm^{-1}	A cm^{-1}	A cm^{-1}	A cm^{-1}
	4240 23,585	4572 21,872	4236 23,607
	4236 23,607	4552 21,968	4272 23,408
4085 24,480	4067 24,588	4072 24,588	4041 24,746
- - - - -	- - - - -	- - - - -	- - - - -
Tm	Yb	Lu	
A cm^{-1}	A cm^{-1}	A cm^{-1}	
4259 23,480	4228 23,652	4681 21,363	
4251 23,524	4235 23,613	4628 21,608	
4056 24,655	4064 24,606	4076 24,534	

(3) **ANALYSIS OF THE DATA**
AND THE RESULTS OF THE INVESTIGATION

Date	Time	Location	Remarks
1-1	A	1-1	1-1
1-1	A	1-1	1-1
1-1	A	1-1	1-1
1-1	A	1-1	1-1
1-1	A	1-1	1-1
1-1	A	1-1	1-1
1-1	A	1-1	1-1
1-1	A	1-1	1-1
1-1	A	1-1	1-1

The results of the investigation are as follows: The data shows that the system is capable of operating at a level of 1-1. The results of the investigation are as follows: The data shows that the system is capable of operating at a level of 1-1.

The results of the investigation are as follows: The data shows that the system is capable of operating at a level of 1-1. The results of the investigation are as follows: The data shows that the system is capable of operating at a level of 1-1.

The results of the investigation are as follows: The data shows that the system is capable of operating at a level of 1-1. The results of the investigation are as follows: The data shows that the system is capable of operating at a level of 1-1.

TABLE 10

(a) WAVELENGTH MEASUREMENTS OF THE PHOSPHORESCENCE
BAND MAXIMA OF THE RARE EARTH 8-HYDROXYQUINOLATES,
2-METHYL-8-HYDROXYQUINOLATES AND ANTHRANILATES

$\text{La}(\text{8HQ})_3^{(b)}$	$\text{Gd}(\text{8HQ})_3$	$\text{Lu}(\text{8HQ})_3$	$\text{La}(2 \text{ Me8HQ})_3$
A cm^{-1}	A cm^{-1}	A cm^{-1}	A cm^{-1}
5600 17,857 5796 17,253 5862 17,059 - - - - -	5660 17,667 5736 17,434 5834 17,141 - - - - -	5632 17,756 5780 17,301 5871 17,033 - - - - -	5612 17,819 5820 17,182 5912 16,915 - - - - -
$\text{La}(\text{AnAc})_3^{(c)}$	$\text{Pr}(\text{AnAc})_3$	$\text{Nd}(\text{AnAc})_3$	$\text{Sm}(\text{AnAc})_3$
A cm^{-1}	A cm^{-1}	A cm^{-1}	A cm^{-1}
4596 21,758 - - - - -	4541 22,022 - - - - -	4467 22,386 - - - - -	4511 22,168 - - - - -
$\text{Dy}(\text{AnAc})_3$	$\text{Ho}(\text{AnAc})_3$	$\text{Er}(\text{AnAc})_3$	$\text{Tm}(\text{AnAc})_3$
A cm^{-1}	A cm^{-1}	A cm^{-1}	A cm^{-1}
4464 22,401	4482 22,311	4475 22,346	4515 22,148

(a) The measurements in this Table are for the band maxima of the phosphorescences. The energy of the triplet state is assumed to be equal to the energy of the lowest wavelength band in the phosphorescence spectra of the 8-hydroxyquinolates and 2-methyl-8-hydroxyquinolates.

(b) The estimated error in the measurements for the 8-hydroxyquinolates and 2-methyl-8-hydroxyquinolates is $\pm 50 \text{ cm}^{-1}$.

(c) The energy of the lowest triplet for the anthranilates could be higher by 1500 cm^{-1} but not lower than the reported values.

TABLE 10--Continued

$\text{Gd}(2 \text{ Me}_8\text{HQ})_3$	$\text{Lu}(2 \text{ Me}_8\text{HQ})_3$		
A cm^{-1}	A cm^{-1}		
5559 17,989 5752 17,385 5846 17,106	5490 18,215 5800 17,241 5960 16,778		

$\text{Eu}(\text{AnAc})_3$	$\text{Gd}(\text{AnAc})_3$	$\text{Tb}(\text{AnAc})_3$	
A cm^{-1}	A cm^{-1}	A cm^{-1}	
4522 22,114	4464 22,401	4558 21,939	

$\text{Yb}(\text{AnAc})_3$	$\text{Lu}(\text{AnAc})_3$	AnAc	AnAc - NaOH
A cm^{-1}	A cm^{-1}	A cm^{-1}	A cm^{-1}
4492 22,262	4525 22,099	4460 22,421	4459 22,426

TABLE 1-1

	(1) (2) (3)	(4) (5) (6)
	A	A
	A	A
	A	A
	A	A
	A	A
	A	A
	A	A
	A	A

2. Graphical Integration.--The actual graphical integration of the densitometer traces for the resolved phosphorescence and fluorescence emission was accomplished by the use of a polar planimeter which gave the area in square inches. A separate conversion factor for the phosphorescence, fluorescence, and total emission was determined by taking an appropriate area in the spectral region of interest (phosphorescence, fluorescence, and total emission) and expressing this in angstroms multiplied by percent transmission and using this as an average value to determine the conversion factors ($Ax\%T/\text{sq in}$). The area was converted to express the integral, $\int D(\lambda)d\lambda$, which represents the integrated optical density.

The fluorescence and phosphorescence areas were determined separately. A check on the integration procedure was made by integration of the total emission as indicated above and comparing this value to the sum of the integrated fluorescence and integrated phosphorescence intensities. The results of the integrations are tabulated in Table 11.

The approximations made in the Appendix I regarding conversion of the $\int T(\lambda)d\lambda$ to $-\log Td\lambda$ were confirmed by actually plotting the curve for gadolinium anthranilate in terms of $\log \frac{1}{T}$ vs. wavelength. The results show the approximation to be valid for these cases.

TABLE 11

AREAS OBTAINED BY GRAPHICAL INTEGRATION FOR THE EMISSION
SPECTRA OF THE RARE EARTH ANTHRANILATES

Compound	Concentration	Fluorescence Area		
		Sq in	A(%T)	$\int D(\lambda) d\lambda$
La(AnAc) ₃	3.46x10 ⁻⁵ M	36.85	36,850	-1,088
Pr(AnAc) ₃	3.48x10 ⁻⁵ M	19.83	19,830	- 911
Nd(AnAc) ₃	3.47x10 ⁻⁵ M	17.39	17,380	- 871
Sm(AnAc) ₃	3.49x10 ⁻⁵ M	17.48	17,470	- 878
Eu(AnAc) ₃	3.51x10 ⁻⁵ M	25.53	17,381	- 977
Gd(AnAc) ₃	3.52x10 ⁻⁵ M	7.30	7,200	- 647
Tb(AnAc) ₃	3.52x10 ⁻⁵ M	19.49	19,490	- 907
Dy(AnAc) ₃	3.54x10 ⁻⁵ M	-	-	-
Ho(AnAc) ₃	3.45x10 ⁻⁵ M	9.44	9,435	- 717
Er(AnAc) ₃	3.45x10 ⁻⁵ M	30.68	30,658	-1,025
Tm(AnAc) ₃	3.44x10 ⁻⁵ M	32.68	32,680	- 647
Yb(AnAc) ₃	3.45x10 ⁻⁵ M	6.19	6,190	- 608
Lu(AnAc) ₃	3.45x10 ⁻⁵ M	39.18	39,180	-1,089

Conversion Factors: For conversion from square inches to
angstroms x percent transmission

Fluorescence: 1000 A(%T)/sq. in.

Phosphorescence: 1816 A(%T)/sq. in.

Total Emission: 1272 A(%T)/sq. in.

Dy(AnAc)₃ was used as the standard for determining the slope
and intercept of the Hurter-Driffield Plot(52) (see Figures
18-20).

TABLE 11--Continued

Phosphorescence Area			Total Emission		
Sq in	A(%T)	$\int D(\lambda) d\lambda$	Sq in	A(%T)	$\int D(\lambda) d\lambda$
23.33	42,385	-1,513	60.19	76,573	-2,453
8.91	50,103	-1,124	28.72	36,537	-1,983
5.71	10,278	- 946	23.12	29,362	-1,850
7.50	13,610	-1,066	24.97	31,766	-1,898
15.07	27,331	-1,341	40.54	51,588	-2,193
36.90	67,374	-1,695	44.29	56,358	-2,247
8.62	15,663	-1,121	28.11	35,761	-1,969
-	-	-	-	-	-
5.10	9,261	- 914	14.53	18,485	-1,568
13.38	24,334	-1,286	43.69	56,015	-2,243
9.95	18,160	-1,179	32.64	54,297	-2,224
2.58	4,540	- 634	8.77	11,170	-1,263
27.59	50,103	-1,578	56.76	72,210	-2,397

PROCEEDINGS OF THE
 BOARD OF SUPERVISORS
 OF THE COUNTY OF ALBANY, NEW YORK
 HELD AT ALBANY, NEW YORK, ON THE 10TH DAY OF JANUARY, 1901.

2d 1st	A (1)	2d 1st	A (1)
27.25	27.25	27.25	27.25
2.71	2.71	2.71	2.71
2.71	2.71	2.71	2.71
7.50	7.50	7.50	7.50
13.07	13.07	13.07	13.07
26.00	26.00	26.00	26.00
8.85	8.85	8.85	8.85
-	-	-	-
2.10	2.10	2.10	2.10
12.30	12.30	12.30	12.30
2.25	2.25	2.25	2.25
2.50	2.50	2.50	2.50
27.25	27.25	27.25	27.25

As shown by equation 4 in Appendix I, it was necessary to determine the variation of integrated optical density at several exposure times for at least one compound. The study was made on dysprosium anthranilate and the results are reported in graphical form in Figures 18, 19, and 20.

3. Evaluation of the Slopes and Intercepts.--The root mean square method for evaluation of the slope and intercept of a straight line as described by G. W. Snedecor³⁹ was used for obtaining the reported values. The sum of the squares of the deviation of the values of log t was obtained by use of equation (1.).

$$(1.) \quad \sum x^2 = \sum X^2 - \frac{(\sum X)^2}{n}$$

$\sum x^2$: sum of the squares of the deviation of log t.

$\sum X^2$: sum of the squares of all the log t values included.

n: number of log t values. The sum of the squares of the deviations was obtained by use of equation (2.).

$$(2.) \quad \sum xy = \sum XY - \frac{(\sum X)(\sum Y)}{n}$$

$\sum xy$: sum of the deviation of (log t)($\int o(\lambda) d\lambda$).

$\sum X$: sum of all the values of log t.

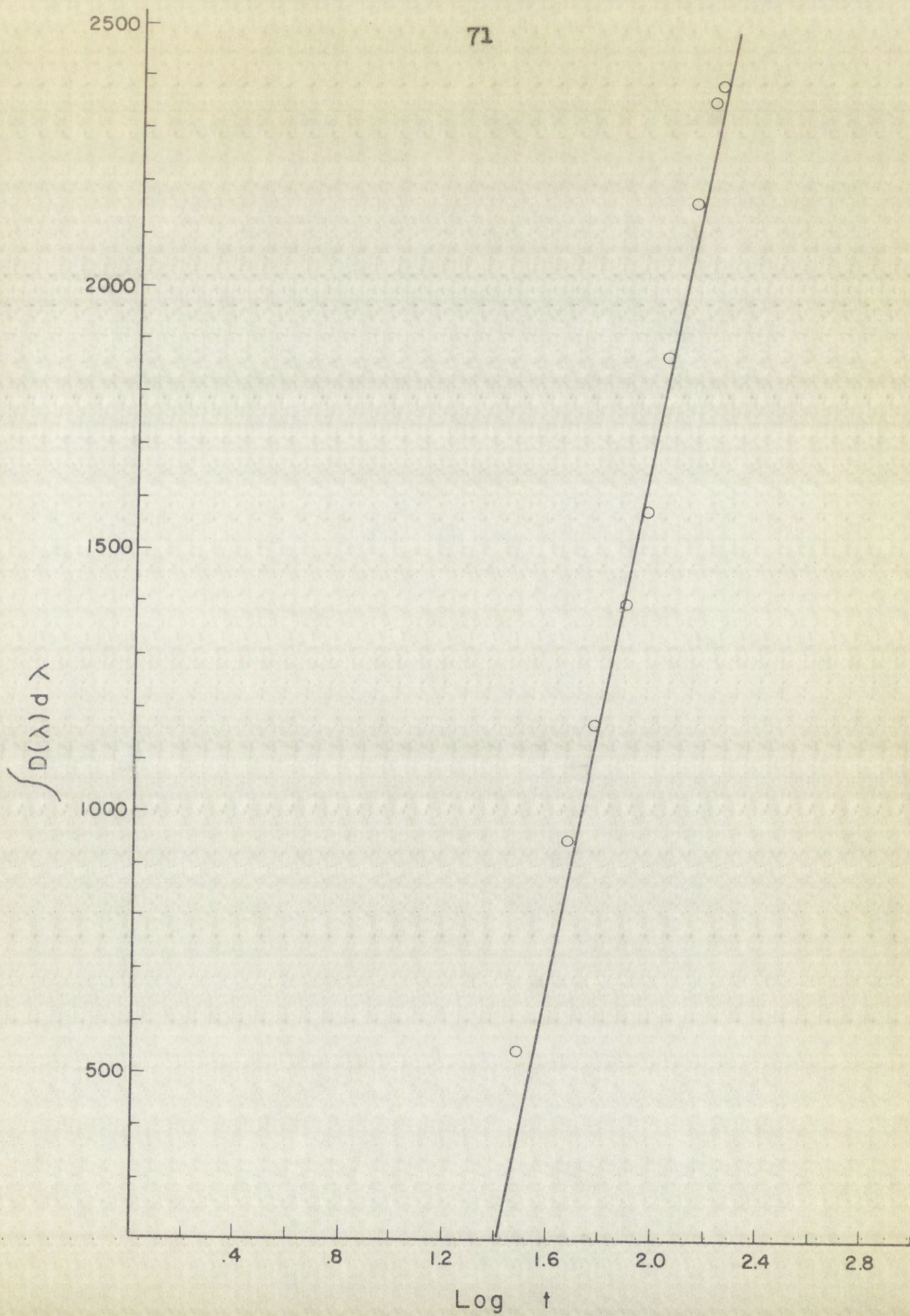
$\sum Y$: sum of all the values of $\int o(\lambda) d\lambda$.

$\sum XY$: sum of the product of the values of (log t)($\int o(\lambda) d\lambda$). The slope of the line was then determined by use of equation (3.).

FIGURE 18 $D_y(\text{AnAc})_3$

Hurter-Drifffield Plot

Total Emission



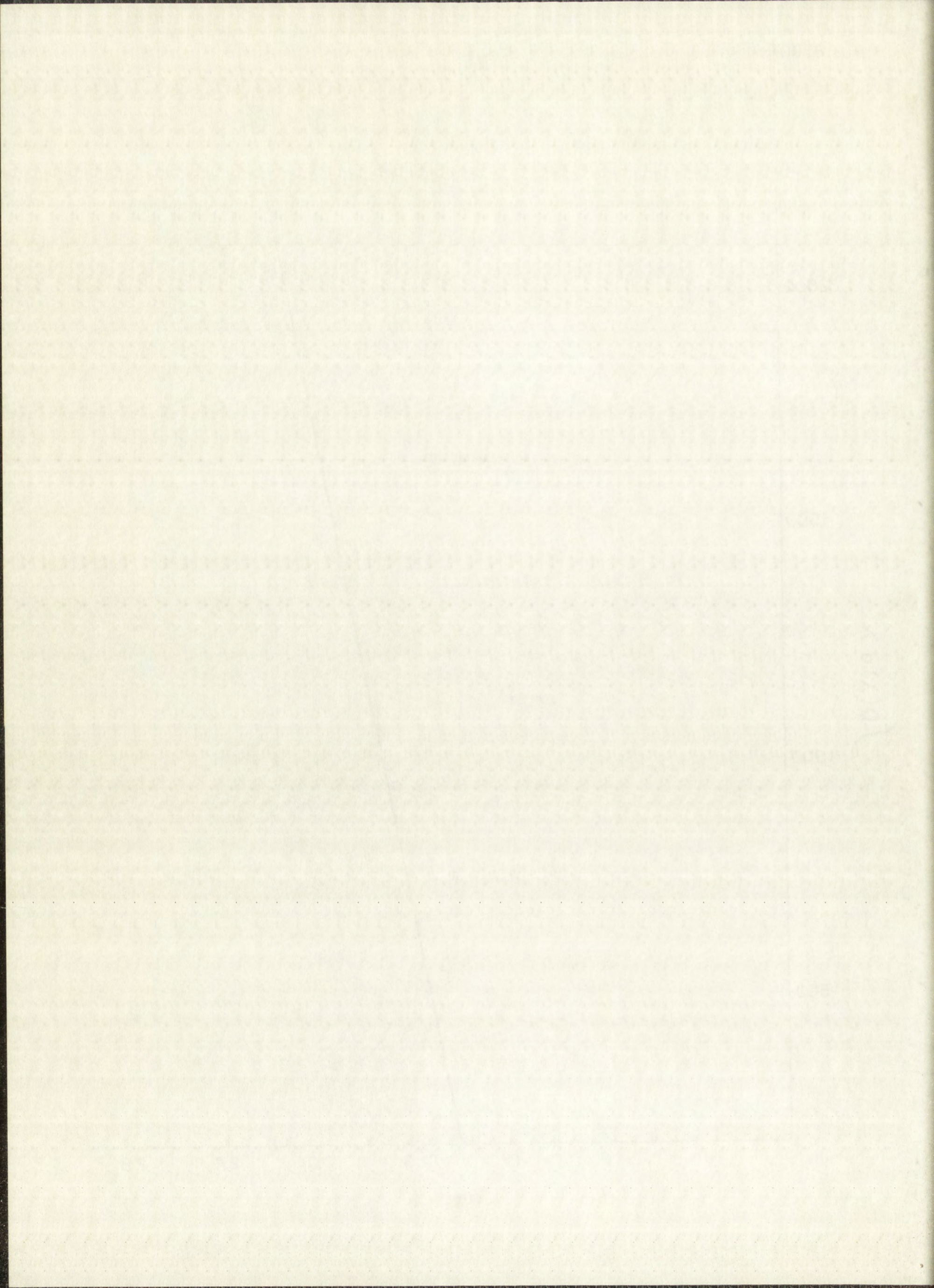
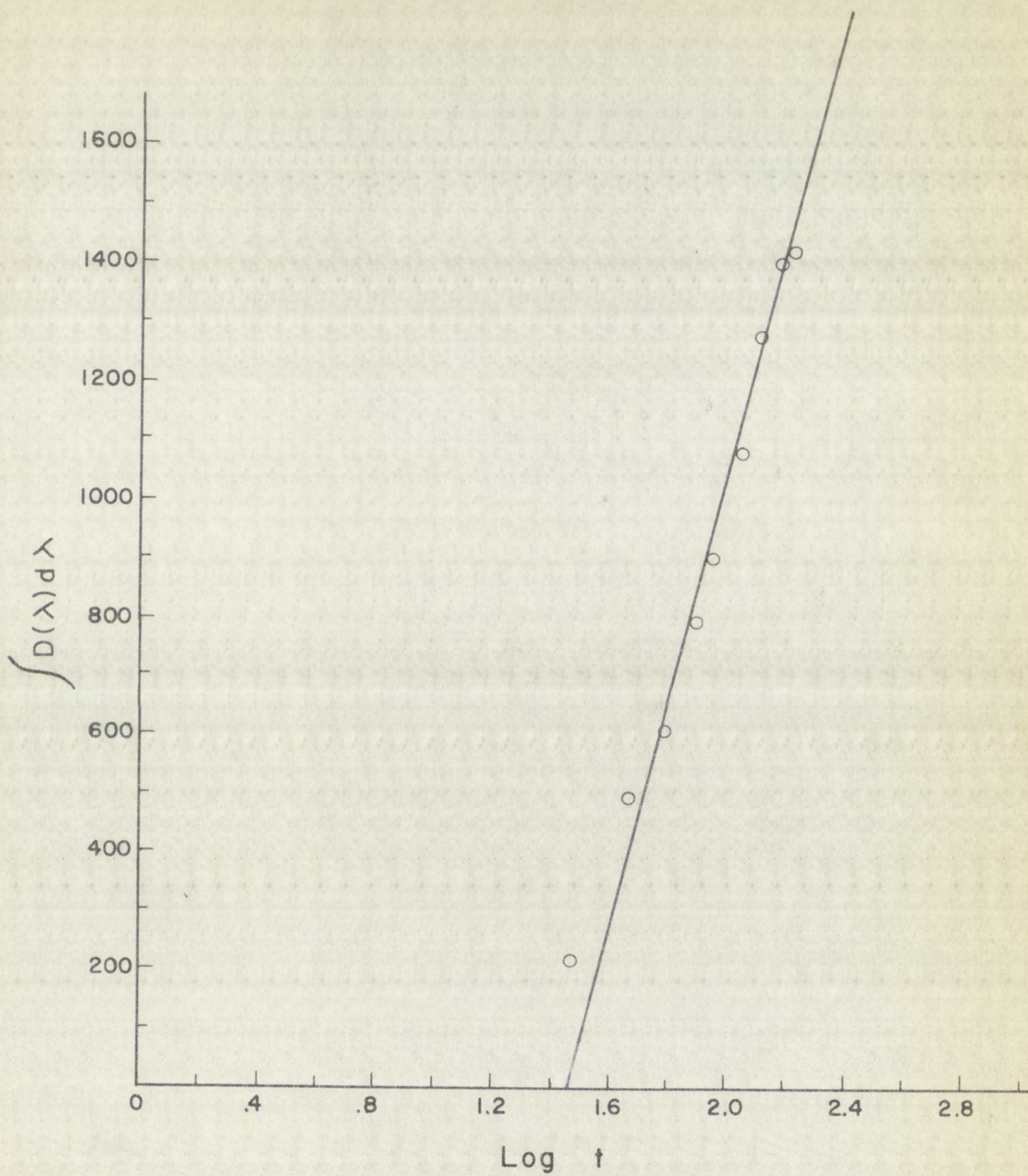


FIGURE 19 $\text{Dy}(\text{AnAc})_3$

Hurter-Drifffield Plot

Phosphorescence



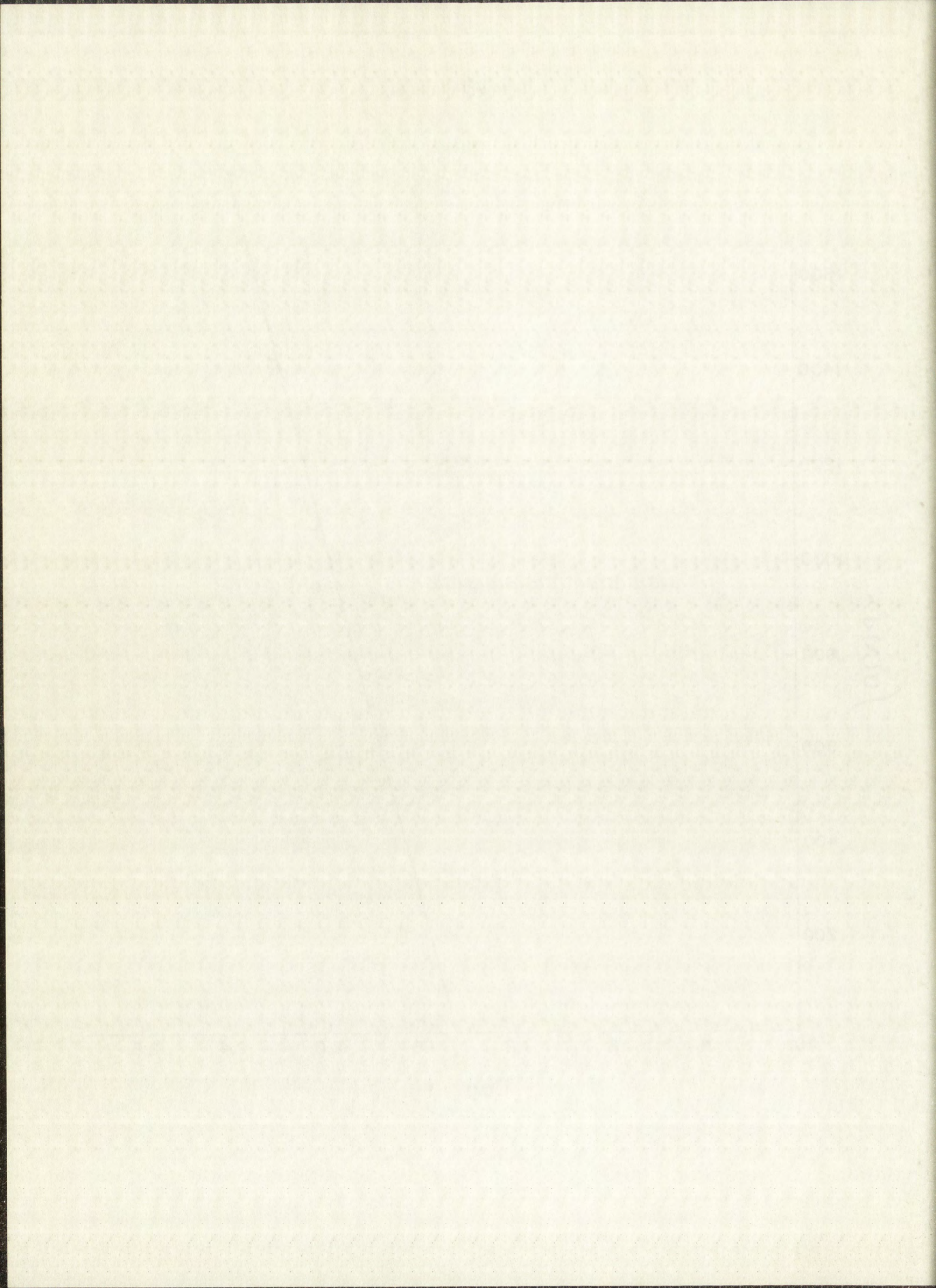
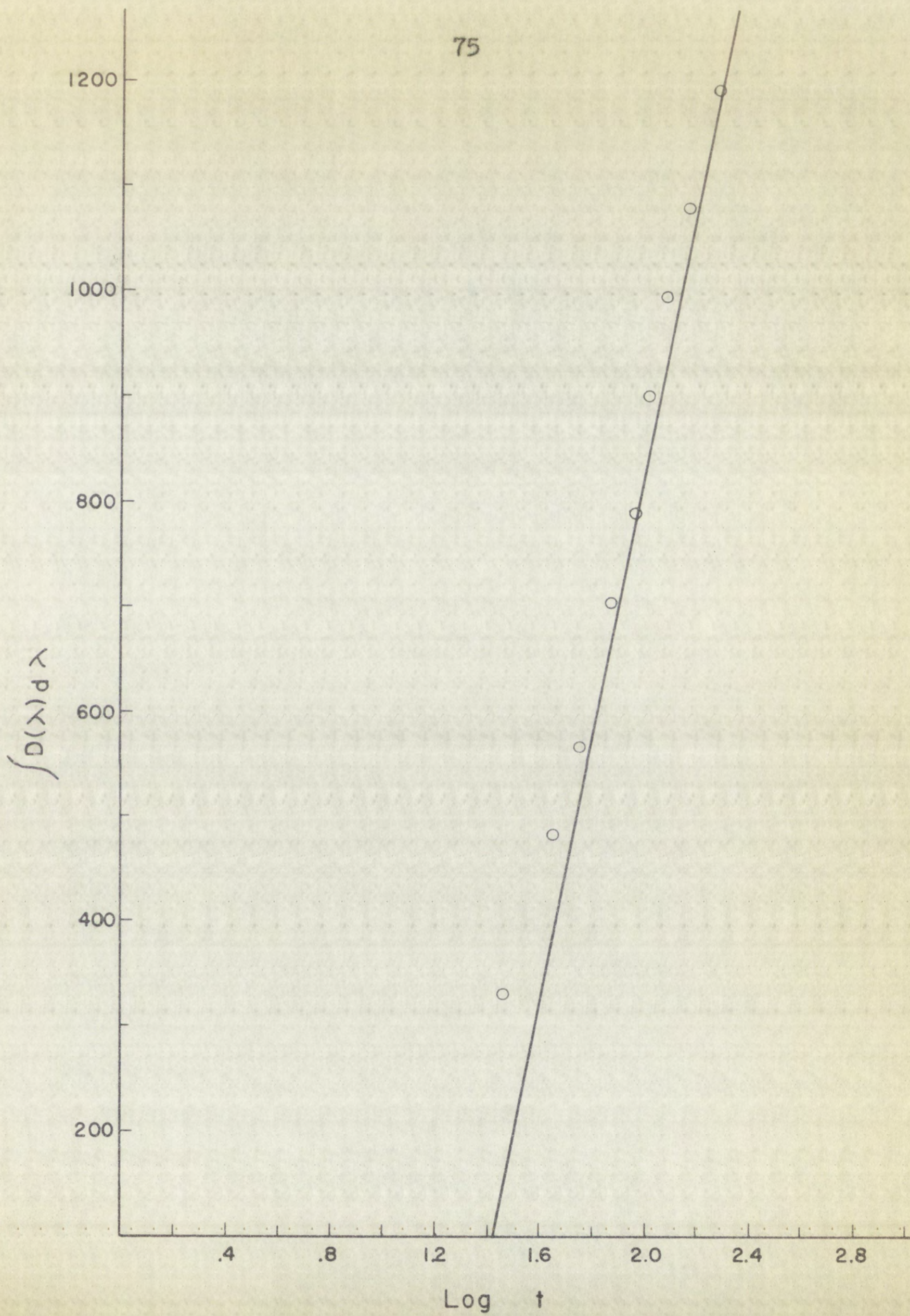


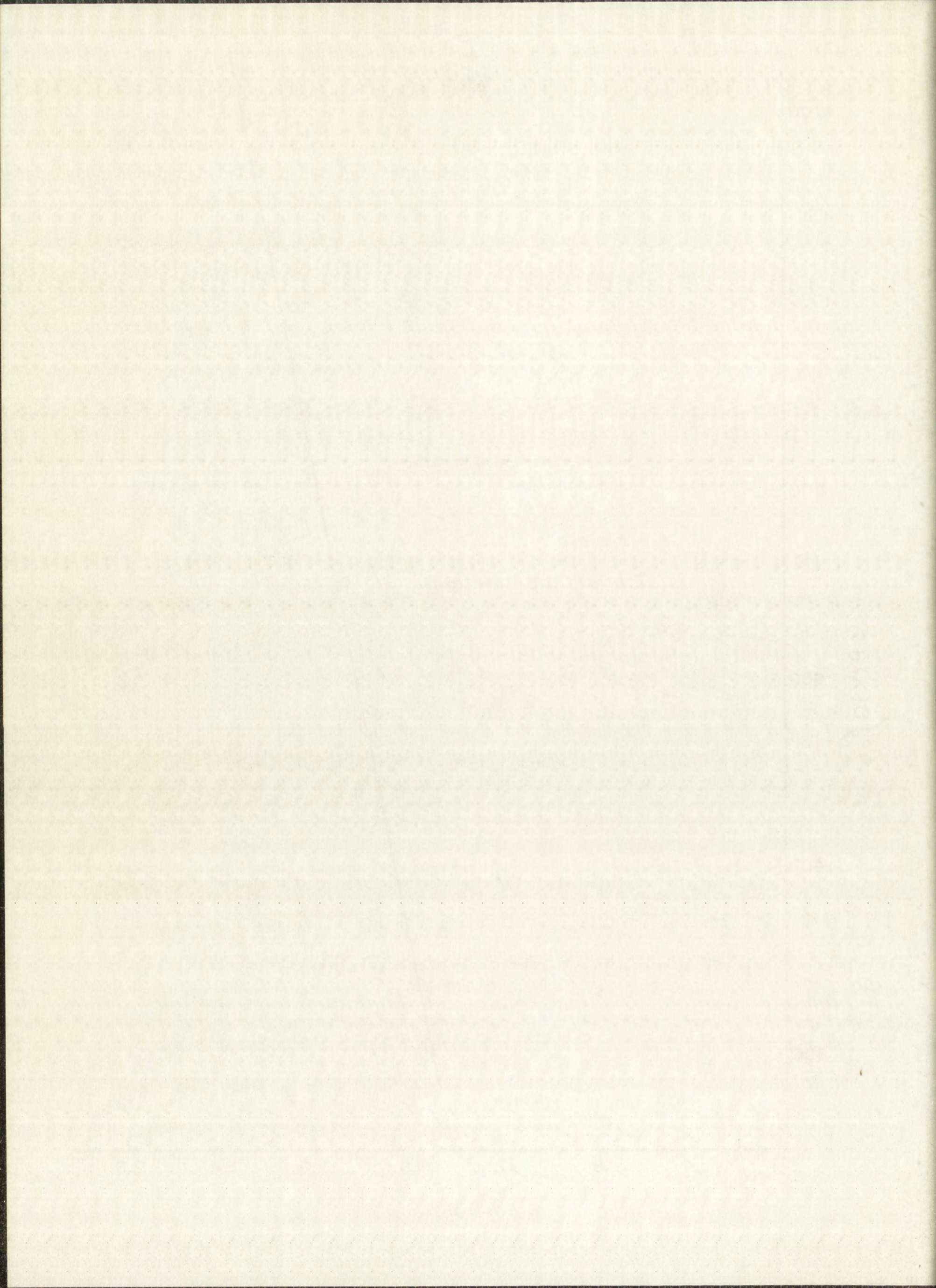
FIGURE 20 $\text{Dy}(\text{AnAc})_3$

Hurter-Drifffield Plot

Fluorescence

75





$$(3.) \quad m(\text{slope}) = \frac{\sum xy}{\sum x^2}$$

The intercept of the line on the integrated optical density axis was determined by use of equation (4.).

$$(4.) \quad b = \bar{y} - m\bar{x}$$

\bar{y} = average of all the values of $\int OD(\lambda) d\lambda$.

\bar{x} = average of all the values of $\log t$.

b = intercept on ordinate.

The approximation $\log i_p - \log i_f - \log i$ as utilized in Appendix I was justified by determining actual values of $\log i_p$ at the wavelength of peak maximum of the phosphorescence and comparing this value to the analogous values obtained from the band maxima of the fluorescence and total emission. The values $\log i_p$, $\log i_f$ and $\log i$ were found to be within $\pm 3\%$ of one another.

The integrated fluorescence and phosphorescence intensities, calculated as shown by Appendix I are reported in Table 12.

The numerical values reported in Table 11 were obtained from the graphical integrations performed. Figure 15 shows a dotted line indicating the resolved fluorescence and phosphorescence for dysprosium anthranilate. A knowledge of the spectral range and peak maximum was the basis used for sketching the phosphorescence emission on a densitometer trace of the total emission, and the fluorescence spectrum

was then determined by subtraction of the phosphorescence spectrum from the total emission spectrum. This resolution of the total emission into the fluorescence and phosphorescence components is the cause of the largest error in these measurements. A conservative estimate of the error places the reliability on the spectral resolution at $\pm 10\%$. Another large source of error involves the difference in the molar absorption coefficients for the anthranilates. Table 6 shows that the variance is about $\pm 15\%$ and they were considered to be equal in the mathematical treatment in Appendix I. The weighing and dilution errors are estimated at $\pm 4\%$. The graphical integration was carried out to an accuracy of $\pm 0.5\%$. The reported integrated intensities in Table 12 are considered to be reliable only within $\pm 25\%$.

The total emission spectrum of an anthranilate chelate extends to about 3900 Å. The glass prisms of the spectrograph absorb some light⁴² from 4100-3900 Å. This glass prism absorption causes some error in the fluorescence intensity measurements. However, the fluorescence spectrum overlaps the absorption spectrum in the expected manner and both the quantum yields of lanthanum and lutecium anthranilate approximate that of gadolinium anthranilate in the final analysis (see Table 13). Since there is considerable difference in the intensity distribution between the former pair and the gadolinium compound, it is assumed that the error arising from prism absorption is negligible.

was then determined by...
apoptosis from the...
of the total...
responder...
these...
placed the...
Another large...
molar...
showed that...
altered to be...
Appendix I...
at...
accuracy of...
Table II...
the...
extends to...
graph...
absorption...
measurements...
absorption...
the...
that of...
Table I...
also...
compound...
morphology is negligible.

TABLE 12
 INTEGRATED INTENSITIES OF THE RARE EARTH ANTHRANILATE

Compound	$I_f \Delta\lambda$	$I_p \Delta\lambda$	$I \Delta\lambda$	Exposure Time
	$\pm 25\%$	$\pm 25\%$	$\pm 25\%$	Seconds
La(AnAc) ₃	3.067	3.474	6.364	25
Pr(AnAc) ₃	1.030	1.200	2.402	45
Nd(AnAc) ₃	.417	.362	.807	120
Sm(AnAc) ₃	.961	1.117	2.241	45
Eu(AnAc) ₃	.293	.335	.6117	210
Gd(AnAc) ₃	1.612	5.418	6.716	20
Tb(AnAc) ₃	.894	.896	1.782	60
Dy(AnAc) ₃	.4643	.5381	1.002	--
Ho(AnAc) ₃	1.236	1.393	2.262	30
Er(AnAc) ₃	.902	.877	1.785	75
Tm(AnAc) ₃	4.028	.721	1.648	80
Yb(AnAc) ₃	.242	.247	.499	120
Lu(AnAc) ₃	3.068	3.762	6.080	25

INTERNATIONAL INSTITUTE OF PURE AND APPLIED CHEMISTRY

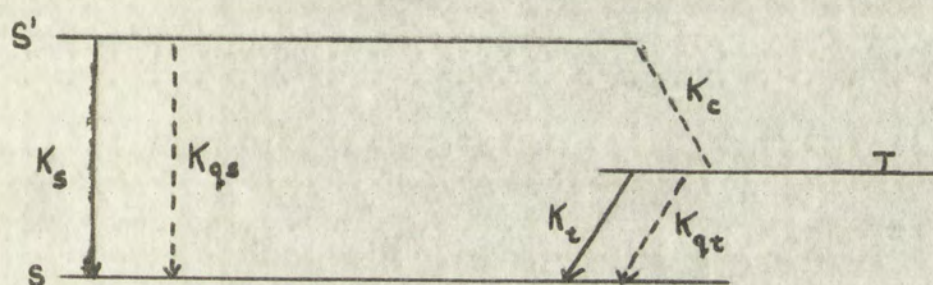
ELEMENTS		Atomic Weight	Symbol
Latin Name	English Name		
Hydrogen	Hydrogen	1.008	H
Helium	Helium	4.003	He
Lithium	Lithium	6.941	Li
Beryllium	Beryllium	9.012	Be
Boron	Boron	10.811	B
Carbon	Carbon	12.011	C
Nitrogen	Nitrogen	14.007	N
Oxygen	Oxygen	15.999	O
Fluorine	Fluorine	18.998	F
Neon	Neon	20.180	Ne
Sodium	Sodium	22.990	Na
Magnesium	Magnesium	24.305	Mg
Aluminum	Aluminum	26.982	Al
Silicon	Silicon	28.086	Si
Phosphorus	Phosphorus	30.974	P
Sulfur	Sulfur	32.06	S
Chlorine	Chlorine	35.453	Cl
Argon	Argon	39.948	Ar
Potassium	Potassium	39.098	K
Calcium	Calcium	40.078	Ca
Scandium	Scandium	44.956	Sc
Titanium	Titanium	47.88	Ti
Vanadium	Vanadium	50.942	V
Chromium	Chromium	51.996	Cr
Manganese	Manganese	54.938	Mn
Iron	Iron	55.845	Fe
Cobalt	Cobalt	58.933	Co
Nickel	Nickel	58.69	Ni
Copper	Copper	63.546	Cu
Zinc	Zinc	65.38	Zn
Gallium	Gallium	69.723	Ga
Germanium	Germanium	72.63	Ge
Arsenic	Arsenic	74.922	As
Selenium	Selenium	78.96	Se
Bromine	Bromine	79.904	Br
Krypton	Krypton	83.80	Kr
Rubidium	Rubidium	85.468	Rb
Strontium	Strontium	87.62	Sr
Yttrium	Yttrium	88.906	Y
Zirconium	Zirconium	91.224	Zr
Niobium	Niobium	92.906	Nb
Molybdenum	Molybdenum	95.94	Mo
Technetium	Technetium	98	Tc
Ruthenium	Ruthenium	101.07	Ru
Rhodium	Rhodium	102.905	Rh
Palladium	Palladium	106.42	Pd
Silver	Silver	107.868	Ag
Cadmium	Cadmium	112.411	Cd
Indium	Indium	114.818	In
Tin	Tin	118.710	Sn
Antimony	Antimony	121.757	Sb
Tellurium	Tellurium	127.6	Te
Iodine	Iodine	126.905	I
Xenon	Xenon	131.29	Xe
Cesium	Cesium	132.905	Cs
Barium	Barium	137.327	Ba
Lanthanum	Lanthanum	138.905	La
Cerium	Cerium	140.12	Ce
Praseodymium	Praseodymium	140.908	Pr
Neodymium	Neodymium	144.24	Nd
Europium	Europium	151.964	Eu
Gadolinium	Gadolinium	157.25	Gd
Terbium	Terbium	158.925	Tb
Dysprosium	Dysprosium	162.50	Dy
Ho		164.930	Ho
Erbium	Erbium	167.259	Er
Thulium	Thulium	168.930	Tm
Ytterbium	Ytterbium	173.054	Yb
Lutetium	Lutetium	174.967	Lu
Hafnium	Hafnium	178.49	Hf
Tantalum	Tantalum	180.948	Ta
Tungsten	Tungsten	183.84	W
Rhenium	Rhenium	186.207	Re
Osmium	Osmium	190.23	Os
Iridium	Iridium	192.222	Ir
Rhodium	Rhodium	192.22	Rh
Palladium	Palladium	195.084	Pd
Silver	Silver	196.967	Ag
Cadmium	Cadmium	196.242	Cd
Mercury	Mercury	200.59	Hg
Thallium	Thallium	204.38	Tl
Lead	Lead	207.2	Pb
Bismuth	Bismuth	208.980	Bi
Polonium	Polonium	209	Po
Astatine	Astatine	210	At
Radium	Radium	226	Ra
Actinium	Actinium	227	Ac
Thorium	Thorium	232.038	Th
Protactinium	Protactinium	231.036	Pa
Uranium	Uranium	238.029	U
Np		237	Np
Plutonium	Plutonium	244	Pu
Am		243	Am
Cm		247	Cm
Bk		247	Bk
Cf		251	Cf
Es		252	Es
Fm		257	Fm
Mendelevium	Mendelevium	258	Md
No		259	No
Lr		262	Lr

4. Crossing Constants.--Upon excitation with near UV light a chelate molecule achieves an excited state. This excited state is either the first excited singlet or a higher singlet. Any molecules which attain an excited state higher than the first singlet are deactivated by internal conversion to the first excited singlet state.⁽⁴⁾ Deactivation of the first excited singlet can be accomplished by the following paths: (1) energy may radiate from the lowest singlet which is the phenomenon known as fluorescence. (2) energy may cross to a nearby triplet, either the lowest or a higher one, by a radiationless transition and finally radiate from the lowest triplet as phosphorescence. (3) energy may be quenched from either the singlet or the triplet. The following energy level diagram is a schematic representation of the energy levels assumed present in a rare earth chelate.

As can be seen from Figure 21, assuming a steady state condition restricts the system to absorbing the same number of quanta per second as are being deactivated by the various paths originating at the first excited singlet. Under this assumption the fluorescence quantum yield may be expressed in terms of the rate constants.

$$\phi_f = \frac{K_s}{K_s + K_{qs} + K_c}$$

FIGURE 21



LEGEND

- S - ground state singlet
- S' - first excited singlet
- T - lowest or nearby triplet
- K_s - rate constant for fluorescence
- K_{qs} - rate constant for singlet quenching
- K_c - rate constant for crossing from the singlet to triplet
- K_t - rate constant for phosphorescence
- K_{qt} - rate constant for triplet quenching
- Dotted lines - radiationless transitions
- Solid lines - radiative transitions

Phosphorescence involves two processes, the singlet-triplet crossing process and the time radiation process from the triplet state to the ground state. The quantum yield of phosphorescence can be expressed as the product of these two yields.

$$\phi_p = \left(\frac{K_c}{K_s + K_{qs} + K_c} \right) \left(\frac{K_t}{K_t + K_{qt}} \right)$$

In a similar manner the quantum yield of triplet quenching is expressed as follows:

$$\phi_{qt} = \left(\frac{K_c}{K_s + K_{qs} + K_c} \right) \left(\frac{K_{qt}}{K_t + K_{qt}} \right)$$

The expression for the ratio of phosphorescence to fluorescence quantum yields follows:

$$\frac{\phi_p}{\phi_f} = \frac{K_c K_p}{K_s (K_p + K_{qt})}$$

The ratio of phosphorescence to triplet quenching quantum yields is given by the following:

$$\frac{\phi_p}{\phi_{qt}} = \frac{\left(\frac{K_c}{K_s + K_{qs} + K_c} \right) \left(\frac{K_p}{K_p + K_{qt}} \right)}{\left(\frac{K_c}{K_s + K_{qs} + K_c} \right) \left(\frac{K_{qt}}{K_p + K_{qt}} \right)} = \frac{K_p}{K_{qt}}$$

fluorescence of the substance is proportional to the concentration of the substance in the solution. The fluorescence of the substance is proportional to the concentration of the substance in the solution.

$$F = \frac{K \cdot I_0 \cdot c \cdot l}{1 + K \cdot c \cdot l}$$

In a dilute solution, the fluorescence is proportional to the concentration of the substance in the solution. In a dilute solution, the fluorescence is proportional to the concentration of the substance in the solution.

$$F = \frac{K \cdot I_0 \cdot c \cdot l}{1 + K \cdot c \cdot l}$$

The expression for the fluorescence of the substance is proportional to the concentration of the substance in the solution. The expression for the fluorescence of the substance is proportional to the concentration of the substance in the solution.

$$F = \frac{K \cdot I_0 \cdot c \cdot l}{1 + K \cdot c \cdot l}$$

The ratio of the fluorescence of the substance is proportional to the concentration of the substance in the solution. The ratio of the fluorescence of the substance is proportional to the concentration of the substance in the solution.

$$F = \frac{K \cdot I_0 \cdot c \cdot l}{1 + K \cdot c \cdot l}$$

The ratio of the fluorescence of the substance is proportional to the concentration of the substance in the solution. The ratio of the fluorescence of the substance is proportional to the concentration of the substance in the solution.

$$F = \frac{K \cdot I_0 \cdot c \cdot l}{1 + K \cdot c \cdot l}$$

Rearranging the expression to give:

$$K_{qt} = K_p \frac{\phi_{qt}}{\phi_p}$$

Substitution of the expression for K_{qt} results in the following:

$$\frac{\phi_p}{\phi_f} = \frac{K_c}{K_s (1 + \frac{\phi_{qt}}{\phi_p})}$$

Rearranging the equation gives the final expression

$$\frac{K_c}{K_s} = \frac{\phi_p + \phi_{qt}}{\phi_f}$$

This shows that it is possible to evaluate the ratio of the crossing rate constant to the fluorescence rate constant from quantum yield measurements.

5. Quenching Yield of the Triplet State.--Appendix I shows that the quenching yield for the rare earth anthranilates was determined on the basis of the quenching yield of gadolinium anthranilate being zero and the total yield being assumed equal to one. The measured quenching yields for the anthranilates are therefore relative to gadolinium anthranilate and are a measure of the number of quanta which is not radiated as being either phosphorescence or fluorescence. The concentrations of the anthranilates are equal within $\pm 2\%$, so that

SECTION 1. The purpose of this section is to provide for the

the following:

1. The purpose of this section is to provide for the

the following:

1. The purpose of this section is to provide for the

the following:

1. The purpose of this section is to provide for the

the following:

1. The purpose of this section is to provide for the

the following:

1. The purpose of this section is to provide for the

the following:

1. The purpose of this section is to provide for the

the following:

1. The purpose of this section is to provide for the

the following:

any concentration quenching is assumed to be small and nearly equal for members of the same series; for at low concentrations ($10^{-5}M$) very little concentration quenching is expected. The same solvent was also used for each sample. The fluorescence quenching is considered to be negligible at liquid nitrogen temperature because solutions of the anthranilates fluoresce even at room temperature.

In order to approximate the fraction of the total energy (absorbed) that is transferred to the rare earth ion, the calculated quenching yields are attributed to quenching of the lowest triplet state only of the chelates. No quenching of singlet states by the rare earth ions is assumed. The data calculated by use of the last equation, are tabulated in Table 13.

any corresponding...
equal for...
tion (1975)...
The same...
science...
nitrogen...
fluorescence...
In order to...
energy (photon)...
the...
of the...
ing of...
data...
Table 1.

TABLE 13

(a) RELATIVE QUANTUM YIELDS AND CROSSING CONSTANT RATIOS FOR RARE EARTH ANTHRANILATES

Compound	ϕ_f	ϕ_p	ϕ_q	K_c/K_s	$\frac{K_{ci}}{K_c \text{ Gd(AnAc)}_3}$	(b) Magnetic Moments
La(AnAc) ₃	.457	.517	0	1.132	.3368	Diamagnetic
Pr(AnAc) ₃	.153	.179	.642	5.237	1.558	3.53
Nd(AnAc) ₃	.062	.054	.880	15.132	4.502	3.55
Sm(AnAc) ₃	.143	.166	.667	5.822	1.750	1.46
Eu(AnAc) ₃	.044	.050	.909	21.991	6.543	3.37
Gd(AnAc) ₃	.240	.807	0	3.361	1.000	8.0
Tb(AnAc) ₃	.133	.133	.735	6.622	1.970	9.3
Dy(AnAc) ₃	.069	.080	.851	13.492	4.014	10.5
Ho(AnAc) ₃	.184	.207	.663	47.31	1.408	10.4
Er(AnAc) ₃	.134	.131	.734	6.434	1.914	9.5
Tm(AnAc) ₃	.060	.107	.755	14.368	4.275	7.3
Yb(AnAc) ₃	.036	.037	.926	26.733	7.954	4.5
Lu(AnAc) ₃	.457	.560	0	1.223	.3648	Diamagnetic

(a) All the measured numbers in this Table are only accurate to $\pm 25\%$.

(b) The magnetic moments are those for the rare earth trivalent ions expressed in Bohr magnetons.

MEMORANDUM

TO : THE SECRETARY OF DEFENSE

FROM : THE SECRETARY OF THE ARMY

SUBJECT: [Illegible]

DATE: [Illegible]

1. [Illegible]

2. [Illegible]

3. [Illegible]

4. [Illegible]

5. [Illegible]

6. [Illegible]

7. [Illegible]

8. [Illegible]

9. [Illegible]

10. [Illegible]

CHAPTER III

DISCUSSION

A. Absorption and Emission

1. Anthranilates.--The luminescence observed for the rare earth chelates of anthranilic acid under excitation in the near ultraviolet region of the spectrum consisted of two intense broad bands, one a fluorescence and the other a phosphorescence. Line emission characteristic of europium, dysprosium, samarium and ytterbium trivalent ions was also observed for the corresponding anthranilates. The data in Table 10 show that anthranilic acid and sodium anthranilate exhibited fluorescence and phosphorescence bands which were similar to those of the rare earth anthranilates. The fluorescence in all cases is attributed to a singlet-singlet electronic transition and the phosphorescence is considered to be a triplet-singlet electronic transition (following Lewis & Kasha's definition)⁽⁴⁾. Since the molecular band emissions of anthranilic acid and its rare earth chelates were observed to be so similar, the lowest excited electronic states in the chelating agent appear to be perturbed only slightly when the ligand is bonded to the central ion in a chelate.

The general features of the absorption spectra in the near ultraviolet region for the anthranilates of the rare earths and anthranilic acid were also very similar (see Figures 4 & 5). The absorption coefficients at the band maxima for the anthranilates were approximately the same (15% variation). The corresponding absorption coefficient for anthranilic acid, however, was considerably lower (approximately 50%) than that for the chelates (see Table 10).

2. 8-Hydroxyquinolates and 2-Methyl-8-Hydroxyquinolates.--The phosphorescence emission from the parent chelating agent in both cases was so weak that it could not be photographed with a reasonable exposure time. It has been observed that gadolinium, lanthanum and lutecium ions enhance the phosphorescence in chelate compounds. Reliable phosphorescence measurements for the 8-hydroxyquinolates and the 2-methyl-8-hydroxyquinolates were obtained only for the corresponding chelates of gadolinium, lanthanum and lutecium. It was not possible to obtain a satisfactory photograph of the phosphorescence emission of the other chelates in these two series because there is no appreciable enhancement of phosphorescence upon chelation to the other rare earth ions. Extremely weak phosphorescence spectra were observed under prolonged exposures. Because of the extreme weakness and diffuseness of these bands, they are attributed to decomposition or dissociation products. The fluorescence emission,

The present study was designed to determine the effect of the concentration of the solution on the rate of the reaction. The reaction was carried out in a closed system at a constant temperature of 25°C. The concentration of the solution was varied from 0.1 M to 0.5 M. The rate of the reaction was determined by measuring the volume of gas evolved at regular intervals of time. The results are shown in the following table:

Concentration of solution (M)	Rate of reaction (ml/min)
0.1	1.2
0.2	2.4
0.3	3.6
0.4	4.8
0.5	6.0

From the above table, it is evident that the rate of the reaction increases with the increase in the concentration of the solution. This is because the rate of the reaction is directly proportional to the concentration of the solution. The results of the present study are in agreement with the results of the previous studies.

however, was readily photographed for all the chelates of both series. Line emission was observed only for the europium and ytterbium chelates of these series of compounds.

The absorption spectra of the 8-hydroxyquinolates and 2-methyl-8-hydroxyquinolates extended to lower frequencies than those of the parent chelating agents (see Figures 6, 7, 8 and 9). Moeller⁴¹ has shown that these long wavelength peaks also appear in acidic and basic solutions of 8-hydroxyquinoline. This indicates that a similar type electronic transition occurs for 8-hydroxyquinoline in acidic or basic media as occurs for chelates of 8-hydroxyquinoline. The absorption coefficients of the band peaks for the parent chelating agent and the chelates cannot be directly compared because they probably represent two different electronic transitions. The fluorescence bands for the chelates and the parent chelating agents are similar. The electronic transitions causing the molecular band luminescence in the complexes are attributed to slightly perturbed transitions occurring in the chelating agent alone. Investigations⁴³ on other chelates (Al, Tl, Ga) of 8 HQ show that the absorption spectra have features similar to the rare earth chelates.

3. Line Emission.--Excitation of the trivalent rare earth ions with light containing frequencies which are absorbed directly by the ions is followed by characteristic line emission for certain rare earth trivalent ions. Characteristic

line luminescence of certain rare earth trivalent ions is also obtained by irradiation with light absorbed only by the organic part of some chelate compounds. Dieke and co-workers have shown that direct excitation of Gd^{+++} , Sm^{+++} , Tb^{+++} , Eu^{+++} and Dy^{+++} in hydrated chlorides results in strong line emission of varying intensity. The coordinated gadolinium trivalent ion is the brightest line emitter of all, Eu^{+++} and Tb^{+++} follow in intensity, Sm^{+++} and Dy^{+++} are somewhat weaker. The remaining ions of the rare earth series fluoresce only weakly or not at all. The relative line intensities of Eu^{+++} , Tb^{+++} and Sm^{+++} observed for the rare earth chelates parallel those observed for the hydrated chlorides.

B. The Path of Energy Transfer

1. The Existence of Energy Transfer.--The absorption spectra of rare earth chlorides in water solution and the near ultraviolet regions show the existence of several absorption peaks which have molar extinction coefficients in the range of 0.2-100.⁴⁴

The strong absorption peaks which are present in chelate molecules obscure any low intensity peaks which are present in the rare earth ions. The excitation of the rare earth chelate samples was accomplished by appropriate filters as shown in Table 4 in the Experimental Section. Ytterbium

trichloride exhibits an absorption peak at 9725A with molar absorption coefficient of 1.90. The excitation of the rare earth chelate samples is done with light of 3200-4500 A wavelength range, thereby not exciting the 9725A peak. It is apparent that whenever line emission is observed from rare earth chelates energy must transfer from the organic portion of the compound to the ion because the exciting light does not contain the required wavelength range for direct excitation of the 9725A peak of the ytterbium ion.

All the other trivalent ions studied contain absorption peaks which are in the wavelength range of the exciting light used for photographing emission from chelate samples. Enhancement of absorption of the trivalent rare earth ion by the surrounding ligands to make direct excitation of the ion possible is discounted because a comparison of line emission observed for 8 HQ chelates of europium to that observed for rare earth hydrated inorganic salts reveals little or no shift in the position of lines. Any interactions which might enhance the absorption peaks of the ions when chemically bonded in chelates would probably also affect the relative positions of the resonance levels resulting in significant shifts of the lines, which are not experimentally observed.

Weissman³¹ has shown that the intensity of line emission for chelates of europium increases considerably over that observed for the hydrated rare earth chloride whenever a sample

is excited with monochromatic light which is largely absorbed by the chelate molecule. The classification of luminescence in rare earth chelates shows that whenever the ligand is varied for a given ion, line emission is not always observed (see Table 8). The absence of line emission in some cases is further evidence that energy is actually being transferred from the organic portion of the molecule to the rare earth ion. The anomalous behavior of the gadolinium trivalent ion which exhibits no line emission in any of the chelate compounds studied will be discussed later.

2. The Resonance Levels.--The positions of the emitting (resonance) levels for the rare earth ions have been established by absorption and emission studies on hydrated inorganic salts (see Introduction). The resonance level of trivalent ytterbium has also been determined by the use of Yb tris-dibenzoylmethide. Table 14 shows the measured values of the resonance levels for the relatively bright line emitters. The remaining ions fluoresce so weakly that their emitting levels have not been definitely established.

3. The Triplet State.--The data on Table 8 indicate that line emission does not always occur as the ligand is varied for a given rare earth ion. This puzzling behavior was also observed by Crosby and Whan³⁴ in a study of dysprosium, thulium and terbium chelates of benzoylacetone, dibenzoylmethane and tribenzoylmethane. Characteristic Dy^{+++} line

is excited with much more
by the electric field
in the case of the
various other cases (see Table I)
(see Table I) the electric field
further evidence of the
from the electric field
ion. The electric field
which exists in the
points of the
of the electric field
than (see Table I)
established a
inorganic salts (see Table I)
crystalline structure
in the electric field
of the electric field
case. The electric field
existing in the
of the electric field
varied for a
was also observed
thinning and
between the

emission was observed for the dysprosium trisbenzoylacetate but not for dysprosium trisdibenzoylmethide. This behavior was explained by comparing the position of the lowest triplet state to the position of the emitting level of the rare earth ions. It was determined that line emission occurs only when the lowest triplet state of the complex lies above the resonance level of the ion, or possibly only slightly below it.

The triplet state measurements in Table 10 and the resonance levels of the rare earth ions in Table 14 are plotted in Figure 22 on an energy level diagram. Attention is focused on those rare earth ions which emit relatively bright lines while complexed in a chelate compound. Perusal of Figure 22 shows that line emission occurs only in the cases where the triplet state of the complex lies above the resonance level of the ion.

4. The Individual Trivalent Rare Earth Ions.--The chelates of 8-hydroxyquinoline, anthranilic acid and 2-methyl-8-hydroxyquinoline will be discussed here; those of salicylaldehyde will be discussed in Appendix II. Lanthanum and lutecium trivalent ions do not have electronic transitions in the visible and the infrared. No line emission was observed for any chelates of these two ions studied.

These observations agree with the proposal that energy transfer to the rare earth ion occurs via the triplet state

emission was 1.5...
...but not...
...behavior was...
...lowest...
...of the...
...with...
...than...
...only...
...the...
...response...
...of the...
...in...
...of...
...of...
...the...
...the...
...of...
...of...
...and...
...in...
...as...
...these...
...to...

TABLE 14
 RESONANCE LEVELS OF SOME RARE EARTH IONS

Compound	Ion	Resonance Level		Reference
		A	cm ⁻¹	
$\text{Eu}_2(\text{C}_2\text{H}_5\text{SO}_4)_3 \cdot 9\text{H}_2\text{O}$	Eu^{+++}	5257	19,015	30
$\text{Eu}_2(\text{C}_2\text{H}_5\text{SO}_4)_3 \cdot 9\text{H}_2\text{O}$	Eu^{+++}	5795	17,257	30
$\text{GdCl}_3 \cdot 6\text{H}_2\text{O}$	Gd^{+++}	3118	32,066	48
$\text{TbCl}_3 \cdot 6\text{H}_2\text{O}$	Tb^{+++}	4895	20,430	49
$\text{DyCl}_3 \cdot 6\text{H}_2\text{O}$	Dy^{+++}	4772	20,957	27
YbD_3 (a)	Yb^{+++}	9708	10,300	33
$\text{YbCl}_3 \cdot 6\text{H}_2\text{O}$	Yb^{+++}	9708	10,300	23
$\text{SmCl}_3 \cdot 6\text{H}_2\text{O}$	Sm^{+++}	5618	17,800	50
$\text{TmCl}_3 \cdot 6\text{H}_2\text{O}$	Tm^{+++}	4695	21,300	51

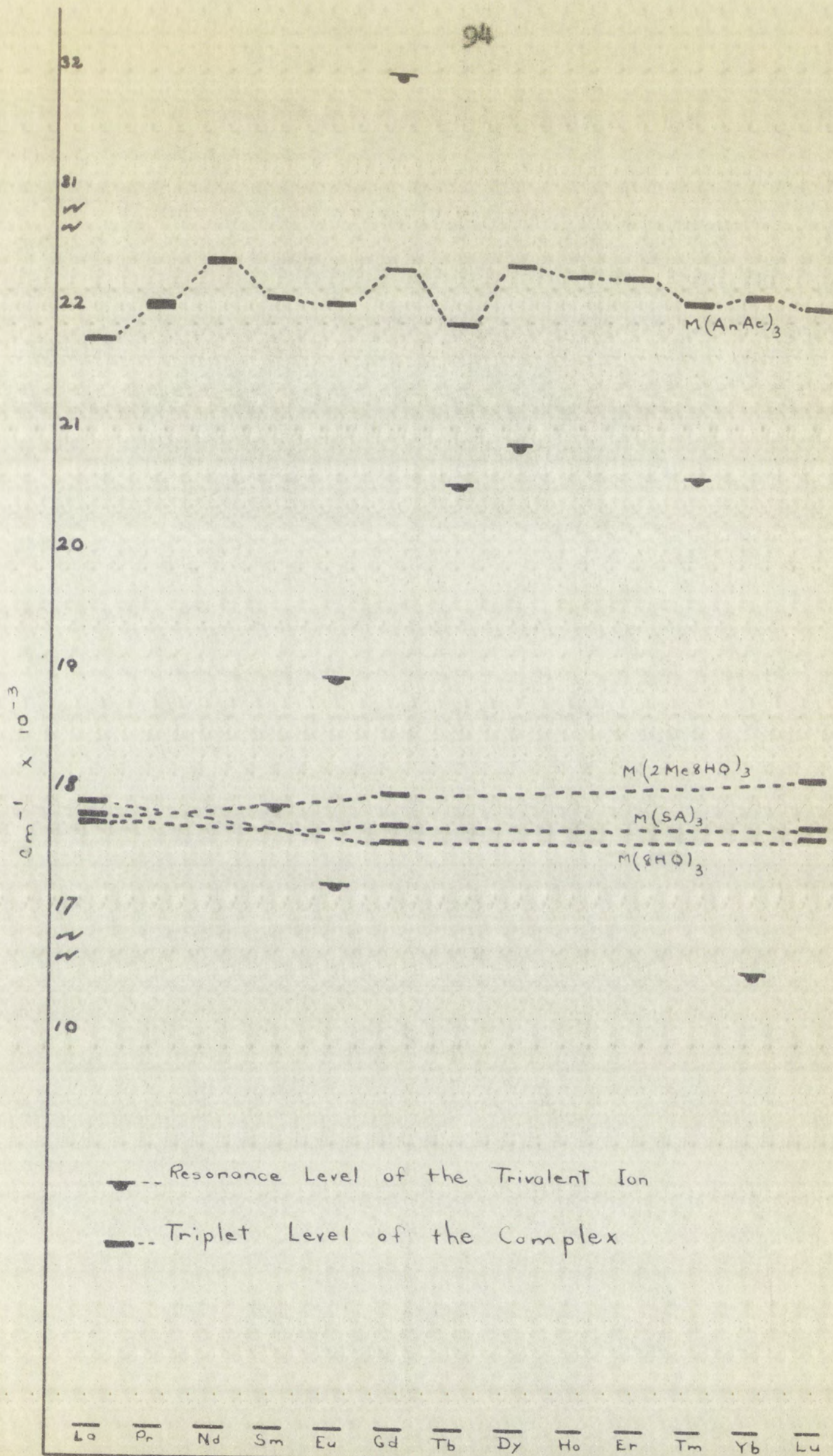
(a) D = Dibenzoylmethide ion

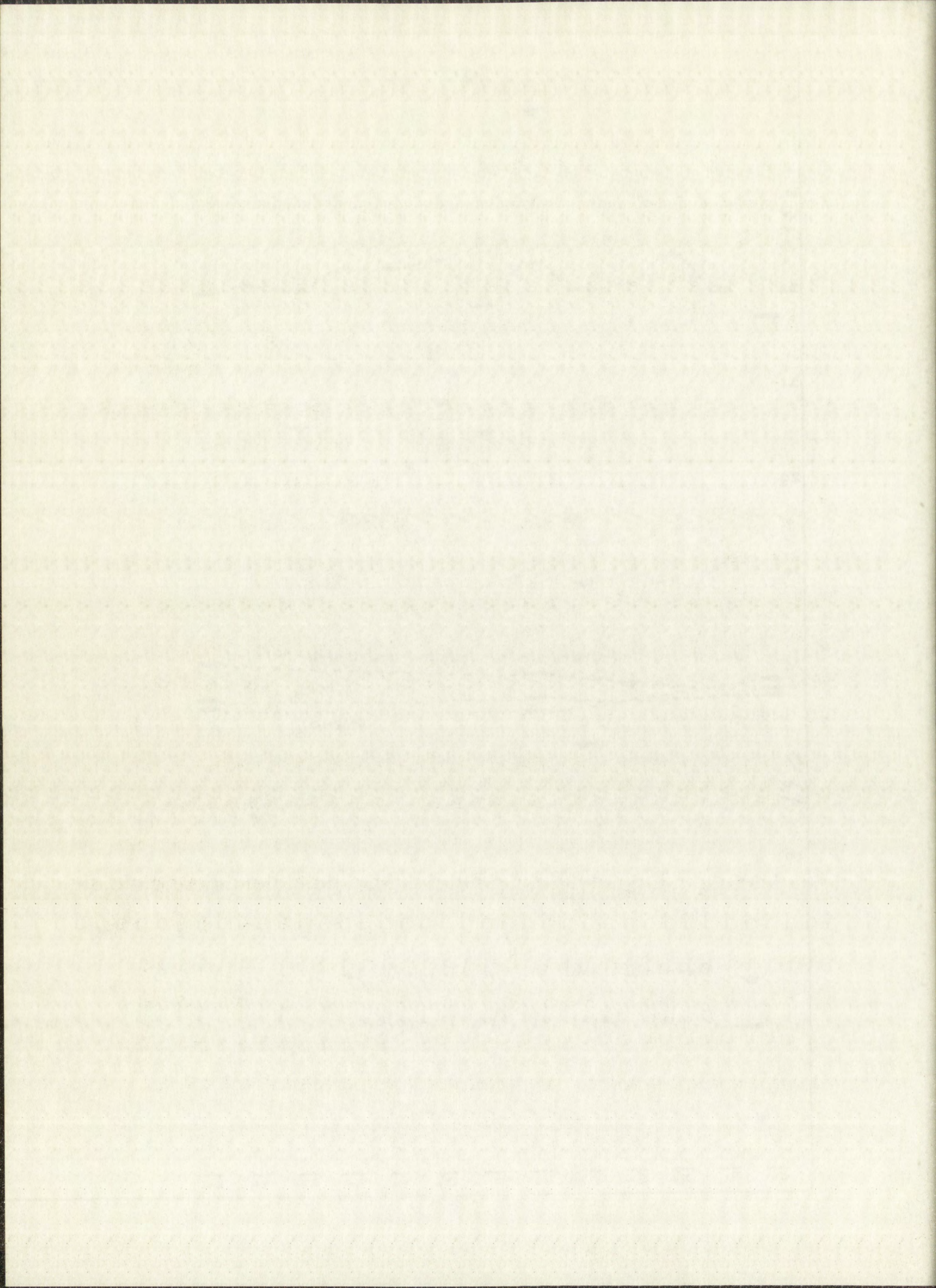
FIGURE 22

Energy Level Diagram

Rare Earth Ions Resonance Levels

Triplet States of Chelates





of the complex. No line emission has been observed for lanthanum and lutecium even in the hydrated chlorides. The effect of lanthanum and lutecium upon chelation is to increase the singlet-triplet mixing of the complexes and consequently increase the phosphorescence yield. As previously indicated, line emission has been observed for the trivalent gadolinium ion in hydrated chlorides and the lowest frequency transition which is a source of line emission lies at 32065 cm^{-1} . Figure 22 shows that it is energetically impossible to transfer energy to the gadolinium ion in any of the chelates studied, because the energy required to excite the resonance level of the gadolinium ion is greater than the exciting light used. Gadolinium enhances the phosphorescence of the complexes to a greater extent than either lanthanum or lutecium.

Praseodymium and neodymium trivalent ions emit characteristic lines in the hydrated chlorides which are weak.⁴⁹ No line emission from chelates of these two ions was observed for the compounds studied. The fact that characteristic line emission is observed in certain cases indicates that there are low energy resonance levels present. The absence of line emission in these two ions for those cases studied is attributed to the following, (i) the inherently weak line emission of the ions, (ii) the weak phosphorescence as in chelates of 8-hydroxyquinoline and 2-methyl-8-hydroxyquinoline,

(iii) inefficient energy transfer due to a greater degree of ionic bonding in the anthranilates. A decrease in efficiency of transfer due to a greater degree of ionic bonding has also been observed by Weissman³¹ in a study of various europium chelates. The dibenzoylmethide of europium was the strongest line emitter followed by the picrate, and finally the platinocyanide emitted no lines at all.

No attempt was made to detect line emission from Ho^{+++} in the chelates studied primarily because of the factors discussed above. The energy level diagram²⁶ for Er^{+++} indicates that any line emission occurring is expected in the infrared region beyond the limits of photographic techniques. Very weak line emission for Ho trisdibenzoylmethide and Ho trisbenzoylacetonate has been reported.³⁵

The trivalent ion of terbium has been observed to be a relatively bright emitter even in the case where energy is not transferred efficiently to the ion (eg. $\text{Tb}(\text{AnAc})_3$). No line emission for terbium chelates of 2-methyl-8-hydroxyquinoline and 8-hydroxyquinoline was photographed. The triplet state lies below the resonance level of terbium in these two cases.

The chelates of dysprosium and ytterbium follow the expected behavior in all three cases. Line emission for Yb^{+++} was first reported by Crosby and Kasha,³³ and later was corroborated by R. E. Whan³⁸ in ytterbium chelates of

benzoylacetone and dibenzoylmethane. Line emission was exhibited by three ytterbium chelates reported here.

Characteristic Sm^{++} lines were present only for samarium anthranilate. The Sm^{++} resonance level lies very close to the triplet states of the corresponding chelates of 2-methyl-8-hydroxyquinoline and 8-hydroxyquinoline. The margin of error for these triplet state measurements makes it difficult to determine whether or not the triplet state energy level lies above the resonance level of the trivalent samarium ion. Since no lines were observed for the samarium chelates in these two cases, the triplet state of the complex is designated to be below the resonance level of Sm^{++} .

5. The Exceptional Case of Europium.--It has definitely been established that the europium trivalent ion possesses two distinct emitting levels.³⁰ Fluorescence and absorption spectra of single crystals of europic ethyl-sulfate nonahydrate have established the observed line emission as originating at energy levels of 17250 cm^{-1} and $19,020\text{ cm}^{-1}$. A close examination of the characteristic line emission for europium 8-hydroxyquinolinolate and europium 2-methyl-8-hydroxyquinolate reveals that the highest frequency line appears at approximately $17,250\text{ cm}^{-1}$. This indicates that the observed line emission of europium 8-hydroxyquinolate and 2-methyl-8-hydroxyquinolate originates at the $17,250\text{ cm}^{-1}$ level and that no line emission originating at the $19,020\text{ cm}^{-1}$

is observed. Long exposures of the line emission in these two chelates still showed no line emission at higher frequencies.

The triplet state measurement for the 8-hydroxyquinolates is at $17,800\text{ cm}^{-1}$ and that for 2-methyl-8-hydroxyquinolate is at $18,000\text{ cm}^{-1}$ (these figures represent averages of the corresponding chelates of trivalent gadolinium, lanthanum and lutecium). It is evident that the triplet state energy levels for these two series of rare earth chelates are between the two measured resonance levels of Eu^{+++} . The lowest frequency line measurement indicates that there is little or no shift in the resonance levels of the ion when chemically bonded in chelates. The anthranilate chelate series exhibits line emission from both resonance levels of europium. The anthranilates have a measured triplet level of about $22,500\text{ cm}^{-1}$.

The observed line emission of the europium 8-hydroxyquinolates and europium 2-methyl-8-hydroxyquinolates has shown that by variation of the ligand for europium it is possible to obtain a chelate with a triplet state which lies between the two existing resonance levels. This observation definitely establishes that the path of energy transfer is via the lowest triplet state or a nearby state.

is observed. Two crystals still remain in the
position.
The first has been removed. The second
later is at 17,000 cm⁻¹. The third
later is at 16,000 cm⁻¹. The fourth
the corresponding value of 16,000 cm⁻¹.
and later. It is 16,000 cm⁻¹.
levels for these two bands. The
the two measured values. The
energy level measurement. The
shift in the resonance. The
banded in crystals. The
the extension from the
anthracene have been
cm⁻¹.
The observed value is 16,000 cm⁻¹.
polarized and oriented. The
shown that by rotation of the
possible to obtain a value of 16,000 cm⁻¹.
between the two values. The
definitely established that the
the lowest crystal state is a

C. Possible Reasons for Radiationless Intersystem Crossing

1. Spin Orbit Coupling.--The radiationless transition probability between the electronic states responsible for fluorescence and phosphorescence is proportional to the square of the matrix element w_{pf} of the perturbation function, w . The matrix element, w_{pf} can be expressed as follows:

$$1. \quad w_{pf} = \int \psi_p^* w \psi_f d\tau$$

ψ_f = eigenfunction of the first excited singlet

ψ_p^* = complex conjugate of the eigenfunction of the phosphorescence state.

To a good approximation the eigenfunctions of the initial and final states can be expressed as a product of the vibrational, rotational and electronic wave functions.¹¹

$$2. \quad \begin{aligned} \psi_f &= \Phi_f^e \Phi_f^v \Phi_f^r \\ \psi_p &= \Phi_p^e \Phi_p^v \Phi_p^r \end{aligned}$$

Φ^e = a function of the positions of the electrons and the nuclei.

Φ^v = a function of the internuclear distance alone.

Φ^r = a function of the orientation of the molecule in space and is independent of internuclear distance.

The electronic wave function (Φ^e) can be further separated into a product of spin and orbital functions.

$$3. \quad \begin{aligned} \Phi_f^e &= (\phi_f^o)(\chi_f^s) \\ \Phi_p^e &= (\phi_p^o)(\chi_p^s) \end{aligned}$$

1. Let us consider a system of two particles, each of mass m , moving in a potential $V(x_1, x_2)$. The Hamiltonian of the system is

$$H = \frac{p_1^2}{2m} + \frac{p_2^2}{2m} + V(x_1, x_2)$$

The wave function $\psi(x_1, x_2)$ satisfies the Schrödinger equation

$$H\psi = E\psi$$

$$1. \psi_0 = \psi_0(x_1, x_2)$$

2. The wave function ψ_0 is a solution of the Schrödinger equation with energy E_0 . The wave function ψ_0 is a function of the coordinates x_1 and x_2 . The energy E_0 is a constant.

3. To a good approximation, the wave function ψ_0 is a function of the coordinates x_1 and x_2 . The energy E_0 is a constant.

$$\psi_0 = \psi_0(x_1, x_2)$$

$$\psi_0 = \psi_0(x_1, x_2)$$

4. The wave function ψ_0 is a function of the coordinates x_1 and x_2 . The energy E_0 is a constant.

5. The wave function ψ_0 is a function of the coordinates x_1 and x_2 . The energy E_0 is a constant.

6. The wave function ψ_0 is a function of the coordinates x_1 and x_2 . The energy E_0 is a constant.

$$\psi_0 = \psi_0(x_1, x_2)$$

$$\psi_0 = \psi_0(x_1, x_2)$$

$$\psi_0 = \psi_0(x_1, x_2)$$

7. The wave function ψ_0 is a function of the coordinates x_1 and x_2 . The energy E_0 is a constant.

The part of the matrix element due to the electronic eigenfunction can be considered as a product of two integrals, which involve the spin and orbital functions.

$$4. \omega_{ps}^e = \left(\int \phi_p^{o*} \omega^o \phi_s \right) \left(\int \chi_p^s \omega^s \chi_p^s \right)$$

If either of these two integrals is zero, the matrix element will be zero and the transition probability between these two states will also be zero. The transition probability between a pure singlet and a pure triplet is zero because the triplet spin function is symmetric with respect to electron interchange and the singlet spin function is antisymmetric with respect to electron interchange. In other words, the selection rule of the conservation of spin is also applicable for non-radiative transitions.¹⁰

In the presence of spin orbit coupling the perturbed triplet level may be designated as a sum of two wave functions representing the pure triplet and pure singlet.

$$5. \psi_p = a \psi_T + b \psi_s$$

The radiationless transition probability between the fluorescence and the phosphorescence levels is proportional to the square of the matrix element, which in turn can be approximated as follows:⁹

$$6. \omega_{pf} = \int (a \psi_T + b \psi_s)^* \omega \psi_s d\tau$$

$$\text{where } a^2 + b^2 = 1$$

$$7. \omega_{pf} = \int b \psi_s \omega \psi_s d\tau$$

The first of these is the fact that the
 eigenfunction can be written as a sum of two
 which involve the same energy levels.

$$\psi_2 = \frac{1}{\sqrt{2}} (\psi_1 + \psi_3)$$

If either of these is chosen, the
 element will be zero and the wavefunction
 these two states will also be zero. The
 strictly between a pair of states is
 because the triplet state is not allowed
 to electron interactions and the
 antisymmetric. The triplet state is
 other words, the triplet state is the
 is also applicable for the triplet state.
 In the case of the triplet state, the
 triplet level may be higher than the
 representing the two states and the

$$\psi_2 = \frac{1}{\sqrt{2}} (\psi_1 + \psi_3)$$

The triplet state is the
 fluorescence and the triplet state is
 to the square of the triplet state and is
 approximated as follows:

$$\psi_2 = \frac{1}{\sqrt{2}} (\psi_1 + \psi_3)$$

 where ψ_1 and ψ_3 are the

$$\psi_1 = \frac{1}{\sqrt{2}} (\psi_1 + \psi_3)$$

The magnitude of the matrix element is directly dependent on the degree of spin orbit coupling. For a strong perturbation the coefficient, b , becomes greater and therefore the radiationless transition becomes more probable.

The spin orbit interaction, which is the magnetic interaction between the orbital motion of the electron and the electron spin magnetic moment definitely enhances the singlet-triplet radiationless transition in atoms and probably also in molecules⁹.

The ratio of the crossing rate constant to the fluorescence rate constant in Table 13 shows that for the rare earth anthranilate chelates the intersystem crossing probability is on the same order of magnitude as the singlet to ground state transition probability. That a paramagnetic effect is unspecific is demonstrated by the fact that the crossing rate constants for the anthranilates have no simple relationship to the magnetic moments of the ions. The data in Table 13 show only that the crossing rate constants are larger for the anthranilates of paramagnetic rare earth ions than for corresponding chelates of diamagnetic ions (La^{+++} and Lu^{+++}).

The lack of a direct relationship between the crossing constant of the rare earth anthranilate chelates and the magnetic susceptibilities of the rare earth ions implies the existence of some other important effect. The importance of



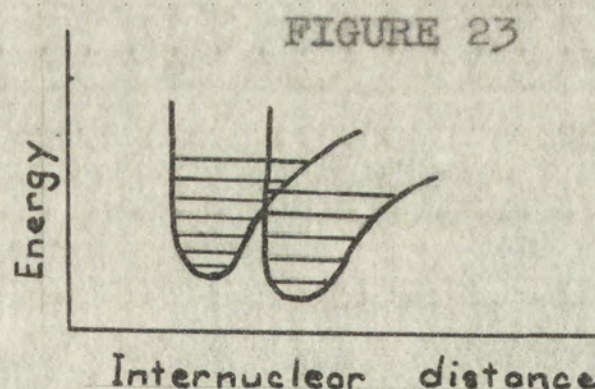
vibrational interaction for singlet-triplet radiationless transitions will be discussed in the following section.

2. Vibrational Interaction.--For the singlet-triplet radiationless transition, the portion of the matrix element depending on the vibrational eigenfunction is expressed as follows:

$$8. \omega_{ST}^v = \int \Phi_S^v \omega^v \Phi_T^v d\tau$$

The function ω^v is the perturbation function which depends on nuclear coordinates. The magnitude of the vibrational matrix element depends on two factors: (i) the degree of change in nuclear position of the singlet with respect to the triplet, thereby affecting the crossing of potential energy surfaces, (ii) the change in angular momentum of the singlet compared to the triplet¹⁰.

Figure 42 represents schematically the potential well surfaces (as demonstrated by Kauzman¹¹) for the singlet and triplet levels of typical organic compounds.



S = schematic potential well surface of the first excited singlet of the anthranilates.

T = schematic potential well surface of the lowest triplet of the anthranilates.

The function ω_{st} is defined as the ratio of the
 transition probability P_{st} to the stationary probability π_s
 of state s . It is a function of the state s and the target state t .
 depending on the value of t .

$$\omega_{st} = \frac{P_{st}}{\pi_s}$$

The function ω_{st} is a function of the state s and the target state t .
 It is a function of the state s and the target state t .
 It is a function of the state s and the target state t .
 It is a function of the state s and the target state t .
 It is a function of the state s and the target state t .

Figure 1 shows the function ω_{st} for a Markov chain with three states.
 The function ω_{st} is a function of the state s and the target state t .



Figure 1 shows the function ω_{st} for a Markov chain with three states.
 The function ω_{st} is a function of the state s and the target state t .
 The function ω_{st} is a function of the state s and the target state t .
 The function ω_{st} is a function of the state s and the target state t .

As shown in Figure 23, the position of the minimum of the singlet with respect to the triplet is probably very similar for the different rare earth chelates of the anthranilate series. The first factor mentioned above consequently, has only a small effect on the magnitude of the vibrational matrix element for different members of the anthranilate series. The second factor, however, certainly varies in magnitude from ion to ion for the rare earth anthranilate series. The transition probability will be small whenever the alteration of angular momentum is large.

The data in Table 13 show a variation in the crossing constant from ion to ion, but show no apparent functional relationship to the magnetic moments of the trivalent ions. The effect of paramagnetism on the crossing constants seem to be the same for different members of the series regardless of the magnetic moments. The variation in the experimentally determined crossing constants for different members of the series is probably not significant because of the large experimental error.

D. Possible Reasons for Radiative Triplet-Singlet Transitions

1. Spin-Orbit Coupling.--The triplet to singlet radiative transition probability is proportional to the integral of the dipole moment across the electronic wave functions of both states. Mixing of the singlet and triplet makes this transition

allowed¹¹.

The same wave function that describes the phosphorescence state in the singlet to triplet radiationless transition also describes it in the triplet to singlet radiative transition (see equations). The transition probability for the triplet to singlet radiative transition is not as large as that for the first excited singlet to triplet radiationless transition. The transition probability for the singlet to triplet radiationless transition is the same order of magnitude as the singlet-singlet radiative transition ($\sim 10^8 \text{ sec}^{-1}$). On the other hand, the transition probability for the triplet-singlet radiative transition is approximately 10 sec^{-1} . The reason for this large difference perhaps lies in a consideration of the vibrational portion of the matrix element.

2. Vibrational Interaction.--Since the phosphorescence state can be approximately described as a sum of a singlet and triplet with proper coefficients, assuming non-zero spin orbit coupling, it is certain that the triplet-singlet transition is allowed. The vibrational term for this transition, however is smaller in general than for the singlet-triplet radiationless transition. The alterations of nuclear position are smaller for the triplet-singlet transition than for the corresponding alterations for the singlet-triplet transition. Some of the variation in the observed mean life of phosphorescence for the different members of the anthranilate series could be

due to variations in the nuclear positions. In other words, the vibrational part of the matrix element might play an important role in the magnitude of the transition probability for the singlet-triplet transitions. As in the case of the singlet-triplet radiationless transition, the magnetic susceptibilities of the rare earth ions have no direct relationship to the triplet to ground state transition probability (see Table 13).

The fact that the phosphorescence quantum yields are relatively higher for gadolinium, lanthanum and lutecium anthranilates merely indicates that no energy is being transferred to the rare earth ion. This experimental fact is not surprising because there are no levels in the rare earth ion below the lowest triplet state of the complex.

E. Possible Reasons for Energy Transfer to the Rare Earth Ion

1. Spin Transfer.--The process of energy transfer to the metal ion in rare earth chelates involves two systems of electronic levels. One system is that of the complex and the other is that of the rare earth ion. The path of energy transfer proceeds via the lowest or a nearby triplet. The resultant spin of the initial state of the complex involved in the energy transfer process can be approximated from the coupling of spins of the ground configuration of the ion and the lowest triplet state of the complex. The resultant spin of the final state

for this process can be obtained from the spin coupling of the lowest triplet state of the complex and the resonance level of the ion.

Consider the ytterbium trivalent chelates as a typical example:

$$M(S = \frac{1}{2})A_3(S = 1) = M(S = \frac{1}{2})A_3(S = 0)$$

MA_3 = the rare earth chelate

S = the spin quantum number

The resultant electron spin of the initial state is $S = \frac{1}{2}$ or $3/2$; that for the final state can only be $S = \frac{1}{2}$. If the orientation of spins is such that the resultant spin for the initial state is $\frac{1}{2}$, then the process of energy transfer to the rare earth ion with subsequent line emission is allowed because spin is conserved.

Table 15 shows that the spin can be conserved by proper spin orientation of the metal ion and the rest of the complex respectively for other members of the rare earth series for which line emission has been observed. The spin transfer process is completely independent of the rare earth ion magnetic susceptibilities. Porter and Wright⁴⁵ have shown that the phosphorescence quenching of naphthalene due to paramagnetic ions in solution is not directly related to the magnetic susceptibilities. The quenching yields for the anthranilates shown in Table 13 do not show a direct relationship to the paramagnetism of the rare earth ions.

TABLE 15

(a) GROUND STATE AND RESONANCE LEVEL CONFIGURATIONS
OF THE RARE EARTH TRIVALENT IONS

Ion	Ground State	(b) Spin	(c) Spin Resultant	(d) Level Resonance	Spin	(e) Spin Resultant
La ⁺⁺⁺	1s ₀	0	1	3p ₀	1	1
Pr ⁺⁺⁺	3H ₄	1				
Nd ⁺⁺⁺	4I _{9/2}	3/2				
Sm ⁺⁺⁺	6H _{5/2}	5/2	3,2,1	5D ₁ , 5D ₀	2	2
Eu ⁺⁺⁺	7F ₀	3				
Gd ⁺⁺⁺	8S _{7/2}	7/2				
Tb ⁺⁺⁺	7F ₆	3	3,2,1	5D ₄	2	2
Dy ⁺⁺⁺	6H _{15/2}	5/2	7/2, 5/2, 3/2	6F _{11/2}	5/2	5/2
Ho ⁺⁺⁺	5I ₈	2				
Er ⁺⁺⁺	4I _{15/2}	3/2				
Tm ⁺⁺⁺	3H ₆	1				
Yb ⁺⁺⁺	2F _{7/2}	1/2	1/2, 3/2	2F _{5/2}	1/2	1/2
Lu ⁺⁺⁺	1s ₀	0				

(a) Only the ions from which line emission was observed in this study are considered.

(b) Spin quantum number of the ground state.

(c) The numbers in this column are the resultant electron spin of mixing the triplet of the complex and the resonance level of the ion.

(d) The numbers in this column are the resonance level configuration of the trivalent rare earth ions.

(e) The numbers in this column are the resultant electron spin of mixing the singlet of the complex and the ground state of the ion.

(a) GROUPED DATA (b) INDIVIDUAL DATA

Ion	Grouped Data	Individual Data
Li+++	1.0	1.0
Na+++	2.0	2.0
K+++	3.0	3.0
Rb+++	4.0	4.0
Ca+++	5.0	5.0
Sc+++	6.0	6.0
Ti+++	7.0	7.0
V+++	8.0	8.0
Cr+++	9.0	9.0
Mn+++	10.0	10.0
Fe+++	11.0	11.0
Co+++	12.0	12.0
Ni+++	13.0	13.0
Cu+++	14.0	14.0
Zn+++	15.0	15.0
Ga+++	16.0	16.0
Ge+++	17.0	17.0
As+++	18.0	18.0
Se+++	19.0	19.0
Br+++	20.0	20.0
Kr+++	21.0	21.0
Rb+++	22.0	22.0
Sr+++	23.0	23.0
Y+++	24.0	24.0
Zr+++	25.0	25.0
Nb+++	26.0	26.0
Mo+++	27.0	27.0
Tc+++	28.0	28.0
Ru+++	29.0	29.0
Rh+++	30.0	30.0
Pd+++	31.0	31.0
Ag+++	32.0	32.0
Cd+++	33.0	33.0
In+++	34.0	34.0
Sn+++	35.0	35.0
Pb+++	36.0	36.0
Bi+++	37.0	37.0
Po+++	38.0	38.0
At+++	39.0	39.0
Tl+++	40.0	40.0
Pb+++	41.0	41.0
Bi+++	42.0	42.0
Po+++	43.0	43.0
At+++	44.0	44.0
Rn+++	45.0	45.0

(c) Only the first three ions are shown in this table. The remaining ions are shown in the following tables.

(d) The following table shows the relative concentrations of the ions in the atmosphere.

(e) The following table shows the relative concentrations of the ions in the ocean.

(f) The following table shows the relative concentrations of the ions in the soil.

(g) The following table shows the relative concentrations of the ions in the rocks.

(h) The following table shows the relative concentrations of the ions in the plants.

(i) The following table shows the relative concentrations of the ions in the animals.

(j) The following table shows the relative concentrations of the ions in the human body.

The conservation of spin by proper spin orientation suggests that the spin part of the matrix element in the electronic transitions for the energy transfer and line emission process is equal in magnitude for different members of the rare earth anthranilates. The fact that the quenching yields are not the same for different rare earth ions in the same chelate series probably lies in a consideration of the vibrational portion of the matrix element.

2. Vibrational Interaction.--The radiationless transition probability from the lowest or a nearby triplet of the complex to the resonance level of the ion varies from ion to ion. This variation is experimentally demonstrated in the anthranilate series by quenching yields. The nuclear position with respect to crossing of these two potential energy surfaces certainly varies from ion to ion. As in the case of the singlet-triplet radiationless transition, the magnitude of the vibrational matrix element probably depends on the alteration of nuclear positions. The transition probability between the lowest or a nearby triplet and the resonance level varies because of existing differences in magnitude of the spin matrix element and in the nuclear position.

Whenever large amounts of energy are transferred to the ion (eg. europium anthranilate), the nuclear positions and consequently the crossing of potential energy surfaces is such that the magnitude of the matrix element is relatively large,

The orientation of spin by proper spin orientation suggests that the spin part of the matrix element in the electronic transition for the energy transfer and thus electron process is equal in magnitude for different members of the rare earth anion. The fact that the quenching yields are not the same for different rare earth ions in the same crystal series probably lies in a consideration of the vibrational portion of the matrix element.

3. Vibrational Interaction.--The vibrational interaction probably from the lowest or a nearby triplet of the complex to the resonance level of the ion varies from ion to ion. This variation is experimentally demonstrated in the magnetic series by quenching yields. The nuclear position with respect to crossing of these two potential energy surfaces certainly varies from ion to ion. As in the case of the singlet-triplet radiativeless transitions, the magnitude of the vibrational matrix element probably depends on the orientation of nuclear positions. The transition probability between the lowest or a nearby triplet and the resonance level varies because of existing differences in magnitude of the spin matrix element and in the nuclear position.

However large amounts of energy are transferred to the ion (e.g. europium anion), the nuclear positions and consequently the crossing of potential energy surfaces is such that the magnitude of the matrix element is relatively large.

but it is difficult to say whether the change of nuclear positions alone determines the magnitude of the vibrational matrix element. It is certainly true that the alteration of nuclear position and the alteration of angular momentum both have a significance in the two systems such that the transition probability is greater for the triplet to resonance level than for triplet-singlet transition.

F. Electronic Transitions for Other Rare Earth Chelate Series

Although quantum yields have not been measured on all of the chelate series studied, the electronic transitions occurring in the rare earth chelates are probably all controlled by spin orbit coupling, spin transfer and vibrational interaction.

Visual estimates of the mean lives of line emission and phosphorescence indicate that in most cases the mean lives of the lines are shorter than that of the phosphorescence. Trivalent terbium and europium lines in all chelate samples can be seen through the phosphoroscope indicating that the mean life of these lines is equal to or greater than 10^{-4} sec. Whenever line emission is shorter lived than the phosphorescence, energy transfer probably occurs from higher vibrational levels of the triplet to some vibronic levels of the metal ion. This type of transfer may be important for some of the chelates in this study (eg. Sm^{+++} , Dy^{+++} chelates).

but it is difficult to see how it could be
positioned along the axis of the crystal
matrix element. It is also possible
of nuclear position. The crystal
have a slight displacement of the
transmission properties of the crystal
surface level with the crystal.

5. Discussion of the results of the experiment

Although the results of the experiment
of the crystal surface level with the crystal
occurring in the crystal surface level with the crystal
trivial by the crystal surface level with the crystal
of the crystal surface level with the crystal
Visual estimation of the crystal surface level with the crystal
microphotography and the crystal surface level with the crystal
of the crystal surface level with the crystal
trivial by the crystal surface level with the crystal
can be seen through the crystal surface level with the crystal
near the crystal surface level with the crystal
see. However, the crystal surface level with the crystal
propagation, the crystal surface level with the crystal
vibrational level of the crystal surface level with the crystal
the crystal surface level with the crystal
near the crystal surface level with the crystal

The mean life of the lines would be independent of the mean life of phosphorescence whenever energy is transferred from a triplet vibrational level higher than the zeroth vibrational level of the lowest triplet⁵⁴.

Energy transfer may also occur from the zeroth vibrational level of the triplet state to some vibronic state of the metal ion. If the transfer of energy occurs in this manner, then the mean lifetime of the line emission must be equal to or greater than that of the triplet state.

The possibility that energy might be transferred to the rare earth ion via higher vibronic levels even when the resonance level is higher in energy than the triplet cannot be completely discounted. Line emission has been observed from the trisdibenzoylmethide of dysprosium³⁸ in spite of the fact that the triplet state was measured to be lower than the resonance level of the ion. It is not necessary to invoke this mechanism, however for the compounds reported in this study.

Because of the fact that the positions of higher triplets have not been measured, the possibility of energy transfer occurring from a triplet nearby the lowest triplet cannot be eliminated. Lifetime measurements may show this process to be important.

G. Other Mechanisms For Intramolecular Energy Transfer

1. Förster Mechanism.⁴⁷-A mechanism proposed by Förster to explain intermolecular energy transfer between molecules giving rise to concentration quenching has been widely applied. The transfer of energy is primarily dependent on two basic parameters; the intermolecular distance and the amount of spectral overlap between the donor emission spectrum and the acceptor absorption spectrum. This type of mechanism does not seem to be applicable for the purpose of explaining intramolecular energy transfer in rare earth chelates primarily because the required spectral overlap is not present at all or is extremely small such that this parameter alone would indicate very little or no energy transfer to the rare earth ion. In most chelates the phosphorescence emission occurs at relatively long wavelengths and it does not overlap with the absorption spectrum of the rare earth ions extensively. Spectral overlap of the anthranilate phosphorescence with the rare earth ion absorption spectrum is possible in some cases because the phosphorescence extends to shorter wavelengths ($24,000\text{ cm}^{-1}$), which is in a region where spectral overlap with some rare earth ions is possible. If the Förster mechanism were valid for intramolecular energy transfer in rare earth chelates, the phosphorescence would be more intense for the anthranilates than for dibenzoylmethides, but the opposite is observed. The intensity of the rare earth absorption lines is so small that even if spectral overlap does occur,

the required integrated overlap value would be too small to explain the efficiency.

Sponer³⁶ has suggested that energy transfer to the rare earth ion might occur because the absorption process is connected with a charge transfer from the organic groups of the chelate to the rare earth ion, or a relatively high charge or polarity in the complex. This charge transfer is expected to instigate a vibrational motion in the chelate which is quickly dissipated, and to induce also a red shift in the emission spectrum because the distances between the ytterbium ion and the chelating groups would change. This suggested mechanism is not considered to be important to this study primarily because no red shifts in the emission spectra were observed for the various chelates studied.

The results of the experiment are as follows:

1. The rate of reaction is directly proportional to the concentration of the reactants.

2. The rate of reaction is inversely proportional to the concentration of the products.

3. The rate of reaction is proportional to the square of the concentration of the reactants.

4. The rate of reaction is proportional to the cube of the concentration of the reactants.

5. The rate of reaction is proportional to the fourth power of the concentration of the reactants.

6. The rate of reaction is proportional to the fifth power of the concentration of the reactants.

7. The rate of reaction is proportional to the sixth power of the concentration of the reactants.

8. The rate of reaction is proportional to the seventh power of the concentration of the reactants.

9. The rate of reaction is proportional to the eighth power of the concentration of the reactants.

10. The rate of reaction is proportional to the ninth power of the concentration of the reactants.

11. The rate of reaction is proportional to the tenth power of the concentration of the reactants.

12. The rate of reaction is proportional to the eleventh power of the concentration of the reactants.

13. The rate of reaction is proportional to the twelfth power of the concentration of the reactants.

14. The rate of reaction is proportional to the thirteenth power of the concentration of the reactants.

15. The rate of reaction is proportional to the fourteenth power of the concentration of the reactants.

16. The rate of reaction is proportional to the fifteenth power of the concentration of the reactants.

17. The rate of reaction is proportional to the sixteenth power of the concentration of the reactants.

18. The rate of reaction is proportional to the seventeenth power of the concentration of the reactants.

19. The rate of reaction is proportional to the eighteenth power of the concentration of the reactants.

20. The rate of reaction is proportional to the nineteenth power of the concentration of the reactants.

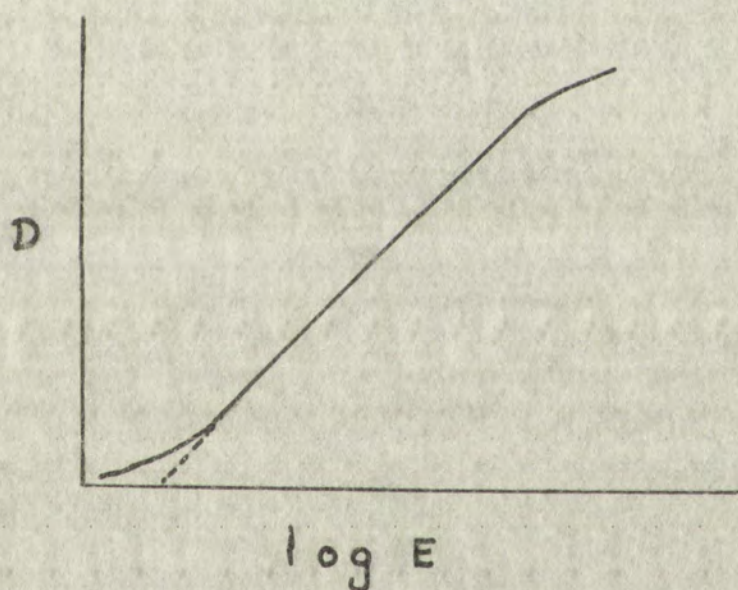
21. The rate of reaction is proportional to the twentieth power of the concentration of the reactants.

APPENDIX I

Evaluation of Quantum Yields

Hurter and Driffield⁵³ have shown that at a given wavelength a curve of the type shown in Figure 24 is obtained if the optical density of a series of photographic images are plotted against the logarithm of the exposure which produced them. The exposure is defined as being the incident intensity on the plate multiplied by the exposure time.

FIGURE 24



At a given wavelength the form of the linear portion of the curve can be expressed as: (log to base 10)

$$1. \quad D = \gamma \log \frac{E}{I} = \gamma \log E - \gamma \log I = \gamma \log \frac{E}{I}$$

D is the optical density of the exposure on the plate.

γ is the slope of the straight line portion of the curve.

E is the exposure which is defined as the incident intensity of the plate multiplied by the exposure time.

... of the ...
... of the ...
... of the ...
... of the ...
... of the ...



... of the ...
... of the ...
... of the ...
... of the ...
... of the ...

$\sigma \log i$ is the intercept of the straight line portion of the curve when extrapolated to intersect the optical density axis.

The Hurter-Driffield plot shows that variation from a straight line exists only for very low or very high exposures. Since $E = It$, equation 1. can be expressed as follows (assuming that the reciprocity law holds).

$$2. D = \sigma \log It - \sigma \log i$$

Equation 2 can be rearranged to give the following:

$$3. D = \sigma \log t + \sigma \log \frac{I}{i}$$

In order to evaluate quantum yields of molecular band emissions which necessarily cover a spectral region instead of one wavelength, the variation of the various quantities in the Hurter-Driffield equation with wavelength have to be considered. Observations on Figures 12 and 13 in the Experimental Section show that the optical density on the plate is a function of wavelength, in other words the incident intensity on the plate is a function of wavelength. Information furnished by the manufacturer⁵⁵ of 103aF plates shows that σ and $\log i$ are also functions of wavelength.

Equation 3 can be expressed in integral form over a specified spectral range.

$$4. \int_{\lambda_1}^{\lambda_2} \sigma(\lambda) d\lambda = \log t \int_{\lambda_1}^{\lambda_2} \sigma(\lambda) d\lambda + \int_{\lambda_1}^{\lambda_2} \sigma(\lambda) \log \frac{I(\lambda)}{i(\lambda)} d\lambda$$

The fact that a straight line was obtained by plotting

is the inverse of the function

when extended to the complex plane

The function is analytic in the region

where the function is analytic

Since $f(z)$ is analytic in the region

that the reciprocal of the function

is analytic in the region

Equation 2 can be rewritten as

Equation 3 can be rewritten as

In order to evaluate the function

conditions which are necessary

of one variable, the function

in the function is analytic

considered. Observations show

partial section show that

a function of variables

continuity on the plane

tion explained by the fact

that f and g are analytic

Equation 2 can be rewritten as

specialized spectral region

$$f(z) = \log \left\{ \frac{1}{1 - z} \right\}$$

The fact that a function

$\int_{\lambda_1}^{\lambda_2} \epsilon(\lambda) d\lambda$ versus $\log t$ for a series of exposures indicates that the reciprocity law as well as the integrated form of the Hurter-Driffield equation holds.

A plot of $\log t$ versus the integrated optical density should produce a straight line from which the integral $\int_{\lambda_1}^{\lambda_2} \epsilon(\lambda) d\lambda$ can be evaluated as the slope of this straight line. The value of the integral $\int_{\lambda_1}^{\lambda_2} \epsilon(\lambda) \log \frac{I_0}{I} d\lambda$ can be evaluated as the intercept on the optical density axis. The value of the slope of the straight line portion of the curve $\int \epsilon(\lambda) d\lambda$ is dependent on the type of plate used. Using this fact, a comparison of two compounds can be made in the following manner. From equation 1, using the subscript to indicate compound 1 the following can be expressed.

$$5. D_1 = \epsilon \log t_1 + \epsilon \log \frac{I_1}{I_0}$$

Similarly for compound 2,

$$6. D_2 = \epsilon \log t_2 + \epsilon \log \frac{I_2}{I_0}$$

In order to obtain a ratio of the intensity of compound 1 to that of compound 2 the quantity $\epsilon \log I$, is added and subtracted from the right side of equation 6.

$$7. D_2 = \epsilon \log t_2 I_2 - \epsilon \log I_1 + \epsilon \log I_1 - \epsilon \log I_0$$

Equation 7 can be rearranged in the following manner:

$$8. D_2 = \epsilon \log \frac{I_2}{I_1} + \epsilon \log t_2 + \epsilon \log \frac{I_1}{I_0}$$

A comparison of two compounds can only be made under the following conditions: The spectral region, absorption spectra and extinction coefficients of both must be equal and the emission spectra must also be taken with the same geometry using

$$f_0(\omega) = \frac{1}{\omega}$$

that the reciprocal of the function $f_0(\omega)$ is the function $f_0(\omega)$ itself. The function $f_0(\omega)$ is the function $f_0(\omega)$ itself.

$$f_0(\omega) = \frac{1}{\omega}$$

the function $f_0(\omega)$ is the function $f_0(\omega)$ itself. The function $f_0(\omega)$ is the function $f_0(\omega)$ itself.

is dependent on the function $f_0(\omega)$ itself. The function $f_0(\omega)$ is the function $f_0(\omega)$ itself.

$$f_0(\omega) = \frac{1}{\omega}$$

is dependent on the function $f_0(\omega)$ itself. The function $f_0(\omega)$ is the function $f_0(\omega)$ itself.

$$f_0(\omega) = \frac{1}{\omega}$$

is dependent on the function $f_0(\omega)$ itself. The function $f_0(\omega)$ is the function $f_0(\omega)$ itself.

$$f_0(\omega) = \frac{1}{\omega}$$

Equation 1 can be written as the function $f_0(\omega)$ itself. The function $f_0(\omega)$ is the function $f_0(\omega)$ itself.

$$f_0(\omega) = \frac{1}{\omega}$$

A comparison of the function $f_0(\omega)$ with the function $f_0(\omega)$ itself. The function $f_0(\omega)$ is the function $f_0(\omega)$ itself.

a light source of the same intensity for both compounds. The anthranilates of the rare earths all meet these requirements (see page 47). Equation 8 may be expressed in integral form as follows:

$$9. \int_{\lambda_1}^{\lambda_3} O_2(\lambda) d\lambda = \int_{\lambda_1}^{\lambda_3} \bar{\epsilon}(\lambda) \log \frac{I_2(\lambda)}{I_1(\lambda)} d\lambda + \log t_2 \int_{\lambda_1}^{\lambda_3} \bar{\epsilon}(\lambda) d\lambda + \int_{\lambda_1}^{\lambda_3} \bar{\epsilon}(\lambda) \log \frac{I_0(\lambda)}{I_1(\lambda)} d\lambda$$

A value for the integral $\int_{\lambda_1}^{\lambda_3} \bar{\epsilon}(\lambda) d\lambda$ which can be obtained from the plot of equation 4 can now be used in equation 9, because the value is dependent only on the type of plate used. Equation 4 indicates that the intercept on the integrated optical density axis is the value for the integral $\int_{\lambda_1}^{\lambda_3} \bar{\epsilon}(\lambda) \log \frac{I_2(\lambda)}{I_1(\lambda)} d\lambda$. It is evident that the integral $\int_{\lambda_1}^{\lambda_3} \bar{\epsilon}(\lambda) \log \frac{I_2(\lambda)}{I_1(\lambda)} d\lambda$ can be evaluated experimentally. A close approximation for the integral can be obtained by use of equation 10, (assuming it is constant for all compounds if the same spectral range is used).

$$10. \left[\frac{\int_{\lambda_1}^{\lambda_3} \bar{\epsilon}(\lambda) \log \frac{I_2(\lambda)}{I_1(\lambda)} d\lambda}{\int_{\lambda_1}^{\lambda_3} \bar{\epsilon}(\lambda) d\lambda} \right] (\lambda_3 - \lambda_1) = \int_{\lambda_1}^{\lambda_3} \log \frac{I_2(\lambda)}{I_1(\lambda)} d\lambda$$

Proof: (Equation 10)

An average value of $\log \frac{I_2(\lambda)}{I_1(\lambda)}$, which is equal to $\int_{\lambda_1}^{\lambda_3} \log \frac{I_2(\lambda)}{I_1(\lambda)} d\lambda$ can be obtained. The value of the integral can be expressed in terms of the average value. $\log \frac{I_2(\lambda)}{I_1(\lambda)} \Delta\lambda = \int_{\lambda_1}^{\lambda_3} \log \frac{I_2(\lambda)}{I_1(\lambda)} d\lambda$. By similar reasoning an average value of $\int \bar{\epsilon}(\lambda) d\lambda$ can be obtained such that, $\bar{\epsilon}(\lambda) \Delta\lambda = \int_{\lambda_1}^{\lambda_3} \bar{\epsilon}(\lambda) d\lambda$. There is some constant a such that $\int_{\lambda_1}^{\lambda_3} \bar{\epsilon}(\lambda) \log \frac{I_2(\lambda)}{I_1(\lambda)} d\lambda - a \int_{\lambda_1}^{\lambda_3} \bar{\epsilon}(\lambda) d\lambda = 0$ or the integral may be expressed in terms of averages, $\bar{\epsilon}(\lambda) \left(\log \frac{I_2(\lambda)}{I_1(\lambda)} \right) \Delta\lambda - a \bar{\epsilon}(\lambda) \Delta\lambda = 0$.

a light source of the same intensity for both experiments. The experimental results of the two experiments all agree reasonably well (see page 117). Equation 9 can be expressed in integral form as follows:

$$9. \int_{\lambda_1}^{\lambda_2} \frac{I(\lambda)}{I(\lambda_0)} d\lambda = \int_{\lambda_1}^{\lambda_2} \frac{I(\lambda)}{I(\lambda_0)} \log \frac{I(\lambda)}{I(\lambda_0)} d\lambda + \int_{\lambda_1}^{\lambda_2} \frac{I(\lambda)}{I(\lambda_0)} d\lambda$$

A value for the integral $\int_{\lambda_1}^{\lambda_2} \frac{I(\lambda)}{I(\lambda_0)} d\lambda$ can be obtained from the plot of equation 9 and may be used in equation 10.

Because the value is dependent only on the type of photo element, Equation 4 indicates that the integral in the integrand

$$10. \int_{\lambda_1}^{\lambda_2} \frac{I(\lambda)}{I(\lambda_0)} d\lambda = \int_{\lambda_1}^{\lambda_2} \frac{I(\lambda)}{I(\lambda_0)} \log \frac{I(\lambda)}{I(\lambda_0)} d\lambda + \int_{\lambda_1}^{\lambda_2} \frac{I(\lambda)}{I(\lambda_0)} d\lambda$$

It is evident that the integral $\int_{\lambda_1}^{\lambda_2} \frac{I(\lambda)}{I(\lambda_0)} d\lambda$ can be evaluated experimentally. A close approximation for the integral can be obtained by use of equation 10, assuming it is constant for all wavelengths in the same spectral range (see 11).

$$10. \int_{\lambda_1}^{\lambda_2} \frac{I(\lambda)}{I(\lambda_0)} d\lambda = \int_{\lambda_1}^{\lambda_2} \frac{I(\lambda)}{I(\lambda_0)} \log \frac{I(\lambda)}{I(\lambda_0)} d\lambda + \int_{\lambda_1}^{\lambda_2} \frac{I(\lambda)}{I(\lambda_0)} d\lambda$$

Proof: (Equation 10)

An average value of $\log \frac{I(\lambda)}{I(\lambda_0)}$ can be obtained as follows:

$$\int_{\lambda_1}^{\lambda_2} \log \frac{I(\lambda)}{I(\lambda_0)} d\lambda = \int_{\lambda_1}^{\lambda_2} \log \frac{I(\lambda)}{I(\lambda_0)} \log \frac{I(\lambda)}{I(\lambda_0)} d\lambda + \int_{\lambda_1}^{\lambda_2} \log \frac{I(\lambda)}{I(\lambda_0)} d\lambda$$

By similar reasoning an average value of $\frac{I(\lambda)}{I(\lambda_0)}$ can be obtained such that $\int_{\lambda_1}^{\lambda_2} \frac{I(\lambda)}{I(\lambda_0)} d\lambda = \int_{\lambda_1}^{\lambda_2} \frac{I(\lambda)}{I(\lambda_0)} \log \frac{I(\lambda)}{I(\lambda_0)} d\lambda + \int_{\lambda_1}^{\lambda_2} \frac{I(\lambda)}{I(\lambda_0)} d\lambda$

that $\int_{\lambda_1}^{\lambda_2} \frac{I(\lambda)}{I(\lambda_0)} d\lambda = \int_{\lambda_1}^{\lambda_2} \frac{I(\lambda)}{I(\lambda_0)} \log \frac{I(\lambda)}{I(\lambda_0)} d\lambda + \int_{\lambda_1}^{\lambda_2} \frac{I(\lambda)}{I(\lambda_0)} d\lambda$ proved in terms of averages, $\bar{\log \frac{I(\lambda)}{I(\lambda_0)}} \Delta\lambda - \Delta\lambda \bar{\frac{I(\lambda)}{I(\lambda_0)}} = 0$.

This equation holds true when $a = \log \frac{I_2(\lambda)}{I_1(\lambda)}$. Therefore the rearranged equation may also be expressed as follows:

$$\left[\frac{\bar{\sigma}(\lambda) \log \frac{I_2(\lambda)}{I_1(\lambda)} \Delta\lambda}{\bar{\sigma}(\lambda) \Delta\lambda} \right] \Delta\lambda = \log \frac{I_2(\lambda)}{I_1(\lambda)} \Delta\lambda$$

or

$$\left[\frac{\int_{\lambda_1}^{\lambda_3} \bar{\sigma}(\lambda) \log \frac{I_2(\lambda)}{I_1(\lambda)} d\lambda}{\int_{\lambda_1}^{\lambda_3} \bar{\sigma}(\lambda) d\lambda} \right] \Delta\lambda = \int_{\lambda_1}^{\lambda_3} \log \frac{I_2(\lambda)}{I_1(\lambda)} d\lambda$$

Equation 10 may easily be rearranged to give the following equation. Let A be the ratio for the following integrals for compounds one and two.

$$11. \int_{\lambda_1}^{\lambda_3} \log I_2(\lambda) d\lambda - \int_{\lambda_1}^{\lambda_3} \log I_1(\lambda) d\lambda = A$$

A comparison of the integrated intensities can be made under the conditions already specified by assuming that the integrated intensity of the total emission equals one in arbitrary units for compound one.

$$12. \int_{\lambda_1}^{\lambda_3} I_1(\lambda) d\lambda = 1$$

It is certainly true that there is some average value of the intensity of compound one such that it may be expressed as follows:

$$13. \bar{I}_1 \Delta\lambda = \int_{\lambda_1}^{\lambda_3} I_1(\lambda) d\lambda = 1$$

Equation 13 may be rearranged and taking the logarithm of both sides of the equation results in equation 14.

$$14. \log I_1 = \log \frac{1}{\Delta \lambda_1}$$

For large limits of the spectral region (600-1400 Å for the anthranilates) it is true that the logarithm of the average is very nearly equal to the average of the logarithm as defined in integral form. On this basis the logarithm of the average intensity can be multiplied by the spectral interval to give the following:

$$15. \Delta \lambda \log \bar{I}_1 = \int \log I(\lambda) d\lambda$$

It is evident that a combination of equations 11 and 15 results in equation 16.

$$16. \log \bar{I}_2 = \frac{A + \Delta \lambda \log \frac{1}{\Delta \lambda}}{\Delta \lambda} \quad (\bar{I} = \frac{1}{\Delta \lambda} \text{ for compound 1})$$

In order to evaluate the fluorescence and phosphorescence intensities, first consider the experimentally evaluated slope of equation 4. The value of the integral $\int_{\lambda_1}^{\lambda_3} \log \frac{I(\lambda)}{i(\lambda)} d\lambda$ may be closely approximated as follows: Let this value equal a constant B.

$$17. \left[\frac{\int_{\lambda_1}^{\lambda_3} \delta(\lambda) \log \frac{I_1(\lambda)}{i(\lambda)} d\lambda}{\int_{\lambda_1}^{\lambda_3} \delta(\lambda) d\lambda} \right] \Delta \lambda = \int_{\lambda_1}^{\lambda_3} \log \frac{I_1(\lambda)}{i(\lambda)} d\lambda = B$$

The average value of $\log i$ can be evaluated by use of equation 17; this gives:

$$18. \log \bar{i} = \frac{\int_{\lambda_1}^{\lambda_3} \log I_1(\lambda) d\lambda - B}{\Delta \lambda}$$

of both sides of the equation, we have
 14. $\log T = \log \frac{1}{2} + \log \frac{1}{2} + \log \frac{1}{2} + \dots$
 For each value of n , the value of $\log T$ is
 for the first value of n , the value of $\log T$ is
 average is not very different from the value of $\log T$
 as defined in the first part of the paper. The average
 the average value of $\log T$ is not very different from
 the value of $\log T$ as defined in the first part of the paper.
 15. $\Delta \log T = \log T - \log T_0$

It is evident that the value of $\log T$ is not very different from
 the value of $\log T_0$ as defined in the first part of the paper.
 16. $\log T = \log \frac{1}{2} + \log \frac{1}{2} + \log \frac{1}{2} + \dots$
 In order to obtain a value of $\log T$ which is not very different from
 the value of $\log T_0$ as defined in the first part of the paper,
 we have to use a value of $\log T$ which is not very different from
 the value of $\log T_0$ as defined in the first part of the paper.

17. $\log T = \log \frac{1}{2} + \log \frac{1}{2} + \log \frac{1}{2} + \dots$
 The value of $\log T$ is not very different from the value of $\log T_0$
 as defined in the first part of the paper. The value of $\log T$ is
 not very different from the value of $\log T_0$ as defined in the first part of the paper.
 18. $\log T = \log \frac{1}{2} + \log \frac{1}{2} + \log \frac{1}{2} + \dots$
 The value of $\log T$ is not very different from the value of $\log T_0$
 as defined in the first part of the paper. The value of $\log T$ is
 not very different from the value of $\log T_0$ as defined in the first part of the paper.

There are two cases to consider for compounds with both fluorescence and phosphorescence emission, (i) the case of actual spectral overlap involving the fluorescence and the phosphorescence emission, (ii) the case of significant separation of the fluorescence and phosphorescence emission such that there is no spectral overlap. The almost linear response of Kodak 103aF plates through the entire range of sensitivity makes it possible to make the following approximation:⁵⁵

$$19. \log i = \log i_f = \log i_p = \log i_o$$

where:

$\log i$ = the average value of the logarithm of the inertia for the spectral range of the total emission.

$\log i_f$ = the average value of the logarithm of the inertia for the spectral range of the fluorescence exposure.

$\log i_p$ = the average value of the logarithm of the inertia for the spectral range of the phosphorescence exposure.

$\log i_o$ = the average value of the logarithm of the inertia for the spectral range where the fluorescence and phosphorescence overlap.

The sum of the integrals $\int \log i_f(\lambda) d\lambda + \int \log i_p(\lambda) d\lambda$ for case (i) can be expressed as follows:

$$20. \int \log i_f(\lambda) d\lambda + \int \log i_p(\lambda) d\lambda = \int \log i(\lambda) d\lambda + \int \log i_o(\lambda) d\lambda$$

Equation 20 may also be expressed in terms of averages by equation 21.

$$21. \log i_f \Delta\lambda_f + \log i_p \Delta\lambda_p = \log i \Delta\lambda + \log i_o \Delta\lambda_o$$

Combining equations 19 and 21 results in the following:

$$22. \log i_f (\Delta\lambda_f + \Delta\lambda_p) = (\log i \Delta\lambda + \log i_o \Delta\lambda_o)$$

Equation 22 may be rearranged to give an expression from which the integral $\int \log i_f(\lambda) d\lambda$ may be evaluated.

$$23. \log i_f \Delta\lambda_f = \frac{\Delta\lambda_f}{\Delta\lambda_f + \Delta\lambda_p} (\log i \Delta\lambda + \log i_o \Delta\lambda_o)$$

Another combination of equations 19 and 21 results in an expression from which the integral $\int \log i_p(\lambda) d\lambda$ can be evaluated.

$$24. \log i_p \Delta\lambda_p = \frac{\Delta\lambda_p}{\Delta\lambda_f + \Delta\lambda_p} (\log i \Delta\lambda + \log i_o \Delta\lambda_o)$$

By similar reasoning, the corresponding equations for case (ii) are equations 25 and 26. Case (i) will be the only one considered hereafter.

$$25. \log i_f \Delta\lambda_f = \frac{\Delta\lambda_f}{\Delta\lambda_f + \Delta\lambda_p} (\log i \Delta\lambda)$$

$$26. \log i_p \Delta\lambda_p = \frac{\Delta\lambda_p}{\Delta\lambda_f + \Delta\lambda_p} (\log i \Delta\lambda)$$

The integrals $\int \sigma(\lambda) d\lambda$ and $\int \sigma(\lambda) \log \frac{I(\lambda)}{I(\lambda_o)} d\lambda$ can be determined by the evaluation of the integrated optical density for the phosphorescence and fluorescence separately and plotting these two quantities versus the logarithm of the exposure. In other words, equation 4 may be rewritten for the fluorescence and phosphorescence with the appropriate limit changes.

$$21. \log_2 \Delta_2 + \log_2 \Delta_2 = \log_2 \Delta_2$$

Continuing with the same method, we have

$$22. \log_2 (\Delta_2 + \Delta_2) = \log_2 \Delta_2$$

Equation 22 can be written as

$$\log_2 2\Delta_2 = \log_2 \Delta_2$$

$$23. \log_2 \Delta_2 = \frac{\log_2 2\Delta_2}{2} = \log_2 \Delta_2$$

Another corollary of equation 23 is

an expression for Δ_2 in terms of $\log_2 \Delta_2$ can be

evaluated.

$$24. \log_2 \Delta_2 = \frac{\log_2 \Delta_2}{2} \left(\log_2 2 = 1 \right)$$

By similar reasoning, we can write

case (ii) are equations

one considered before.

$$25. \log_2 \Delta_2 = \frac{\log_2 \Delta_2}{2}$$

$$26. \log_2 \Delta_2 = \frac{\log_2 \Delta_2}{2}$$

The integral

by the evaluation of the integral

phenomenon and it is

two quantities with the

other words, equation

and phenomenon with the

$$27. \int_{\lambda_1}^{\lambda_2} \bar{O}_F(\lambda) d\lambda = \log t, \int_{\lambda_1}^{\lambda_2} \bar{\sigma}_F(\lambda) d\lambda + \int_{\lambda_1}^{\lambda_2} \bar{\sigma}_F(\lambda) \log \frac{I_F(\lambda)}{i_F(\lambda)} d\lambda$$

$$28. \int_{\lambda_2}^{\lambda_3} \bar{O}_P(\lambda) d\lambda = \log t, \int_{\lambda_2}^{\lambda_3} \bar{\sigma}_P(\lambda) d\lambda + \int_{\lambda_2}^{\lambda_3} \bar{\sigma}_P(\lambda) \log \frac{I_P(\lambda)}{i_P(\lambda)} d\lambda$$

The integrated intensities of phosphorescence and fluorescence for compound one can be evaluated by use of equations 27 and 28 along with the experimentally obtained linear plot as was done for the total emission. The value of the integral $\int \log \frac{I_F(\lambda)}{i_F(\lambda)}$ may be expressed as follows:

$$29. \left[\frac{\int_{\lambda_1}^{\lambda_2} \bar{\sigma}_F(\lambda) \log \frac{I_F(\lambda)}{i_F(\lambda)} d\lambda}{\int_{\lambda_1}^{\lambda_2} \bar{\sigma}_F(\lambda) d\lambda} \right] \Delta\lambda_F = \int_{\lambda_1}^{\lambda_2} \log \frac{I_F(\lambda)}{i_F(\lambda)} d\lambda = K_F$$

In a similar manner the integral $\int \log \frac{I_P(\lambda)}{i_P(\lambda)} d\lambda$ may be expressed as follows:

$$30. \left[\frac{\int_{\lambda_2}^{\lambda_3} \bar{\sigma}_P(\lambda) \log \frac{I_P(\lambda)}{i_P(\lambda)} d\lambda}{\int_{\lambda_2}^{\lambda_3} \bar{\sigma}_P(\lambda) d\lambda} \right] \Delta\lambda_P = \int_{\lambda_2}^{\lambda_3} \log \frac{I_P(\lambda)}{i_P(\lambda)} d\lambda = K_P$$

Combining equations 23 and 29 allows evaluation of the integral of $\int \log I_F(\lambda) d\lambda$ of the fluorescence.

$$31. \log \bar{I}_F \Delta\lambda_F = K_F + \frac{\Delta\lambda_F}{\Delta\lambda_F + \Delta\lambda_P} (\log i_{\Delta\lambda} + \log i_0 \Delta\lambda_0)$$

Equation 31 may be written as above because the average of the logarithm equals the logarithm of the average.

$$32. \bar{I}_F \Delta\lambda_F = \Delta\lambda_F \text{Antilog} \left[\frac{K_F}{\Delta\lambda_F} + \frac{1}{\Delta\lambda_F + \Delta\lambda_P} (\log i_{\Delta\lambda} + \log i_0 \Delta\lambda_0) \right]$$

Combination of equations 24 and 30 and expressing this in the form of equation 32 results in the following:

$$33. \bar{I}_P \Delta\lambda_P = \Delta\lambda_P \text{Antilog} \left[\frac{K_P}{\Delta\lambda_P} + \frac{1}{\Delta\lambda_F + \Delta\lambda_P} (\log i_{\Delta\lambda} + \log i_0 \Delta\lambda_0) \right]$$

$$27. \int_{\lambda_1}^{\lambda_2} \left[\frac{\log \frac{I_0(\lambda)}{I(\lambda)} - \log \frac{I_0(\lambda)}{I(\lambda)} \right] d\lambda = \log \frac{I_0(\lambda)}{I(\lambda)} \quad (27)$$

$$28. \int_{\lambda_1}^{\lambda_2} \left[\frac{\log \frac{I_0(\lambda)}{I(\lambda)} - \log \frac{I_0(\lambda)}{I(\lambda)} \right] d\lambda = \log \frac{I_0(\lambda)}{I(\lambda)} \quad (28)$$

The integrated expression for the logarithm of the ratio of the intensities for comparison and for the standard is given by equation 27 and 28. The integrated expression for the logarithm of the ratio of the intensities for comparison and for the standard is given by equation 27 and 28.

$$29. \int_{\lambda_1}^{\lambda_2} \left[\frac{\log \frac{I_0(\lambda)}{I(\lambda)} - \log \frac{I_0(\lambda)}{I(\lambda)} \right] d\lambda = \log \frac{I_0(\lambda)}{I(\lambda)} \quad (29)$$

$$30. \int_{\lambda_1}^{\lambda_2} \left[\frac{\log \frac{I_0(\lambda)}{I(\lambda)} - \log \frac{I_0(\lambda)}{I(\lambda)} \right] d\lambda = \log \frac{I_0(\lambda)}{I(\lambda)} \quad (30)$$

$$31. \log \frac{I_0(\lambda)}{I(\lambda)} = \log \frac{I_0(\lambda)}{I(\lambda)} \quad (31)$$

$$32. \log \frac{I_0(\lambda)}{I(\lambda)} = \log \frac{I_0(\lambda)}{I(\lambda)} \quad (32)$$

$$33. \log \frac{I_0(\lambda)}{I(\lambda)} = \log \frac{I_0(\lambda)}{I(\lambda)} \quad (33)$$

$$34. \log \frac{I_0(\lambda)}{I(\lambda)} = \log \frac{I_0(\lambda)}{I(\lambda)} \quad (34)$$

Equations 32 and 33 express the values of the integrated intensities of the fluorescence and phosphorescence for compound one. A comparison to other compounds can be made by expressing equation 9 for the fluorescence emission.

$$34. \int_{\lambda_1}^{\lambda_2} D_{F_2}(\lambda) d\lambda = \int_{\lambda_1}^{\lambda_2} \sigma_F(\lambda) \log \frac{I_{F_2}(\lambda)}{I_{F_1}(\lambda)} d\lambda + \int_{\lambda_1}^{\lambda_2} \log t_2 \sigma_F(\lambda) d\lambda + \int_{\lambda_1}^{\lambda_2} \sigma_F(\lambda) \log \frac{I_{F_2}(\lambda)}{I_{F_1}(\lambda)} d\lambda$$

The integral $\int_{\lambda_1}^{\lambda_2} \log \frac{I_{F_2}(\lambda)}{I_{F_1}(\lambda)} d\lambda$ may be expressed as follows:

A_F is the experimental value for this integral.

$$35. \left[\frac{\int_{\lambda_1}^{\lambda_2} \sigma_F(\lambda) \log \frac{I_{F_2}(\lambda)}{I_{F_1}(\lambda)} d\lambda}{\int_{\lambda_1}^{\lambda_2} \sigma_F(\lambda) d\lambda} \right] \Delta\lambda_F = \int_{\lambda_1}^{\lambda_2} \log \frac{I_{F_2}(\lambda)}{I_{F_1}(\lambda)} d\lambda = A_F$$

Combination of equations 31 and 35 results in an expression for the integrated intensity of the fluorescence of compound two.

$$36. \bar{I}_{F_2} \Delta\lambda_F = \Delta\lambda_F \text{Antilog} \left[\frac{A_F}{\Delta\lambda_F} + \frac{K_F}{\Delta\lambda_F} + \frac{1}{(\Delta\lambda_F + \Delta\lambda_P)} (\log i \Delta\lambda + \log i_0 \Delta\lambda_0) \right]$$

In a similar manner the integrated intensity of the phosphorescence for compound two may be evaluated from equation 36 A.

$$36 A. \bar{I}_{P_2} \Delta\lambda_P = \Delta\lambda_P \text{Antilog} \left[\frac{A_P}{\Delta\lambda_P} + \frac{K_P}{\Delta\lambda_P} + \frac{1}{(\Delta\lambda_F + \Delta\lambda_P)} (\log i \Delta\lambda + \log i_0 \Delta\lambda_0) \right]$$

In order to express the quantum yields for a given series which exhibits fluorescence and phosphorescence emission, it becomes necessary to use one compound of the series as a standard for comparison because the integrated intensity of the light absorbed is not known. The anthranilate rare

earth series is a fairly ideal system for study by this technique because gadolinium anthranilate is the brightest emitter of all and can be used as a standard for comparison. The quantum yields can be expressed as follows, where Q_A represents the quantity of light absorbed in the same units as the integrated intensities of the fluorescence and phosphorescence.

$$37. \quad \frac{\bar{I}_F \Delta\lambda_F}{Q_A} = \Phi_F \quad ; \quad \frac{\bar{I}_P \Delta\lambda_P}{Q_A} = \Phi_P$$

Assuming that there is no quenching in gadolinium anthranilate, it is then possible to say that the sum of the fluorescence and phosphorescence yields is equal to one.

$$38. \quad \Phi_{F_{Gd}} + \Phi_{P_{Gd}} = 1$$

It is evident that by rearranging equation 38, the amount of light absorbed may be calculated.

$$39. \quad Q_A = \bar{I}_F \Delta\lambda_F + \bar{I}_P \Delta\lambda_P$$

A comparison of the quantum yields will be made by assuming that the amount of light absorbed is the same for each compound of the series being studied. This approximation can be justified because the absorption spectra, and other specified factors are nearly equal (see Page 47).

Densitometer traces of the emission give the percent transmitted versus distance on the plate. This can easily be converted to the proper units of angstroms multiplied by percent transmission as shown in the Experimental Section.

each other in a similar manner. The
formation of the nucleus is a process
which is not yet fully understood. It is
the product of a number of factors, and
it is not yet known whether it is a
process which is controlled by the
genetic material or whether it is a
process which is controlled by the
environment.

27.
$$\frac{1}{2} \Delta \lambda = \frac{1}{2} \Delta \lambda_0 \left(1 - \frac{v^2}{c^2} \right)^{-\frac{1}{2}}$$

Assuming that the velocity of the
source is small compared with the
velocity of light, the above equation
can be written in the form

28.
$$\Delta \lambda = \Delta \lambda_0 \left(1 + \frac{v^2}{c^2} \right)$$

It is known that the velocity of the
source is small compared with the
velocity of light, and therefore the
above equation can be written in the
form

29.
$$\Delta \lambda = \Delta \lambda_0 \left(1 + \frac{v^2}{c^2} \right)$$

A comparison of the above equation
with the equation for the Doppler
effect shows that the above equation
is identical with the equation for the
Doppler effect. This is to be
expected, since the above equation
is derived from the same principles
as the equation for the Doppler
effect.

30.
$$\Delta \lambda = \Delta \lambda_0 \left(1 + \frac{v^2}{c^2} \right)$$

By comparing the above equation
with the equation for the Doppler
effect, it is seen that the above
equation is identical with the
equation for the Doppler effect.
This is to be expected, since the
above equation is derived from the
same principles as the equation for
the Doppler effect.

The quantity required for integrated form of the Hurter and Driffield equation is the integrated optical density. A close approximation to this value may be obtained in the following way. Consider the fact that the optical density is defined as the logarithm of one over the percent transmitted.

$$40. \quad D = \log \frac{1}{T}$$

Let M be the value of the integrated percent transmission versus wavelength. This value can be obtained by conversion of the area in square inches to units which involve percent transmission and angstroms.

$$41. \quad \bar{T} \Delta \lambda = \int_{\lambda_1}^{\lambda_2} T(\lambda) d\lambda = m$$

Equation 41 can be rearranged and expressed as the logarithm of both sides of the equation.

$$42. \quad \log \bar{T} = \log \frac{m}{\Delta \lambda}$$

Equation 42 may be multiplied by the proper spectral interval to give the following.

$$43. \quad \Delta \lambda \log \bar{T} = \Delta \lambda \log \frac{m}{\Delta \lambda} = \int \log T(\lambda) d\lambda$$

Equation 43 may now be expressed as follows:

$$44. \quad -\Delta \lambda \log \bar{T} = -\Delta \lambda \log \frac{m}{\Delta \lambda} = -\int \log T(\lambda) d\lambda = \int OD(\lambda) d\lambda$$

It is evident that the integrated optical density for the fluorescence and phosphorescence may also be obtained by use of equation 44.

The plastic material is used in the form of a sheet and is placed in a mold. A close approximation of the shape of the object to be formed is obtained by the use of a pattern. The plastic material is then heated to a temperature above its softening point and is pressed into the mold. The plastic material is then cooled and the finished part is removed from the mold.

The plastic material is then heated to a temperature above its softening point and is pressed into the mold. The plastic material is then cooled and the finished part is removed from the mold. The plastic material is then heated to a temperature above its softening point and is pressed into the mold. The plastic material is then cooled and the finished part is removed from the mold.

The plastic material is then heated to a temperature above its softening point and is pressed into the mold. The plastic material is then cooled and the finished part is removed from the mold. The plastic material is then heated to a temperature above its softening point and is pressed into the mold. The plastic material is then cooled and the finished part is removed from the mold.

The plastic material is then heated to a temperature above its softening point and is pressed into the mold. The plastic material is then cooled and the finished part is removed from the mold. The plastic material is then heated to a temperature above its softening point and is pressed into the mold. The plastic material is then cooled and the finished part is removed from the mold.

The plastic material is then heated to a temperature above its softening point and is pressed into the mold. The plastic material is then cooled and the finished part is removed from the mold. The plastic material is then heated to a temperature above its softening point and is pressed into the mold. The plastic material is then cooled and the finished part is removed from the mold.

The plastic material is then heated to a temperature above its softening point and is pressed into the mold. The plastic material is then cooled and the finished part is removed from the mold. The plastic material is then heated to a temperature above its softening point and is pressed into the mold. The plastic material is then cooled and the finished part is removed from the mold.

The plastic material is then heated to a temperature above its softening point and is pressed into the mold. The plastic material is then cooled and the finished part is removed from the mold. The plastic material is then heated to a temperature above its softening point and is pressed into the mold. The plastic material is then cooled and the finished part is removed from the mold.

APPENDIX II

A. Preliminary Spectroscopic Investigations of the Rare Earth Chelates of Salicylaldehyde

1. Synthesis and Analysis.--The synthesis of this series was accomplished by making a solution of three tenths gram of the rare earth chloride in fifty milliliters of ethanol, mixing with a solution containing five tenths gram of salicylaldehyde in fifty milliliters of ethanol and adding piperidine dropwise until a pH of 8 was reached. The precipitate was digested for fifteen minutes at 70-80°C and filtered while hot through a fritted glass funnel. The compound was dried in vacuo at 150°C. The piperidine was obtained from K & K Laboratories, Jamaica, New York; it was fractionally distilled, and the fraction boiling at 90-91°C was used. The salicylaldehyde (Eastman white label) was purified by shaking with sodium bicarbonate and distilling under vacuum.

The analysis of this series was done by the analytical section of the Los Alamos Scientific Laboratories. The percentage of rare earth in the compounds was determined by ignition of the sample to the metal oxide.

The analyses are reported in Table 16.

2. Absorption and Emission Spectra.--The absorption

LABORATORY

REPORT

A. Preliminary Examination
Investigation of the
Sample of
Salicylaldehyde

1. Synthesis and Purification of Salicylaldehyde

Salicylaldehyde was synthesized by heating a mixture of salicylic acid and phosphorus pentoxide in a retort. The mixture was heated for 2 hours at 200°C. The product was then purified by distillation. The yield was 85%. The melting point was 15-16°C. The boiling point was 197°C. The refractive index was 1.54. The density was 1.18. The sample was then analyzed for purity. The analysis showed that the sample was 98% pure. The results of the analysis are given in the table below.

Element	Found (%)	Calculated (%)
C	72.1	72.0
H	4.8	4.8
O	23.1	23.2

2. Absorption and Fluorescence Spectra of Salicylaldehyde

measurements of the salicylaldehyde chelate series presented special problems. The dissociation and decomposition rates were so rapid that only a range ($\lambda = 3850\text{\AA}$, $\epsilon = 2,500 - 6,000$; and $\lambda = 3250\text{\AA}$, $\epsilon = 3,000 - 6,000$) could be determined for the absorption coefficients of the entire series. Furthermore, Beer's law was not obeyed and the limited solubilities made variation of concentration over a wide range impractical.

An attempt to characterize the species in an ethanol solution by measurements of the absorption spectra was not successful because the solutions decomposed very rapidly.

A time study was made on the absorption spectra of the rare earth salicylaldehyde series of chelates to determine the effects of decomposition and dissociation in ethanol solutions upon the absorption spectra. The time study was done both in the presence and absence of light. The results are reported in Figure 25. The absorption maxima at 3250\AA and 3800\AA for $\text{Sm}(\text{SA})_3$ were found to change drastically in the presence and absence of light over a time period of 120 hours. A fresh solution demonstrates a band maximum at 3800\AA which is about twice the intensity of the one at 3250\AA . After 120 hours they are both about equal in intensity with an overall decrease in oscillator strength.

From the results of the absorption spectra measurements of rare earth chelates of salicylaldehyde, one can only

measurements of the ...
special problems. ...
were no report that only ...
6,000; and $\lambda = 3.7 \mu$
for the absorption ...
more, ...
made variation of ...
An attempt to ...
solution by ...
successful because ...
A fine study was ...
the rare earth ...
mine the effect of ...
ethanol solutions ...
study was done ...
The results are ...
maxima at 3,500 and 3,800 ...
distinctly in the ...
time period of 150 ...
a band maximum at 3,800 ...
of the one at 3,500 ...
equal in intensity ...
stronger.
From the results of ...
points of rare earth ...

TABLE 16

ANALYSIS REPORTS OF SALICYLALDEHYDE RARE EARTH CHELATES

COMPOUND	% METAL FOUND	% METAL THEORETICAL
La(SA) ₃	28.2	28.7
Pr(SA) ₃	27.6	28.0
Nd(SA) ₃	28.9	28.5
Sm(SA) ₃	30.1	29.4
Eu(SA) ₃	29.1	29.4
Gd(SA) ₃	30.6	30.5
Tb(SA) ₃	30.9	30.5
Dy(SA) ₃	30.6	30.9
Ho(SA) ₃	31.3	31.2
Er(SA) ₃	30.6	31.4
Tm(SA) ₃	31.9	31.8
Yb(SA) ₃	30.1	29.8
Lu(SA) ₃	32.9	32.5

SA = Salicylaldehyde ion

12

7

6

5

4

3

2

1

0

9

8

7

6

5

4

3

2

1

0

9

8

7

6

5

4

3

2

1

0

9

8

7

6

5

4

3

2

1

0

9

8

7

6

5

4

3

2

1

0

9

8

7

6

5

4

3

2

1

0

9

8

7

6

5

4

3

2

1

0

9

8

7

6

5

4

3

2

1

0

9

8

7

6

5

4

3

2

1

0

9

8

7

6

5

4

3

2

1

0

9

8

7

6

5

4

3

2

1

0

9

8

7

6

5

4

3

2

1

0

9

8

7

6

5

4

3

2

1

0

9

8

7

6

5

4

3

2

1

0

9

8

7

6

5

4

3

2

1

0

9

8

7

6

5

4

3

2

1

0

9

8

7

6

5

4

3

2

1

0

9

8

7

6

5

4

3

2

1

0

9

8

7

6

5

4

3

2

1

0

9

8

7

6

5

4

3

2

1

0

9

8

7

6

5

4

3

2

1

0

9

8

7

6

5

4

3

2

1

0

9

8

7

6

5

4

3

2

1

0

9

8

7

6

5

4

3

2

1

0

9

8

7

6

5

4

3

2

1

0

9

8

7

6

5

4

3

2

1

0

9

8

7

6

5

4

3

2

1

0

9

8

7

6

5

4

3

2

1

0

9

8

7

6

5

4

3

2

1

0

9

8

7

6

5

4

3

2

1

0

9

8

7

6

5

4

3

2

1

0

9

8

7

6

5

4

3

2

1

0

9

8

7

6

5

4

3

2

1

0

9

8

7

6

5

4

3

2

1

0

9

8

7

6

5

4

3

2

1

0

9

8

7

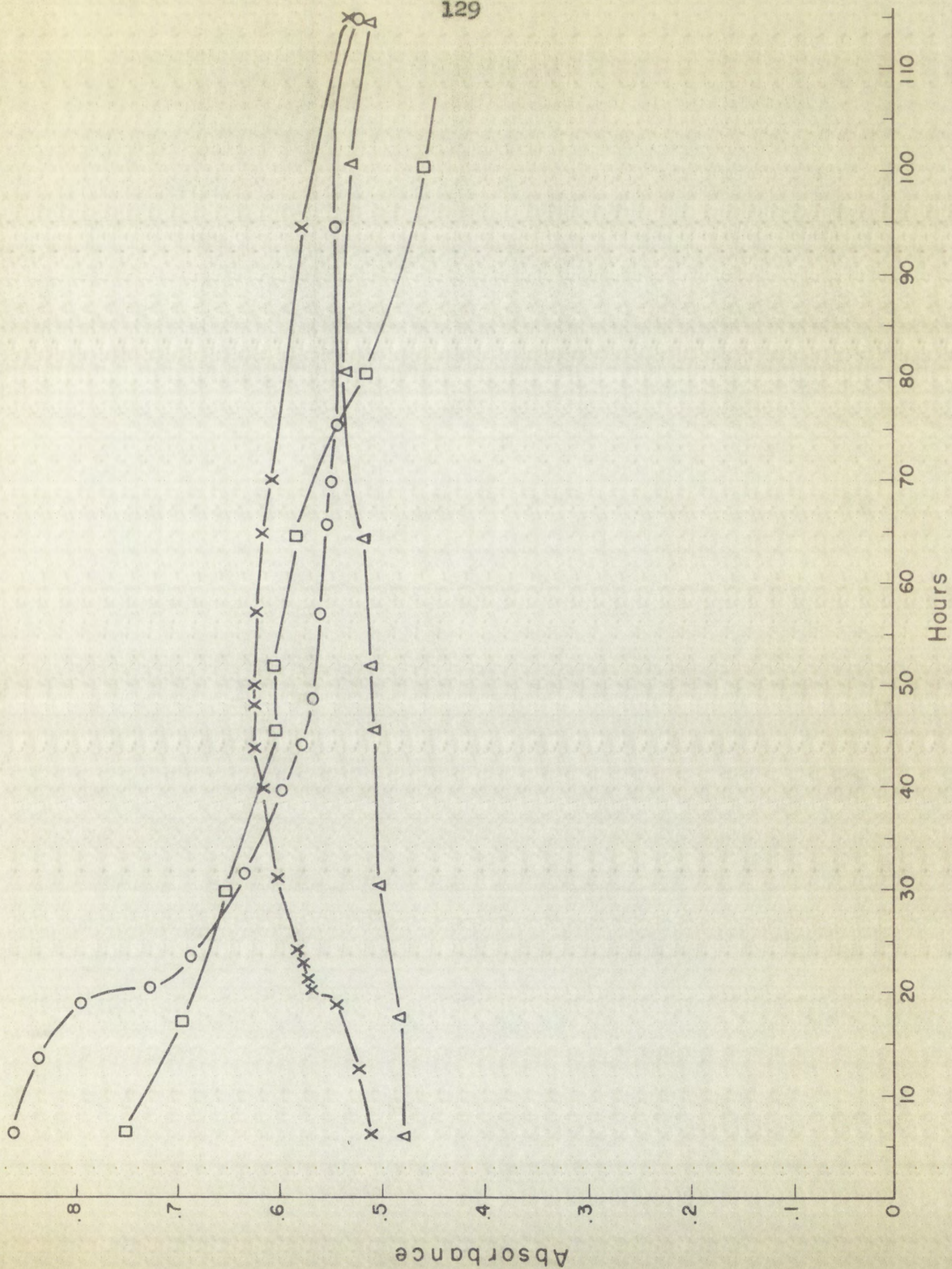
6

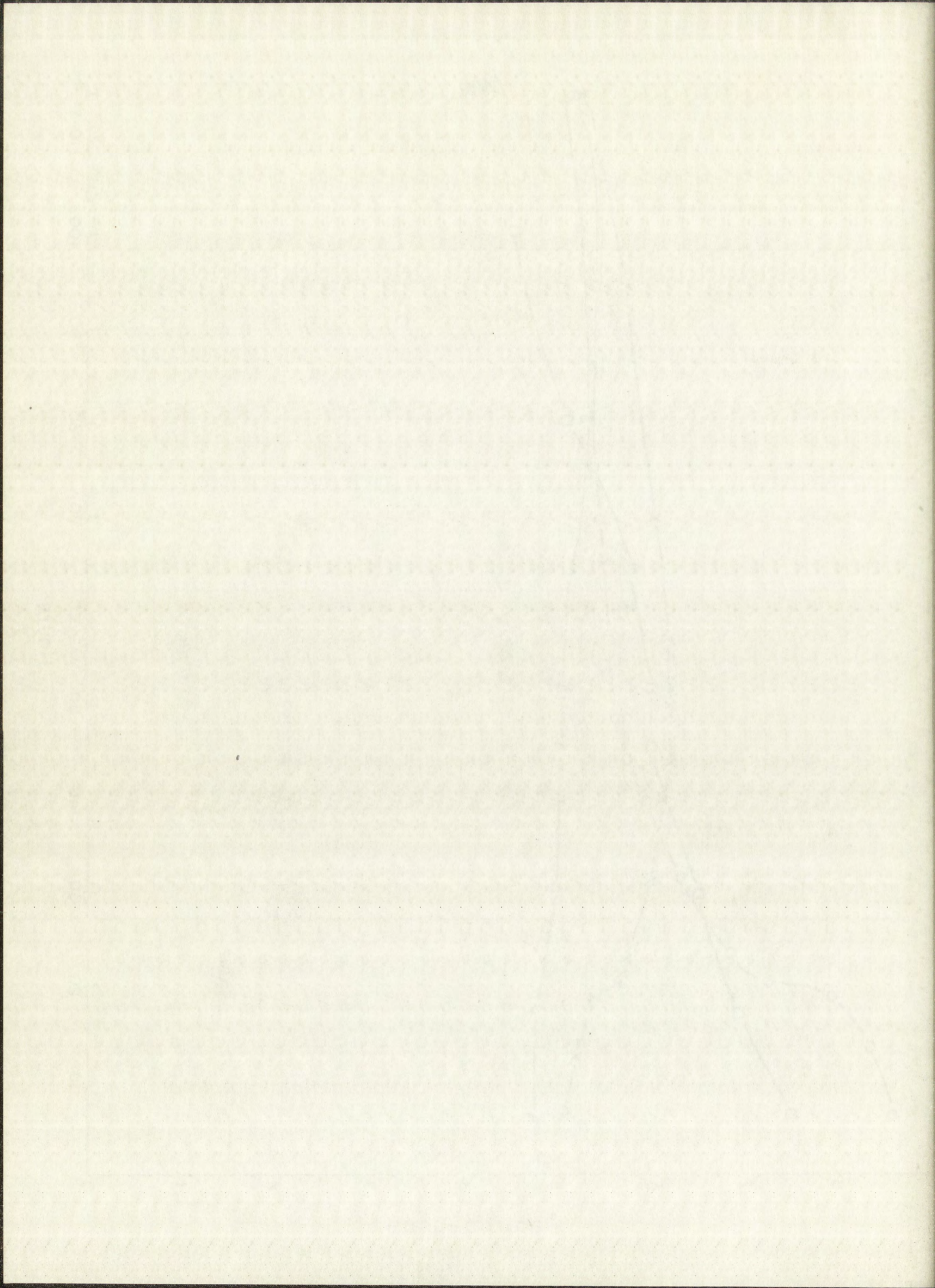
5

FIGURE 25

Decomposition of $\text{Sm}(\text{SA})_3$

- - 3850A peak in light
- ◻ - 3850A peak in dark
- × - 3250A peak in light
- ◼ - 3250A peak in dark





conclude that dissociation and decomposition definitely occur in solution.

The salicylaldehyde rare earth chelate series exhibited the most well defined emission spectra of all the compounds studied. Each member of the series had two different types of emission, a green phosphorescence with a short mean life ($\sim 10^{-3}$ sec.), and a blue after glow with relatively long mean life ($\sim 10^{-1}$ sec.). All of the observed emissions could be easily photographed through the phosphoroscope. The spectra are shown in Figures 26-33.

A triplet-singlet emission is usually a long lived luminescence ($\sim 10^{-4}$ sec. or longer), while a singlet-singlet emission is approximately 10^{-8} seconds in duration.⁷ The measured band maxima are not reported separately as singlets and triplets but instead all are considered to be experimentally determined phosphorescence bands whose origins will be discussed later. The measurements are believed to be accurate within $\pm 25 \text{ cm}^{-1}$. As was previously mentioned, this series of compounds undergoes rapid dissociation and decomposition in solution, however, the wavelength positions of band maxima were not affected by this experimental difficulty. The band intensities decreased somewhat with time as a result of the dissociation and decomposition. The salicylaldehyde chelates of gadolinium, lanthanum and lutecium

collected two different...
depending on the...
Table II and Figure 1...
experiments from the...
ported in Table I.

Photographs of the...
contained mixtures...
responding character...
characteristic...
The emission bands...

position of the...
was observed when...
changed from ethanol...
hexane was used...
was found to be...

current (see Figure...
the rate also...
of the dissociation...
of these results...
3. Solvent effect...

absorption peak...
underwent a...
the solvent from...

107
108
109
110
111
112
113
114
115
116
117
118
119
120
121
122
123
124
125
126
127
128
129
130
131
132
133
134
135
136
137
138
139
140
141
142
143
144
145
146
147
148
149
150
151
152
153
154
155
156
157
158
159
160
161
162
163
164
165
166
167
168
169
170
171
172
173
174
175
176
177
178
179
180
181
182
183
184
185
186
187
188
189
190
191
192
193
194
195
196
197
198
199
200

Original in file

Original in file

FIGURE 26 $\text{Gd}(\text{SA})_3$

Phosphorescence

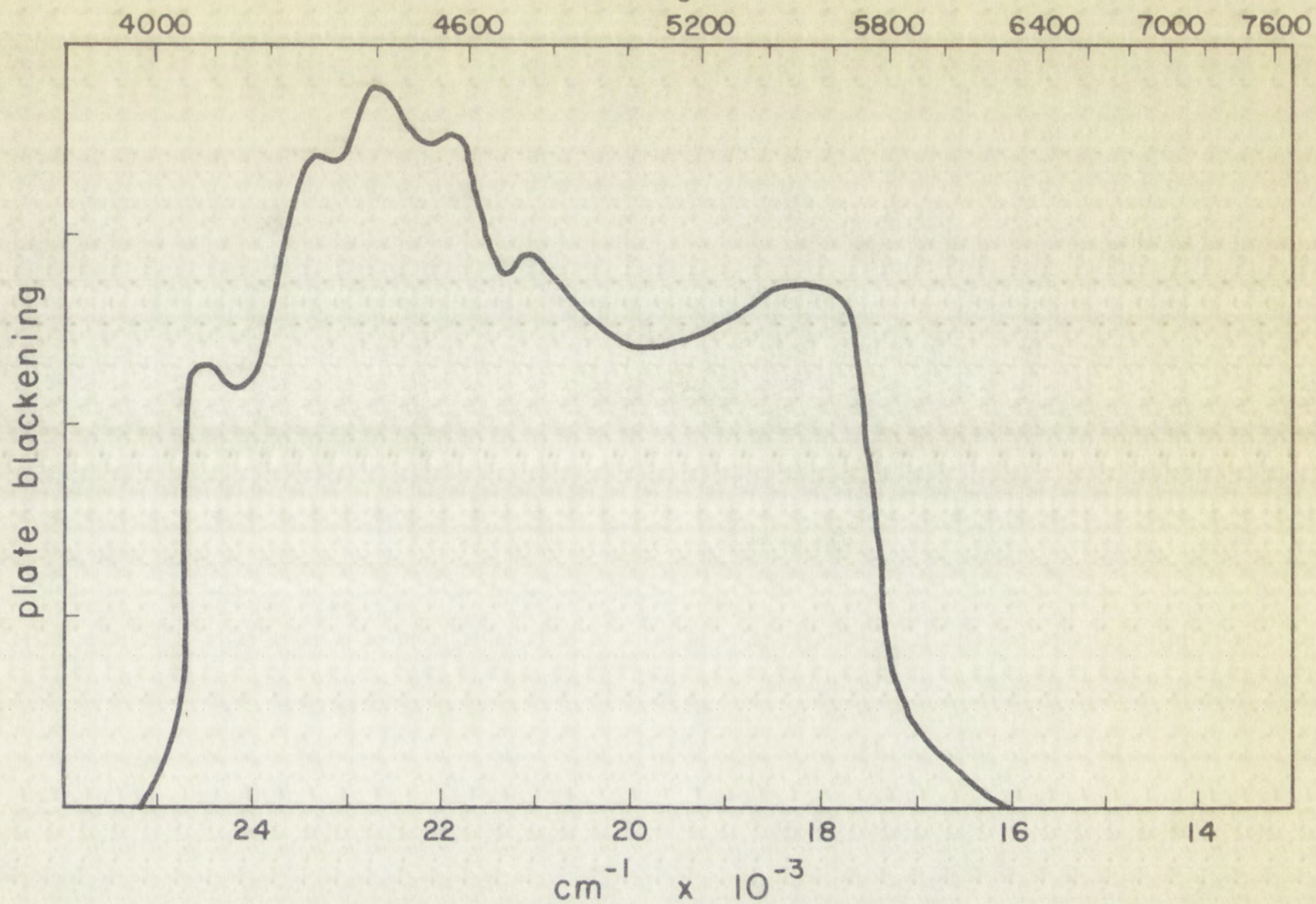
5840-KCr₂(SO₄) FilterFIGURE 27 $\text{Gd}(\text{SA})_3$

Phosphorescence

3389-CuSO₄ Filter

133

wavelength in Å



wavelength in Å

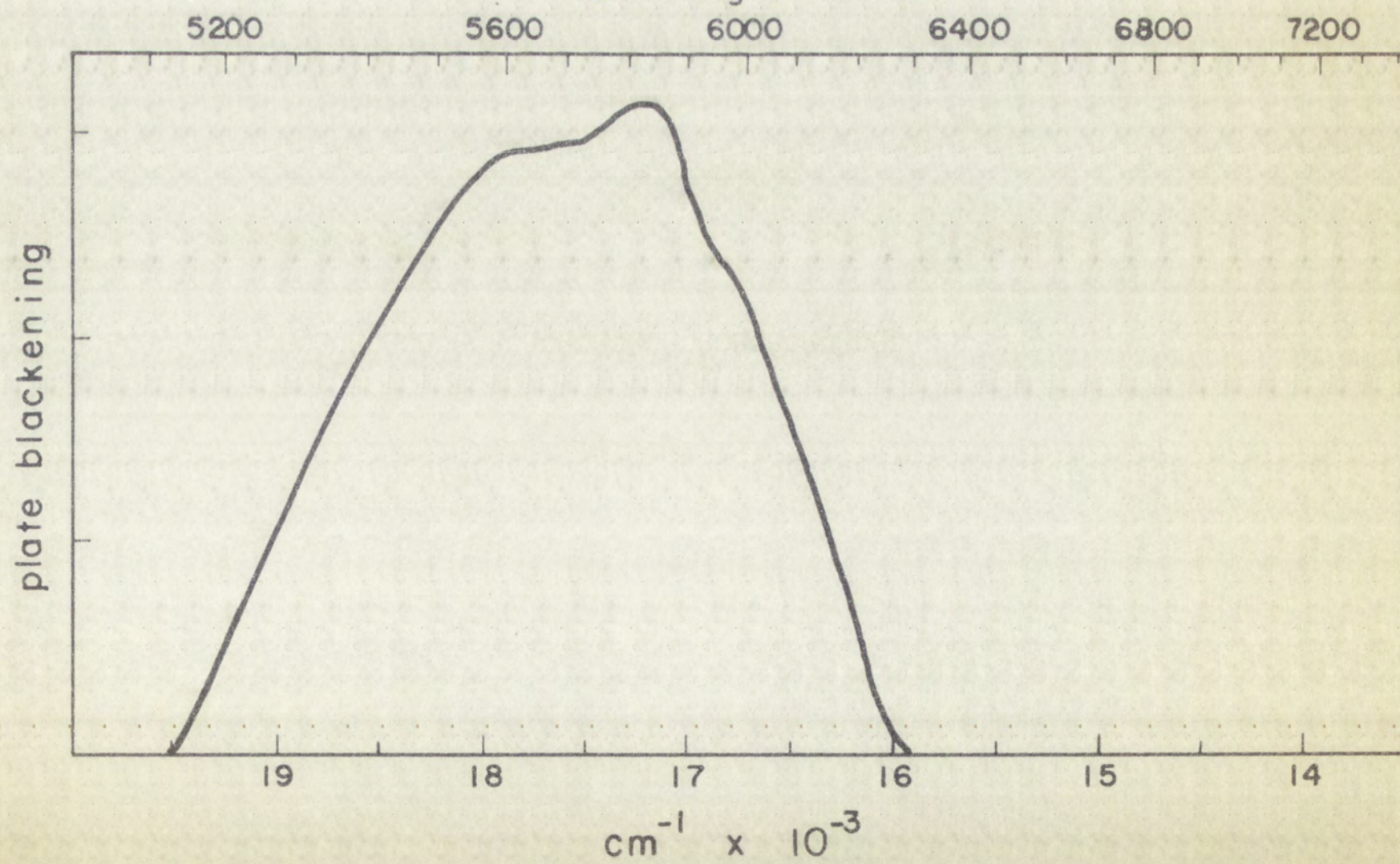
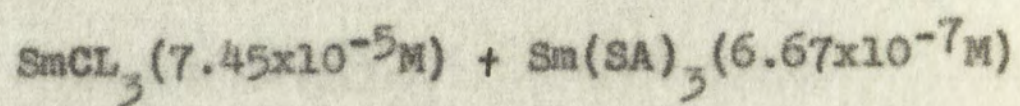
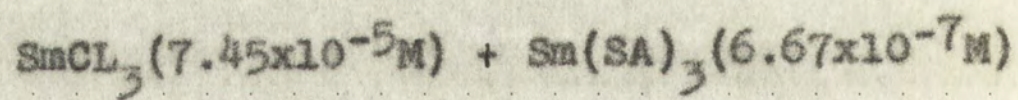


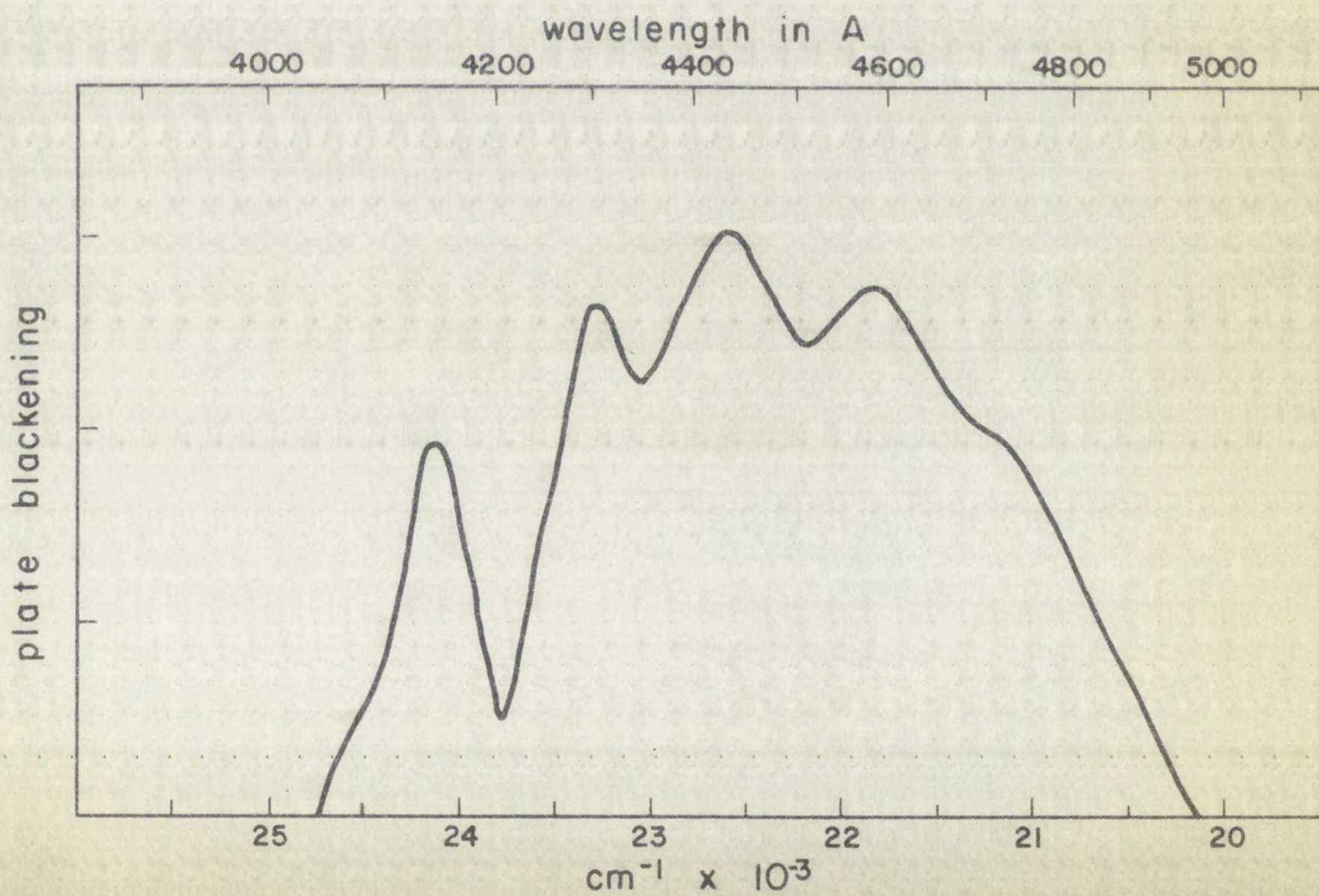
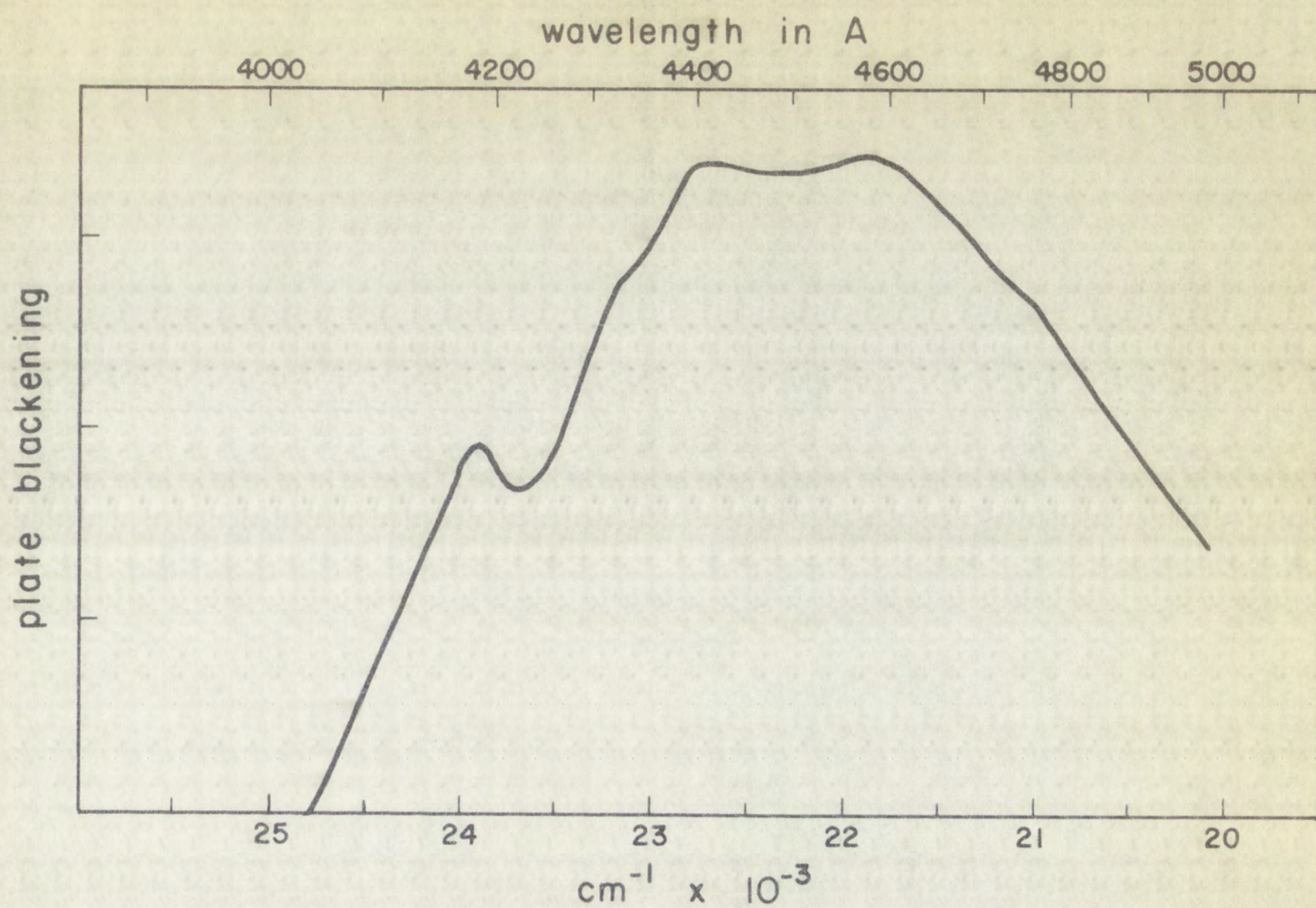
FIGURE 28

Total Emission

FIGURE 29

Phosphorescence

135



1000 900 800 700 600 500 400 300 200 100 0



1000 900 800 700 600 500 400 300 200 100 0

1000 900 800 700 600 500 400 300 200 100 0

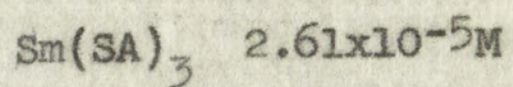


1000 900 800 700 600 500 400 300 200 100 0

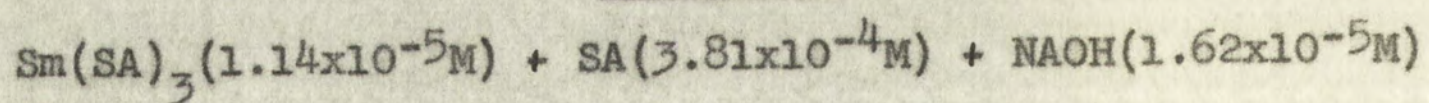
note blackening

blackening

note

FIGURE 30

Total Emission

FIGURE 31

Total Emission

137

plate blackening

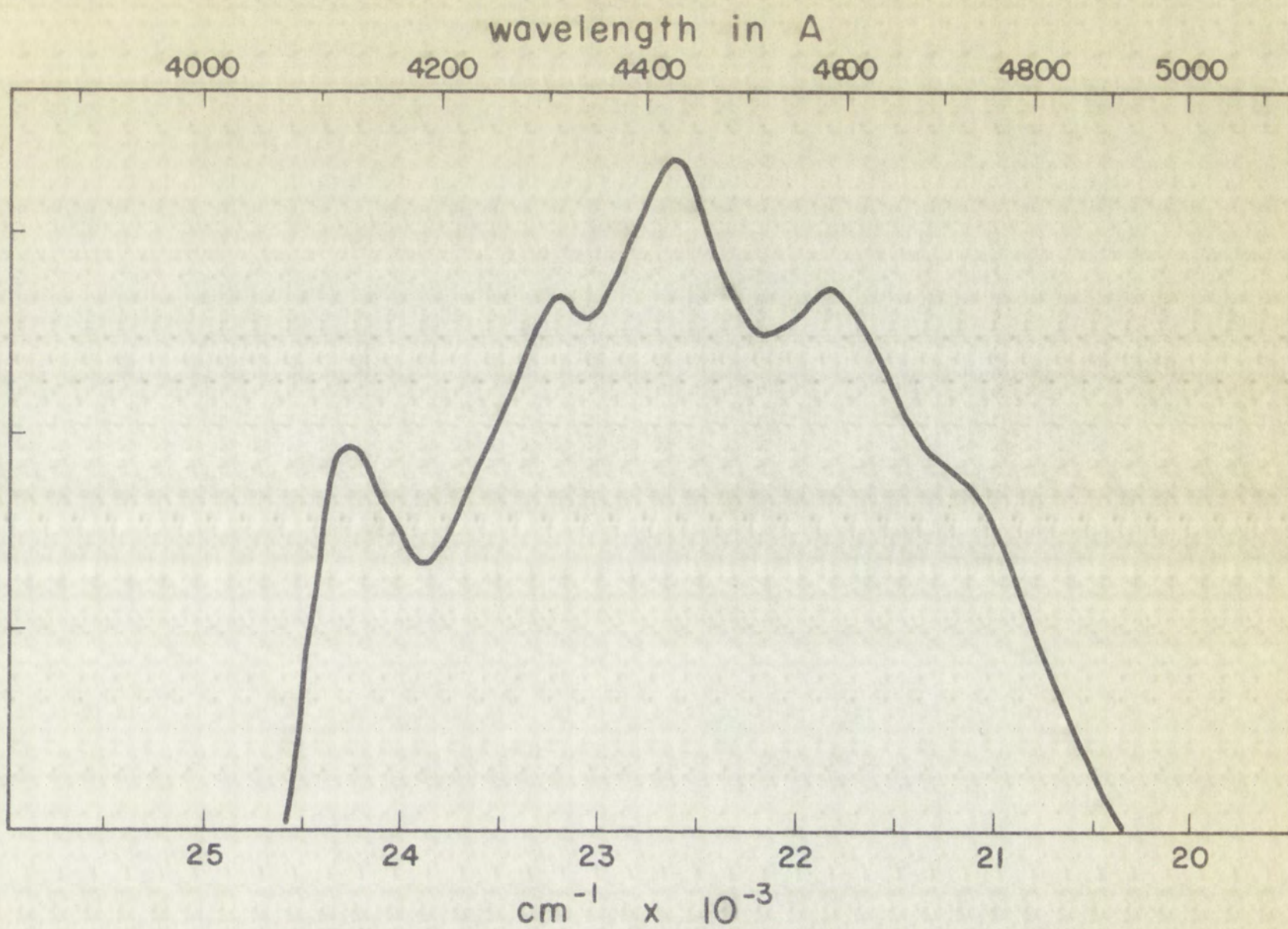
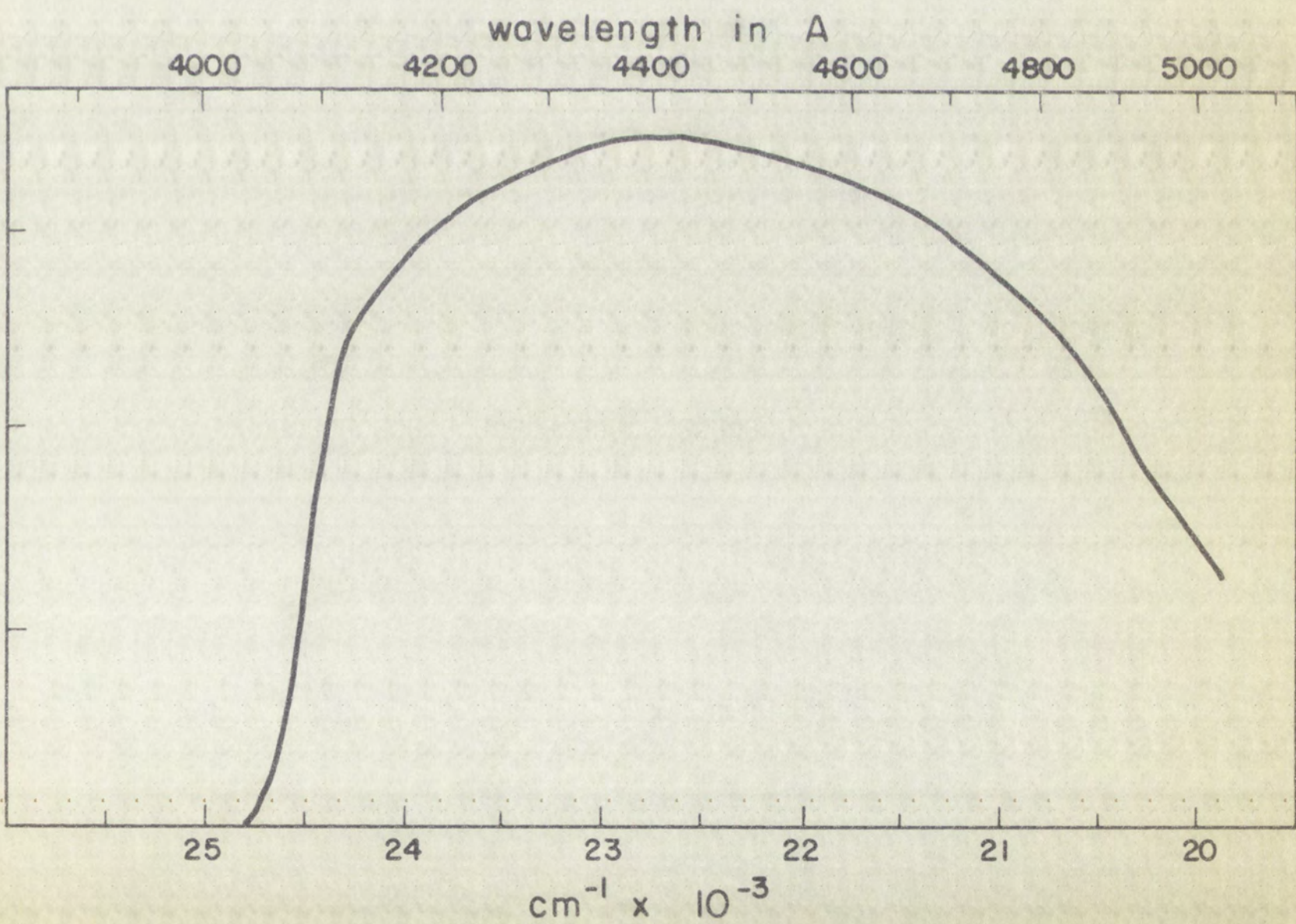


plate blackening



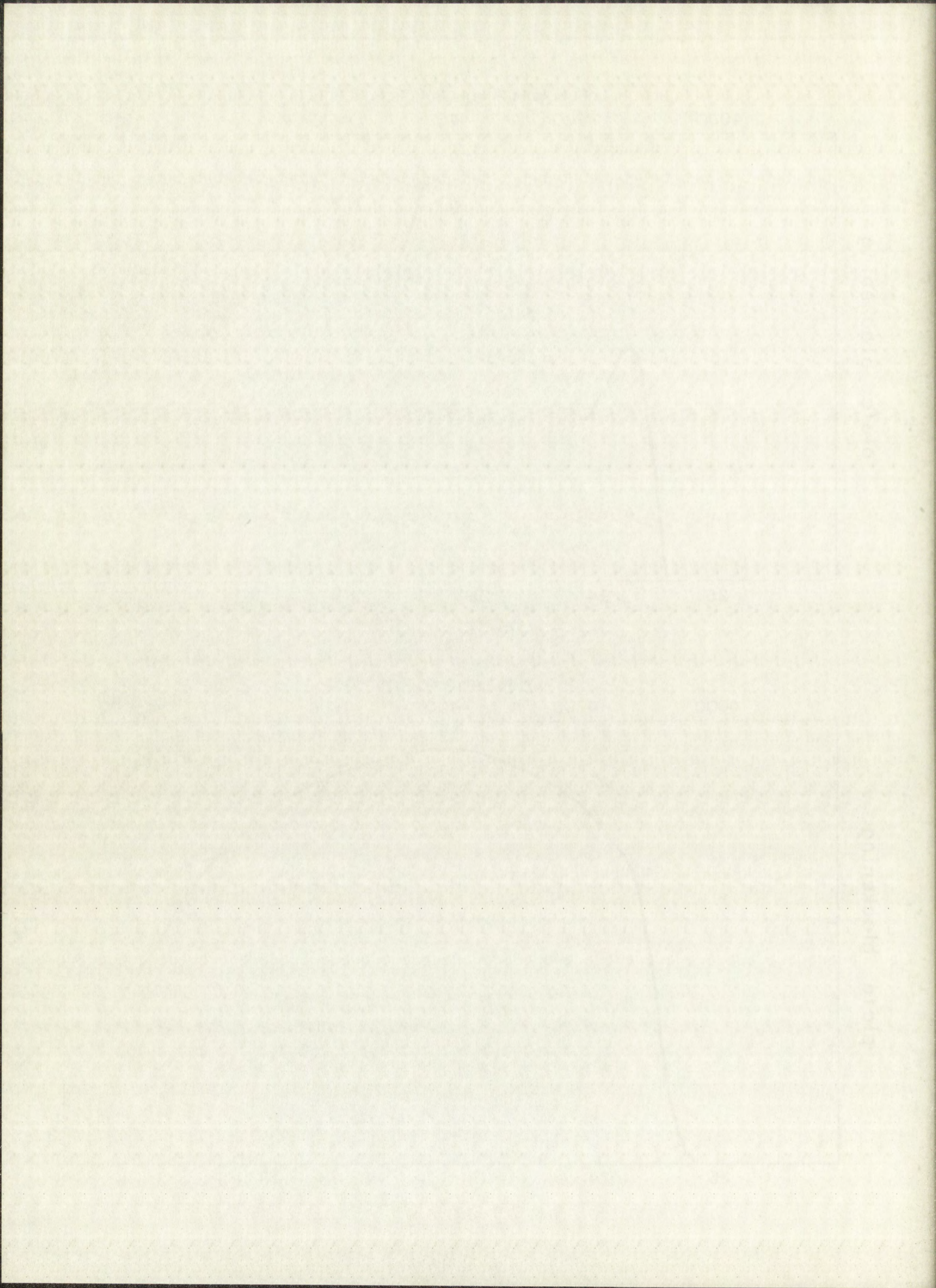
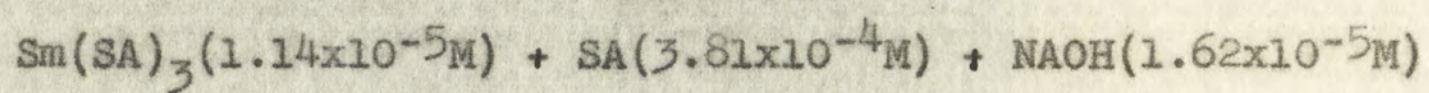
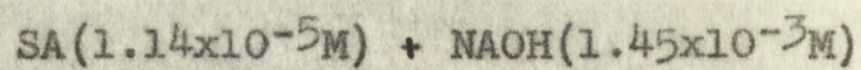


plate blanketing

plate blanketing

FIGURE 32

Phosphorescence

FIGURE 33

Phosphorescence

139

wavelength in Å

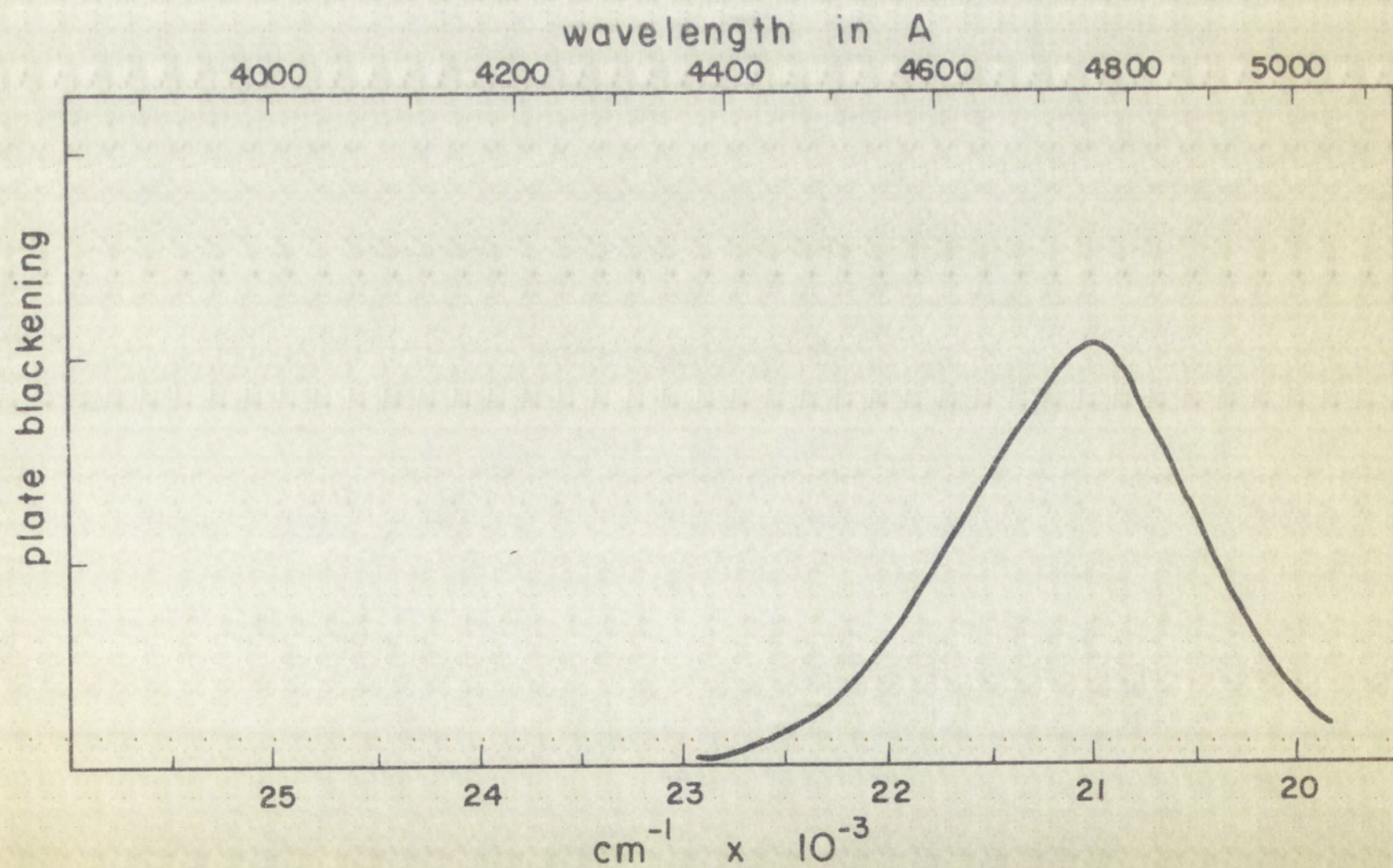
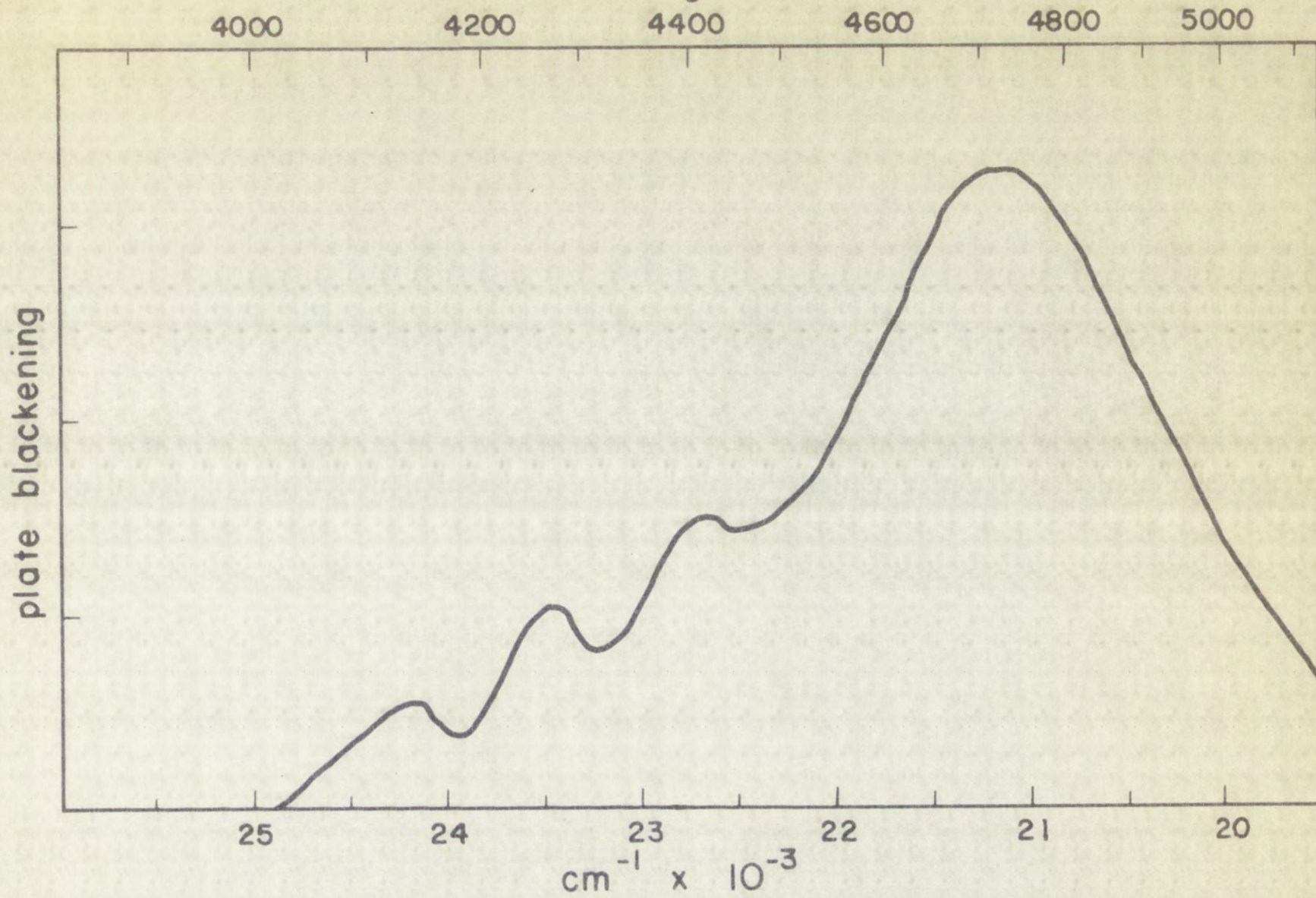




Figure 1: The solid



Figure 2: The solid

NOTHING BUT THE TRUTH
AND NOTHING BUT THE TRUTH

THE TRUTH IS THE ONLY WAY TO THE TRUTH

THE TRUTH IS THE ONLY WAY TO THE TRUTH

THE TRUTH IS THE ONLY WAY TO THE TRUTH

THE TRUTH IS THE ONLY WAY TO THE TRUTH

THE TRUTH IS THE ONLY WAY TO THE TRUTH

THE TRUTH IS THE ONLY WAY TO THE TRUTH

THE TRUTH IS THE ONLY WAY TO THE TRUTH

THE TRUTH IS THE ONLY WAY TO THE TRUTH

THE TRUTH IS THE ONLY WAY TO THE TRUTH

THE TRUTH IS THE ONLY WAY TO THE TRUTH

THE TRUTH IS THE ONLY WAY TO THE TRUTH

THE TRUTH IS THE ONLY WAY TO THE TRUTH

THE TRUTH IS THE ONLY WAY TO THE TRUTH

THE TRUTH IS THE ONLY WAY TO THE TRUTH

THE TRUTH IS THE ONLY WAY TO THE TRUTH

THE TRUTH IS THE ONLY WAY TO THE TRUTH

THE TRUTH IS THE ONLY WAY TO THE TRUTH

THE TRUTH IS THE ONLY WAY TO THE TRUTH

THE TRUTH IS THE ONLY WAY TO THE TRUTH

THE TRUTH IS THE ONLY WAY TO THE TRUTH

THE TRUTH IS THE ONLY WAY TO THE TRUTH

THE TRUTH IS THE ONLY WAY TO THE TRUTH

THE TRUTH IS THE ONLY WAY TO THE TRUTH

THE TRUTH IS THE ONLY WAY TO THE TRUTH

THE TRUTH IS THE ONLY WAY TO THE TRUTH

THE TRUTH IS THE ONLY WAY TO THE TRUTH

THE TRUTH IS THE ONLY WAY TO THE TRUTH

THE TRUTH IS THE ONLY WAY TO THE TRUTH

THE TRUTH IS THE ONLY WAY TO THE TRUTH

THE TRUTH IS THE ONLY WAY TO THE TRUTH

TABLE 17

MEASUREMENTS OF THE PHOSPHORESCENCE BAND MAXIMA FOR
THE RARE EARTH CHELATES OF SALICYLALDEHYDE

$\text{La}(\text{SA})_3^{(a)}$		$\text{Pr}(\text{SA})_3$		$\text{Nd}(\text{SA})_3$		$\text{Sm}(\text{SA})_3$	
A	cm^{-1}	A	cm^{-1}	A	cm^{-1}	A	cm^{-1}
4096	24,414	4120	24,272	4126	24,236	4120	24,272
4280	23,364						
4420	22,624	4275	23,392	4272	23,408	4266	23,441
4585	21,810	4420	22,624	4420	22,624	4424	22,604
4752	21,044	4590	21,786	4590	21,786	4593	21,772
5460	18,315	4753	21,039	4752	21,044	4750	21,053
5810	17,212	5120	19,531	5120	19,531	5120	19,531
-----		-----		-----		-----	
$\text{Ho}(\text{SA})_3$		$\text{Er}(\text{SA})_3$		$\text{Dy}(\text{SA})_3$		$\text{Tm}(\text{SA})_3$	
A	cm^{-1}	A	cm^{-1}	A	cm^{-1}	A	cm^{-1}
4130	24,213	4122	24,844	4120	24,272	4130	24,876
4270	23,419	4274	23,397	4268	23,430	4272	23,408
4418	22,634	4418	22,634	4420	22,624	4415	22,650
4595	21,763	4596	21,758	4589	21,791	4596	21,758
4752	21,044	4753	21,039	4753	21,039	4753	21,039
5120	19,531	5118	19,539	5130	19,531	5119	19,535

(a) The error in the frequency measurements is
+ 25 cm^{-1} .

(b) These three phosphorescence measurements were made
by use of a 3389 Corning filter and copper sulfate solution
(see Table 4 in the Experimental Section).

TABLE 17--Continued

Eu(SA) ₃		Gd(SA) ₃		Tb(SA) ₃		La(SA) ₃ ^(b)	
A cm ⁻¹		A cm ⁻¹		A cm ⁻¹		A cm ⁻¹	
4120	24,271	4081	24,504	4125	24,242	5640	17,730
4268	23,430	4267	23,436	4268	23,430	5850	17,094
4416	22,644	4400	22,727	4420	22,624	5926	16,874
4590	21,786	4591	21,782	4596	21,758		
4753	21,039	4748	21,061	4753	21,039		
5118	19,539	5452	18,342	5120	19,531		
		5805	17,226				
-----		-----		-----		-----	
Yb(SA) ₃		Lu(SA) ₃		Gd(SA) ₃		Lu(SA) ₃	
A cm ⁻¹		A cm ⁻¹		A cm ⁻¹		A cm ⁻¹	
4130	24,876	4110	24,331	5639	17,734	5636	17,743
4270	23,419	4270	23,419	5846	17,106	5847	17,103
4424	22,604	4415	22,650	5929	16,866	5930	16,863
4592	21,777	4592	21,777				
4753	21,039	4745	21,074				
5118	19,539	5450	18,348				
		5810	17,212				

1000

Yp(2A)		Yp(2A)	
A		A	
41.00	24.00	41.00	24.00
42.00	25.00	42.00	25.00
43.00	26.00	43.00	26.00
44.00	27.00	44.00	27.00
45.00	28.00	45.00	28.00
46.00	29.00	46.00	29.00
47.00	30.00	47.00	30.00
48.00	31.00	48.00	31.00
49.00	32.00	49.00	32.00
50.00	33.00	50.00	33.00
51.00	34.00	51.00	34.00
52.00	35.00	52.00	35.00
53.00	36.00	53.00	36.00
54.00	37.00	54.00	37.00
55.00	38.00	55.00	38.00
56.00	39.00	56.00	39.00
57.00	40.00	57.00	40.00
58.00	41.00	58.00	41.00
59.00	42.00	59.00	42.00
60.00	43.00	60.00	43.00
61.00	44.00	61.00	44.00
62.00	45.00	62.00	45.00
63.00	46.00	63.00	46.00
64.00	47.00	64.00	47.00
65.00	48.00	65.00	48.00
66.00	49.00	66.00	49.00
67.00	50.00	67.00	50.00
68.00	51.00	68.00	51.00
69.00	52.00	69.00	52.00
70.00	53.00	70.00	53.00
71.00	54.00	71.00	54.00
72.00	55.00	72.00	55.00
73.00	56.00	73.00	56.00
74.00	57.00	74.00	57.00
75.00	58.00	75.00	58.00
76.00	59.00	76.00	59.00
77.00	60.00	77.00	60.00
78.00	61.00	78.00	61.00
79.00	62.00	79.00	62.00
80.00	63.00	80.00	63.00
81.00	64.00	81.00	64.00
82.00	65.00	82.00	65.00
83.00	66.00	83.00	66.00
84.00	67.00	84.00	67.00
85.00	68.00	85.00	68.00
86.00	69.00	86.00	69.00
87.00	70.00	87.00	70.00
88.00	71.00	88.00	71.00
89.00	72.00	89.00	72.00
90.00	73.00	90.00	73.00
91.00	74.00	91.00	74.00
92.00	75.00	92.00	75.00
93.00	76.00	93.00	76.00
94.00	77.00	94.00	77.00
95.00	78.00	95.00	78.00
96.00	79.00	96.00	79.00
97.00	80.00	97.00	80.00
98.00	81.00	98.00	81.00
99.00	82.00	99.00	82.00
100.00	83.00	100.00	83.00

Absorbance

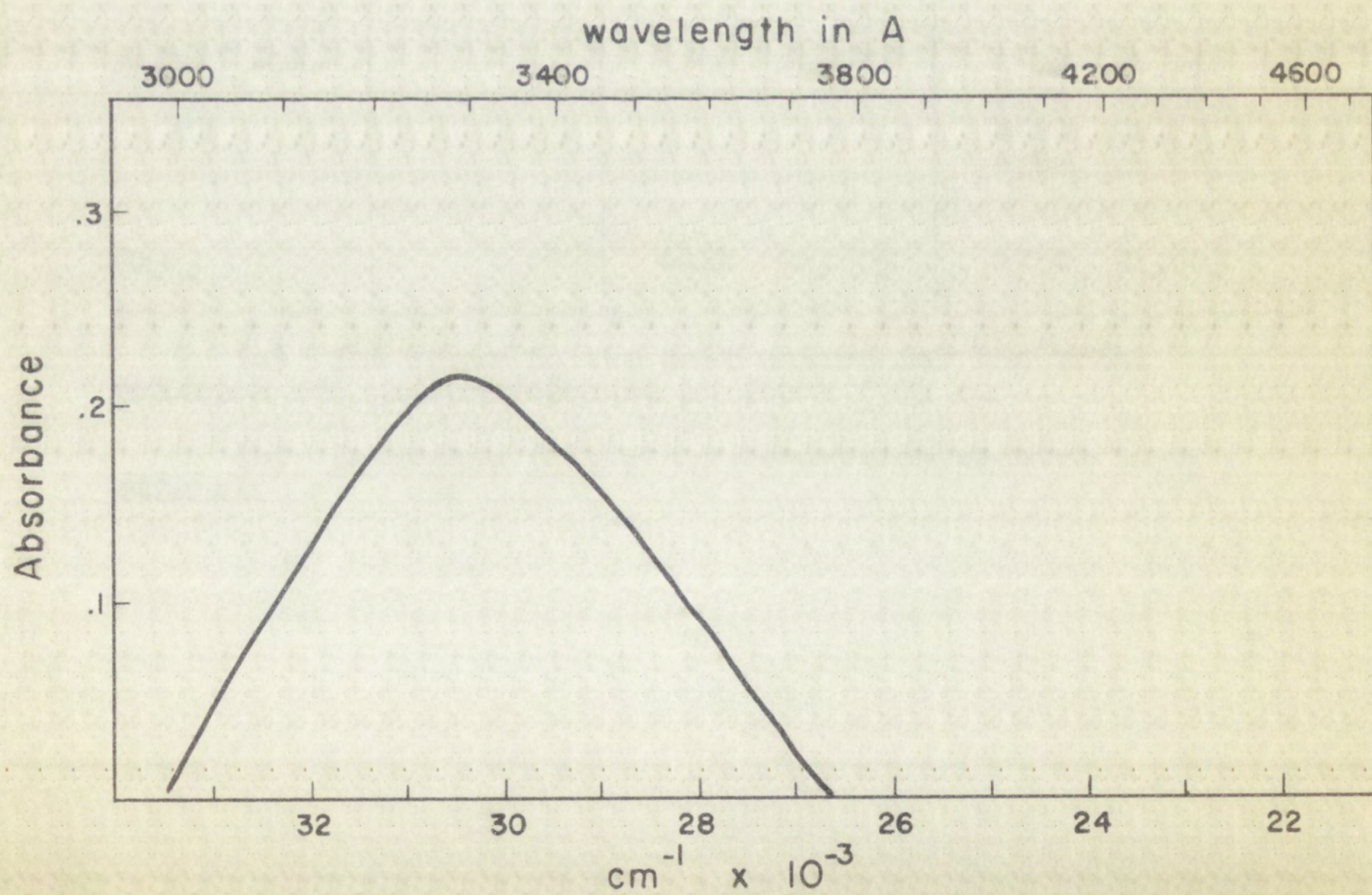
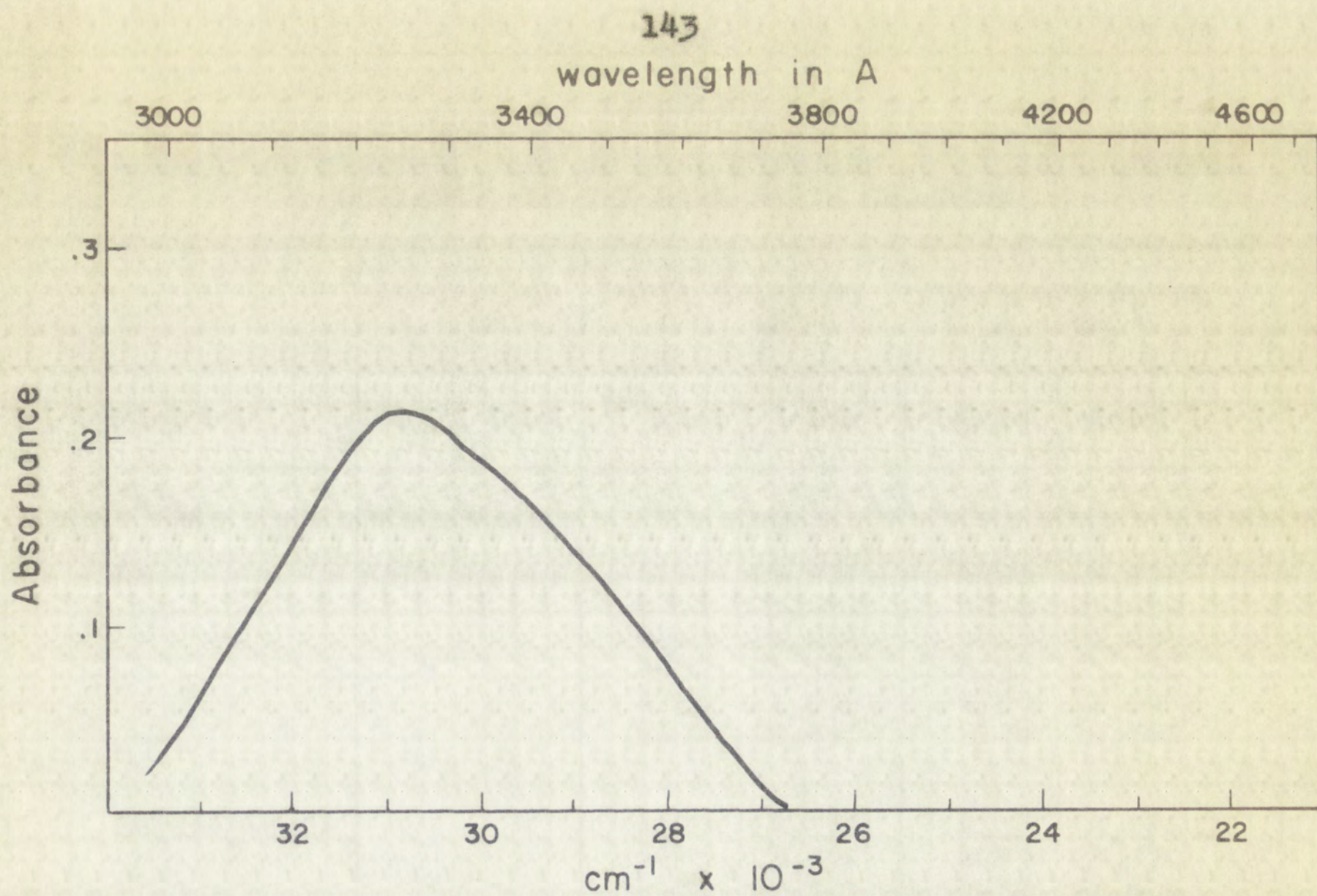
Absorbance

FIGURE 34SA($6.90 \times 10^{-5} \text{M}$)

Abs. Eth.

FIGURE 35SA($6.89 \times 10^{-5} \text{M}$)

Hexane



The blue shift which is observed in the
to hydrogen bonding of the solvent to the
the ground state of the molecule. The
to the first excited state of the molecule
n-electrons are shifted to higher energy
solvent. The result is a shift of the
state and the ground state of the molecule
hexamer; consequently the energy of the
in the absorption spectrum. The energy of
bonding of SA is predicted to be lower
in ethanol, and also, the energy of the
is expected. The energy of the
energy of the excited state is higher than
the corresponding energy of the ground state
if the solvent is ethanol. The energy of
the excited state is higher than the energy
the corresponding energy of the ground state
character of the excited state is higher
shifts because the energy of the excited state
or any other hydrogen bonding solvent.
The energy of the excited state is higher
the possibility that a hydrogen bond is
ethanol was formed in a hydrogen bond
The observed blue shift is higher than
mixture of ethanol and water.

ethanol, but not in hexane.

4. Emission Spectra.--The salicylaldehyde chelates of lanthanum, gadolinium and lutecium demonstrate three different types of emission: (i) a green phosphorescence ($22,000\text{ cm}^{-1}$ - $20,000\text{ cm}^{-1}$, $\sim 10^{-3}$ seconds lifetime) (ii) a yellow phosphorescence ($19,000\text{ cm}^{-1}$ - $16,800\text{ cm}^{-1}$) with a lifetime of approximately 10^{-4} seconds in duration (iii) a relatively long lived ($\sim 10^{-1}$ seconds) blue afterglow ($25,000\text{ cm}^{-1}$ - $22,000\text{ cm}^{-1}$). The remainder of the chelates in this series only show the blue and the green phosphorescence (with the exception of the europium chelate which also shows line emission characteristic of the metal ion). Selective excitation of gadolinium, lanthanum and lutecium chelate samples of this series with near ultraviolet light which is primarily absorbed by the 3850A band (using CuSO_4 solution filter and 3389 Corning filter) is followed by a yellow phosphorescence (see Figure 27). None of the other members of the series demonstrate this long wavelength emission which is attributed to an electronic transition of the type triplet to ground state in either $\text{M}(\text{SA})^{++}$ or $\text{M}(\text{SA})_2^+$ or $\text{M}(\text{SA})_3$ or all three species. The highest energy peak for this lowest lying electronic transition is at $17,734\text{ cm}^{-1}$ for $\text{Gd}(\text{SA})_3$, $17,730\text{ cm}^{-1}$ for $\text{La}(\text{SA})_3$, and $17,743\text{ cm}^{-1}$ for $\text{Lu}(\text{SA})_3$.

A chrome alum solution (see Table 4) and a Corning 5840 filter system for the exciting light selectively excites a

observed, but not in reverse.

... In the case of ...
... gadolinium ...
... of gadolinium ...
... $10,000 \text{ cm}^{-1}$...
... resonance ...
... approximately 10^{-1} ...
... long lived ...
... $22,000 \text{ cm}^{-1}$...
... only show the blue ...
... exception of the ...
... also characteristic ...
... of gadolinium ...
... series with near ...
... formed by the ...
... 3500 ...
... (see Figure 1) ...
... demonstrate ...
... to an electronic ...
... state in which ...
... expected. The ...
... electronic ...
... 10^{-1} ...
... A ...
... filter system for the ...

chelate sample at the 3250A absorption band. The filter system, however, also allows some excitation of the 3850A band. The resulting emission is shown in Figure 26. The band structure appearing from about $20,500\text{ cm}^{-1}$ to about $16,600\text{ cm}^{-1}$ is characteristic of the lanthanum, gadolinium and lutecium chelates of this series. For the remaining members of the series only the bands from $24,900\text{ cm}^{-1}$ to $20,000\text{ cm}^{-1}$ appear.

In the rare earth 2-methyl-8-hydroxyquinolates, and 8-hydroxyquinolates, the chelates of lanthanum, gadolinium and lutecium are the only three of these that show a long wavelength emission. The triplet-singlet electronic transition for these three cases is more apparent because the trivalent rare earth ion has no electronic levels lying below the lowest triplet state of the complexes to provide a quenching path; consequently there is little quenching due to the rare earth ion. By analogy we assign the long wavelength transition observed in the salicylaldehyde chelates of Lu, La, and Gd to a T-S transition of the complex.

The green phosphorescence has a band maximum about $21,150\text{ cm}^{-1}$. This emission is observed for all the rare earth chelates in this series as well as the sodium salt of SA (see Figure 33).

Because dissociation of the metal chelates occurs in solution, the green phosphorescence with band maximum at

approximately $21,150\text{ cm}^{-1}$, which is characteristic of all the salicylaldehyde rare earth chelates, is attributed to an electronic transition of the salicylaldehyde ion.

A densitometer trace of the phosphorescence for the mixture $\text{Sm}(\text{SA})_3 + \text{NaOH} + \text{SA}$, is shown in Figure 31. The phosphorescence band appearing at about $21,150\text{ cm}^{-1}$ has definitely increased in intensity accompanied by a decrease in the other peak intensities compared to the intensities of the $\text{Sm}(\text{SA})_3$ sample (see Figure 30). This increase in intensity probably indicates an increase in the concentration of SA^- . The phosphorescence bands for the mixture $\text{SmCl}_3 + \text{Sm}(\text{SA})_3$ (Figure 29) are at about the same positions as $\text{Sm}(\text{SA})_3$ but a slight increase in relative intensity at $21,150\text{ cm}^{-1}$ and a decrease at $22,600\text{ cm}^{-1}$ also occurred. These changes, small in magnitude, are probably not significant and definitely within experimental error. We conclude that the species (SA^-) is responsible for the green phosphorescence.

The long lived blue ($25,000 - 22,000\text{ cm}^{-1}$) afterglow is also characteristic of all the members of this chelate series. This phosphorescence is observed following selective excitation of a chelate sample with ultraviolet light which is primarily absorbed by the 3250A absorption band. This emission is attributed primarily to an electronic transition of a species which does not have a rare earth ion chemically bonded. Because salicylaldehyde also demonstrates the same type of

emission (see Table 18), the electronic transition responsible for the blue afterglow in the chelates is only slightly perturbed compared to that occurring in salicylaldehyde alone. Although it was not experimentally possible to classify the 3250A absorption band as an $n-\pi^*$ transition in the rare earth chelates of this series, the emission spectrum of salicylaldehyde is almost identical to that observed (range - 25,000 - 22,000 cm^{-1}) for all members of the series. Therefore, the blue afterglow could be due to salicylaldehyde which is a species in solution, or possibly to the hemiacetal of salicylaldehyde and ethanol.

The emission band at about 21,150 cm^{-1} also appearing for salicylaldehyde (see Table 18) is again almost identical in all cases and is probably due to salicylaldehyde. The SA- species may be responsible for the long wavelength tail absorption at approximately 3700 A in the salicylaldehyde absorption spectrum. No absorption peak appears at 3850 A, but the absence of a peak may be due to the very dilute SA-species in solution.

5. The Path of Energy Transfer.--The salicylaldehyde chelate of europium was the only chelate of the entire rare earth series for which line emission could be easily photographed. Very weak line emission from the terbium chelate on prolonged exposures was photographed but these weak lines are considered to be emission from decomposition products or

impurities. Tris-salicylaldehyde Eu^{+++} exhibits line emission which originates at the lower resonance level of Eu^{+++} ($17,250 \text{ cm}^{-1}$). The highest frequency line for this Eu chelate appears at $17,270 \text{ cm}^{-1}$. The line is 30 Å wide but the measurement is sufficiently accurate to definitely show that line emission for the salicylaldehyde chelate of europium only occurs from the lower resonance level.

Figure 22 shows that the energy level responsible for the yellow phosphorescence ($17,700 \text{ cm}^{-1}$) lies between the two resonance levels of Eu^{+++} . On the basis of the fact that the energy transfer to the rare earth ion in the 2-methyl-8-hydroxyquinolate and 8-hydroxyquinolate europium chelates has been established as going via the lowest or a nearby triplet state, the energy transfer for the corresponding salicylaldehyde chelate probably goes via the emitting level lying between the two resonance levels of Eu^{+++} .

Intramolecular energy transfer to the rare earth ion cannot go via the emitting level ($21,150 \text{ cm}^{-1}$) of the salicylaldehyde ion because it is an ionized molecular species in solution and a separate entity. Since the emitting level of the salicylaldehyde ion is sufficiently energetic, intermolecular energy transfer between the species SA^- and the species $\text{M}(\text{SA})_3$ is possible, but apparently does not occur.

The transfer of energy to the rare earth ion from an energy level appearing at about $24,280 \text{ cm}^{-1}$, possibly due to

SA , does not occur. No characteristic line emission for any of the other rare earth trivalent ions in this chelate series is observed. This is further evidence that this band is not associated with a species containing a metal ion.

The transfer of energy to the metal ion is most probably via the energy level at $17,740\text{ cm}^{-1}$ attributed to either $M(\text{SA})_3$ or $M(\text{SA})_2^+$ or $M(\text{SA})^{++}$ or all three species. The potential energy surface of this level crosses with the potential energy surface of the resonance level of the ion allowing the energy to transfer. Energy is being transferred from the zero vibronic level lying at $17,740\text{ cm}^{-1}$ to some vibrational level of the resonance level of the ion.

In summary, $\text{Sm}(\text{SA})_3$ was used as a representative sample for a study of the absorption and emission spectra of the salicylaldehyde rare earth chelates. Because the molar absorption coefficients of $\text{Sm}(\text{SA})_3$ varied with time, the species in solution could not be identified. The absorption peak appearing at about 3850 \AA was ascribed to the neutral species $M(\text{SA})_3$ or $M(\text{SA})_2^+$ or $M(\text{SA})^{++}$ or all three, and the peak at about 3250 \AA to SA or a hemiacetal of SA. Non-reversible destruction of the chelate molecule was also observed. Excess trivalent metal ion in solution and excess salicylaldehyde ion in solution showed evidence of extensive dissociation. The three different types of emission observed were classified in the following manner: (i) green phosphorescence

(lifetime 10^{-3} sec.) attributed to the salicylaldehyde ion, (ii) a yellow phosphorescence (lifetime 10^{-4} sec.) attributed to a triplet to ground state transition occurring in the species, $M(SA)_3$, or $M(SA)_2^+$ or $M(SA)^{++}$ (iii) a blue afterglow (lifetime $\sim 10^{-1}$ sec.) attributed to an electronic transition occurring in SA or a hemiacetal of SA or both species. Energy transfer in salicylaldehyde chelates probably occurs from the level measured to be approximately ($17,700 \text{ cm}^{-1}$).

BIBLIOGRAPHY

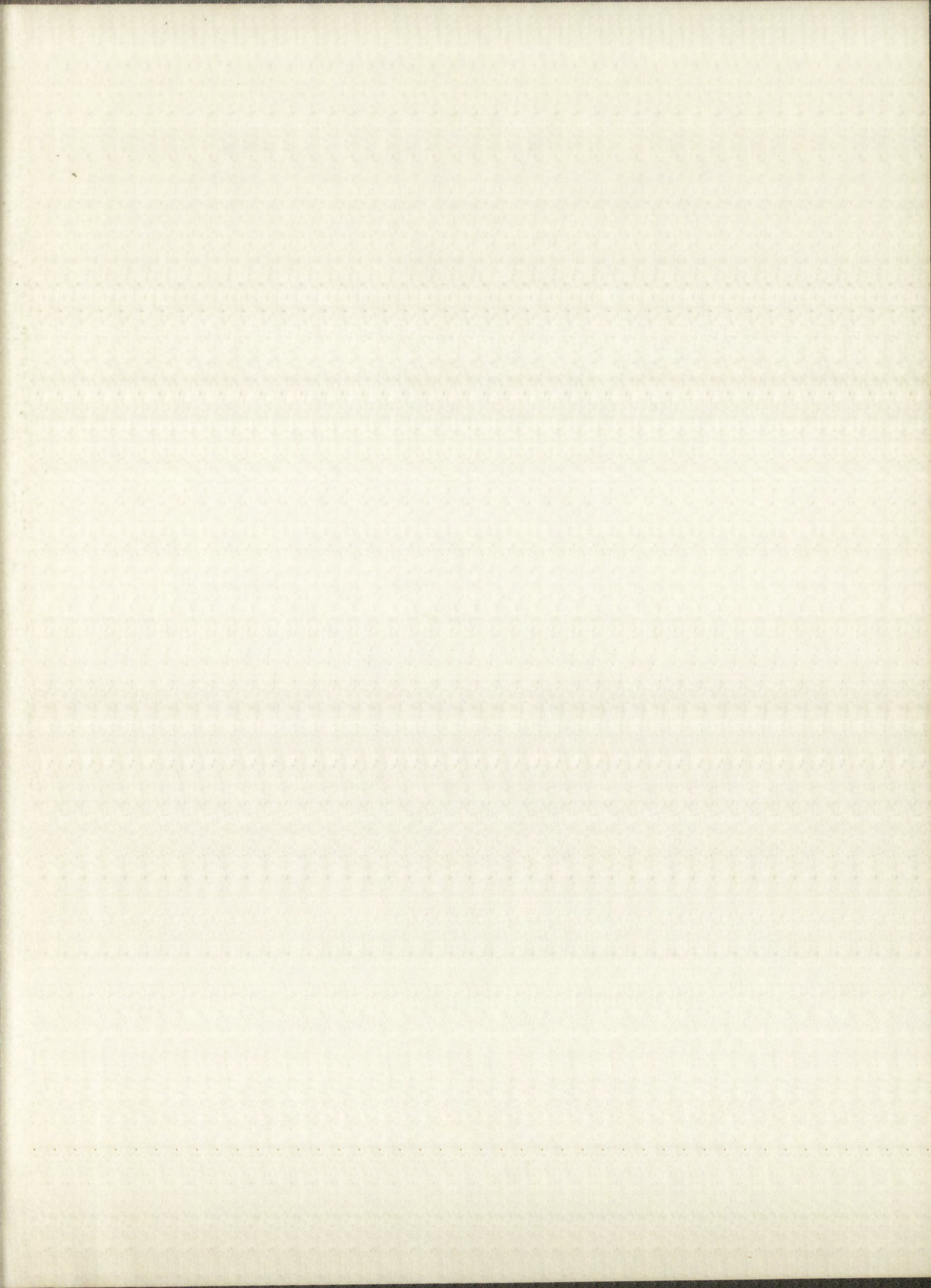
1. Coulson, C. A. *Quart. Rev. Chem. Soc.* 1, 144 (1947).
2. Mulliken, R. S. and Roothaan, C. C. *J. Chem. Rev.* 41, 219 (1947).
3. Platt, J. R. *J. Optical Soc. Am.* 43, 252 (1953).
4. Lewis, G. N. and Kasha, M. *J. Am. Chem. Soc.* 67, 994 (1944).
5. Kasha, M. *Chem. Rev.* 41, 401 (1947).
6. Yuster, P. Phd Thesis, Washington University, St. Louis, Mo. (1949).
7. Kasha, M. *Discussions Faraday Soc.* 9, 14 (1950).
8. Herzberg, G. *Atomic Spectra and Atomic Structure*, New York Dover Publications, p. 125, (1944).
9. McClure, D. *J. Chem. Phys.* 17, 905 (1949).
10. Porter, G. and Wright, M. R. *Discussions Faraday Soc.* 27, 18 (1959).
11. Kauzmann, W. *Quantum Chemistry*, Academic Press Inc. New York, N.Y. P. 581-723 (1957).
12. Evans, D. F. *J. Chem. Soc.* 552, (1959).
13. Kasha, M. *J. Chem. Phys.* 20, 71, (1952).
14. Terrenin, A. and Ermolaev, V. *Trans. Faraday Soc.* 52, 1042 (1956).
15. Förster, Th. *Discussions Faraday Soc.* 27, 7 (1959).
16. Yuster, P. and Weissman, S. I. *J. Chem. Phys.* 17, 1182 (1949).
17. Gilmore, E. H., Gibson, G. E. and McClure, D. S. *J. Chem. Phys.* 20, 829 (1952).

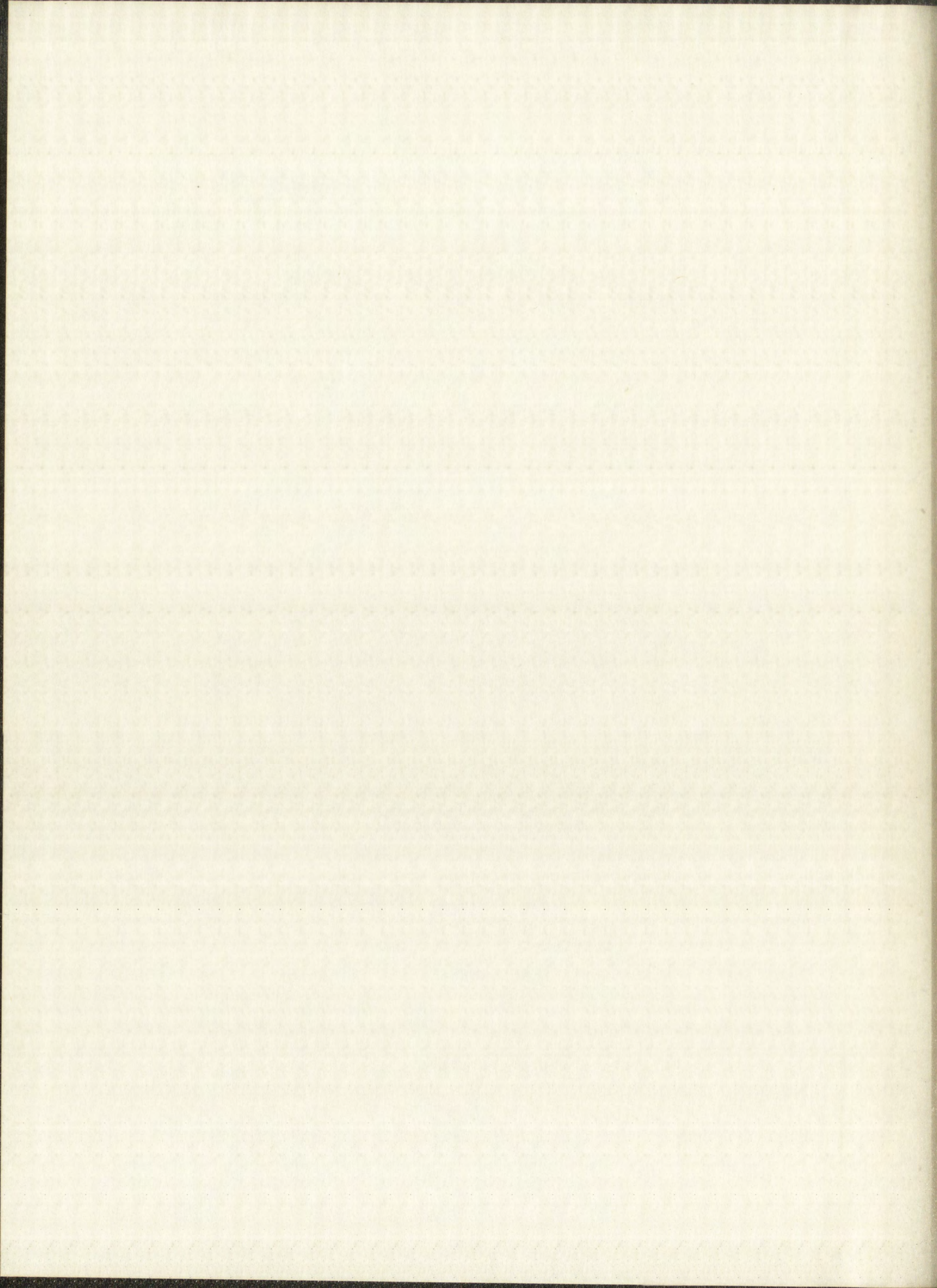
1. Robinson, D. W. (1947)
2. Mullins, J. B. (1947)
3. Pratt, J. W. (1947)
4. Lewis, C. H. (1947)
5. Kester, M. (1947)
6. Young, F. (1947)
7. Kester, M. (1947)
8. Hargrove, J. (1947)
9. McClure, J. (1947)
10. Porter, J. (1947)
11. Kester, M. (1947)
12. Kester, M. (1947)
13. Kester, M. (1947)
14. Kester, M. (1947)
15. Kester, M. (1947)
16. Kester, M. (1947)
17. Kester, M. (1947)

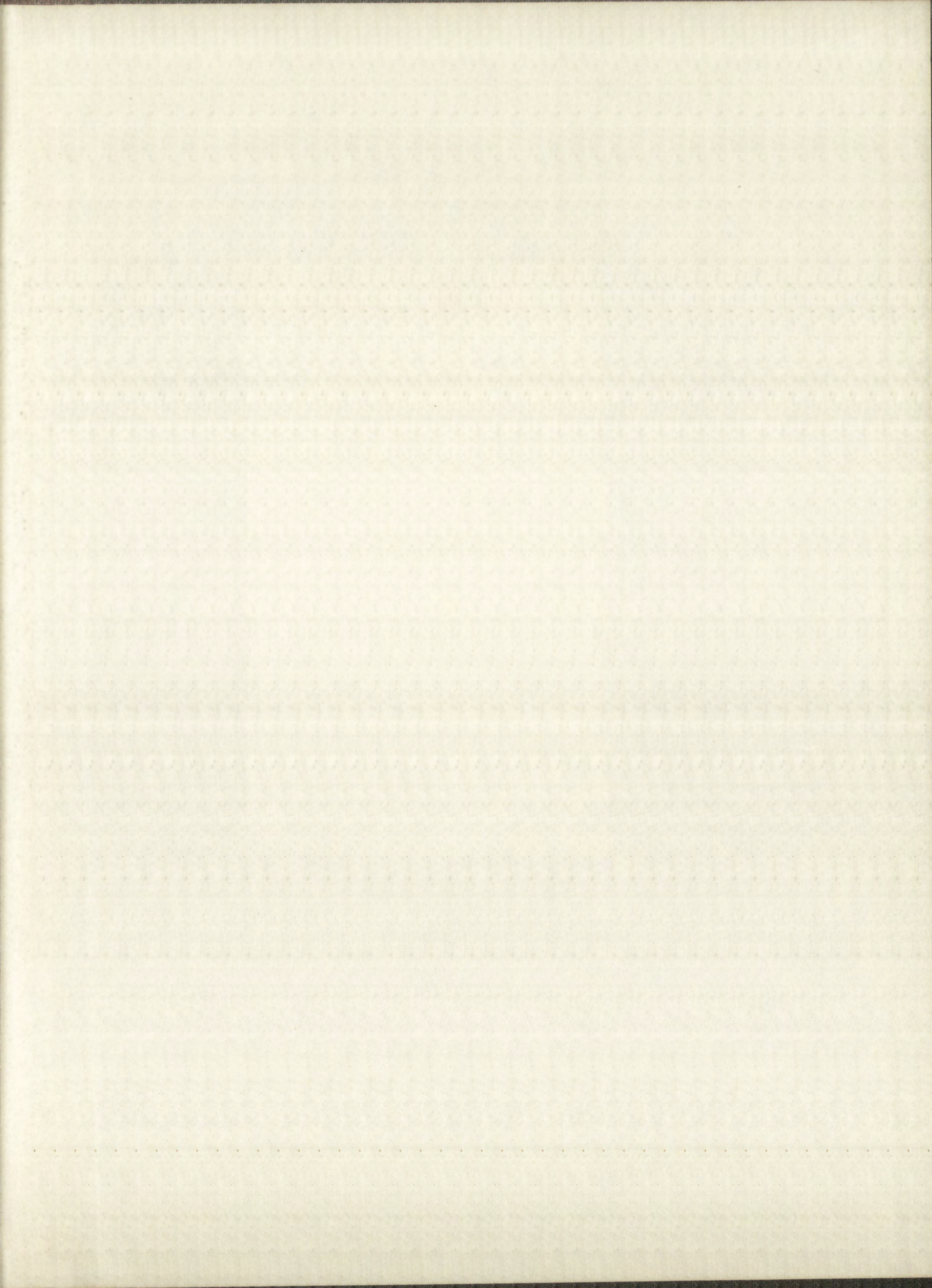
18. Cario, M. and Franck, J. Z. Physik, 17, 202 (1923).
19. McConnell, H. J. Chem. Phys. 20, 700 (1952).
20. Brealey, G. J. and Kasha, M. J. Am. Chem. Soc. 77, 4462 (1955).
21. Deutschbein, O. and Tomaschek, R. Physik Z. 34, 374 (1933).
Tomaschek, R. and Mehnert E. Ann. Physik, 29, 306 (1937).
22. Dieke, G. H. and Hall, L. A. J. Chem. Phys. 27, 465 (1957).
23. Dieke, G. H. and Crosswhite, H. M. J. Optical Soc. 46, 885 (1956).
24. Dieke, G. H. and Heroux, L. Physical Rev. 103, 1227 (1956).
25. Gobrect, H. Z. ges Naturw. 9, 351 (1937).
26. McClure, D. Solid State Physics, Academic Press, New York, 9, p. 454-476, (1959).
27. Dieke, G. H. and Singh, Shobha. J. Optical Soc. Am. 46, 495 (1956).
28. Dieke, G. H. and Sarkup, R. J. Chem. Phys. 29, 741 (1958).
29. Cook, S. P. and Dieke, G. H. J. Chem. Phys. 27, 1213 (1957).
30. Sayre, E. V. and Freed, S. J. Chem. Phys. 24, 1213 (1956).
31. Weissman, S. I. J. Chem. Phys. 10, (1942).
32. Sevchenko, A. N. and Trofimov, A. K. J. Exp. Theor. Phys. 21, 220 (1951).
Sevchenko, A. N. and Morachevsky, A. G. Izv. Akad. Nauk SSSR (ser fiz.) 15, 628 (1951).
33. Crosby, G. A. and Kasha, M. Spectrochimica Acta, 10, 377 (1958).

18. Carlo, M. and ... (1957)
19. McConnell, B. ... (1957)
20. Bresler, G. ... (1957)
21. Tausch, J. ... (1957)
22. ... (1957)
23. ... (1957)
24. ... (1957)
25. ... (1957)
26. ... (1957)
27. ... (1957)
28. ... (1957)
29. ... (1957)
30. ... (1957)
31. ... (1957)
32. ... (1957)
33. ... (1957)

34. Crosby, G. A. and Whan, R. E. J. Chem. Phys. 32, 614 (1960).
35. Crosby, G. A. and Whan, R. E. Naturwissenschaften, 47, 276 (1960).
36. Sponer, H. Radiation Research Supplement 1, 570 (1959).
37. Kolthoff, I. M. and Sandell, E. G. Textbook of Quantitative Inorganic Analysis, 3rd Ed. p. 607-608, (1952).
38. Whan, R. E. Phd. Thesis, University of New Mexico, (1961).
39. Chem. Rubber Handbook, 31st Ed. p. 2255-2257 Chem. Rubber Pub. Co. (1949).
40. Snedecor, G. W. Statistical Methods, 5th Ed. Iowa State College Press, p. 150 (1956).
41. Moeller, T. and Pundsack, F. L. J. Am. Chem. Soc 76, 617 (1954).
42. Nachtrieb, N. H. Principles and Practice of Spectrochemical Analysis, 1st Ed. McGraw-Hill p 12-31 (1950).
43. Ohnesorge, W. E. and Rogers, L. B. Spectrochimica Acta, 15 27 (1959).
44. Holleck, L. and Hartinger, L. Angewandte Chemie, 67, 648 (1955).
45. Herzberg, G. Atomic Spectra and Atomic Structure, New York Dover Publications, p. 209 (1944).
46. Moeller, T. Inorganic Chemistry, John Wiley and Sons Inc., p. 142 (1952).
47. Kronig, R. De L. Z. Physik 50, 347 (1928).
_____. De L. Z. Physik 62, 300 (1930).
48. Förster, Th. Ann. Phys. 6, 55 (1948).
49. Dieke, G. H. and Leopold, L. J. Optical Soc. Am. 47, 944 (1957).







IMPORTANT!

Special care should be taken to prevent loss or damage of this volume. If lost or damaged, it must be paid for at the current rate of typing.

[illegible]

